Understanding the Molecular Mechanism of Signal transduction in LiaSR Two component system in *Bacillus subtilis*

SHAILEE JANI

A THESIS SUBMITTED TO THE FACULTY OF GRADUATE STUDIES

IN PARTIAL FULFILLMENT OF THE REQUIREMENTS

FOR THE DEGREE OF MASTER OF SCIENCE

Graduate Program in Biology

York University

Toronto, Ontario

October 2017

.

Abstract

The *Bacillus subtilis* two-component system (TCS) LiaSR responds to environmental stresses inducing cell envelope damage. Here, the signal transduction mechanisms of LiaS/R are investigated in order to comprehend its uniqueness compared to other TCSs. My results indicate that the soluble portion of LiaS autophosphorylates and plays a bifunctional role towards LiaR. LiaR undergoes phosphorylation by acetyl phosphate in a time dependent manner. LiaR and its mutants bind to distinct regions on the *liaSR* promoter pre and post-phosphorylation. LiaR function is controlled independently by the N and C terminal domains. Characterization of the effector domain mutants created based on the homologous protein from *Enterococcus faecalis* suggested that the dimerization interface of LiaR lies on the N-terminal domain. Additionally, signal transduction between LiaSR and *Staphylococcus aureus* VraSR indicated possible *in vivo* interspecies cross-communication. In conclusion, my research provides comprehensive analysis of the LiaS/R signal transduction pathways regulating cellular responses in *B. subtilis*.

Acknowledgements

First and foremost, I would like to thank my supervisor for her constant support and guidance. Whenever I required advice or assistance relating to experimental work her office door was always open. She allowed me to work independently on my research, but steered me in the right direction and set the pace whenever she thought it was necessary. In addition, both my supervisor and I would like to thank Dr. Michael Scheid for his passionate participation and expert input into my research work. I also whole heartedly thank Dr. Bridget Stutchbury for going above and beyond her role as the program's Graduate Director and offering strong guidance.

A sincere thank you to my lab mates, Mayoorey Murugathasan and Ghazal Tajbakhsh for being there for me and providing encouragement and insightful comments. Earnest thanks to Uzma Muzamal for being an exceptional lab technician and teaching me how to trouble shoot and over come pressure. I'd also like to thank the undergraduate students, Henry Le and Katherine Van, who willingly devoted their precious time involving long working hours. I would like to thank my friends, Jessica D'Angelo, and Veroni Saratha Sri who have supported me throughout the entire process. I will be forever indebted to my family, for their emotional support throughout my life and especially during the two years of my Master's degree. Thank you, Mom for being the positive one, Dad for being the watchful one and Shivansh for being the calm one. I am also grateful to other family members and loved ones who have supported me along the way.

Good judgement comes from experience. Experience comes from bad judgement and persistence….

Table of Contents

List of Tables

List of Figures

Chapter 1

Chapter 2

List of Abbreviations

Ala – Alanine

Asp – Aspartic acid

ATP – Adenosine triphosphate

CESR – cell envelope stress response

EMSA – Electro-mobility shift assay

ESI-MS – Electrospray ionization mass spectrometry

FPLC – Fast protein liquid chromatography

GST – Glutathione S-transferase

His – Histidine

HK – Histidine kinase

IPTG – Isopropyl β- D- 1- thiogalactopyranoside

kDa – Kilodalton

LB – Luria bertani

LC MS – Liquid chromatography mass spectrometry

MRSA – Methicillin resistant staphylococcus aureus

M – molar

Ni-NTA – Nickel-nitrilotriacetic acid

PB – Phosphorylation buffer

PCR – Polymerase chain reaction

PG – Peptidoglycan

PNK – poly nucleotide kinase

RPM – Rotations per minute

RR – Response regulator

SDS-PAGE – Sodium dodecyl sulfate-polyacrylamide gel electrophoresis

TCSs – Two component systems

TB – Terrific Broth

Thr – Threonine

Val – Valine

VRAS – Vancomycin resistant *Staphylococcus aureus*

Chapter 1 : Introduction to the LiaSR TCS

1. Two component systems

Bacterial cells possess various stress signaling systems that sense and respond to specific stimuli, allowing them to cope with changing environmental conditions, usually through differential gene expression (Bury-Moné et al., 2009). A multitude of stress stimuli can activate various response pathways in order to mitigate envelope stress. In bacteria, the three major regulatory mechanisms are: one- component systems (OCSs), two component systems (TCSs), and alternative sigma factors of the extracytoplasmic function (ECF) family (Staroń et al., 2009). The modular design of OCSs is simpler than that of TCSs, with the sensory and regulatory domains fused on a single polypeptide that might bind to DNA modulating gene expression (Ulrich et al., 2005). TCSs are an example of advanced bacterial innovation and have emerged as a result of separation of the sensory and responding domains. Most often, such signaling systems are involved in sensing stressful settings that can potentially harm the microbial cell. In response, they initiate defensive countermeasures via differential expression of target genes involved in stress- resistance and other downstream responses (Ulrich et al., 2005; Storz & Hengge-Aronis, 2000).

1.1. Bacteria and cell envelope stress

Bacterial Gram-positive cell envelopes lack an outer membrane compared to their Gram-negative counterparts. The outer membrane possesses a relatively thin layer of peptidoglycan (PG) that plays a major role in protecting Gram-negative organisms from environmental stresses by providing an additional stabilizing layer around the cell. Gram-positive microorganisms are surrounded by thicker layers of peptidoglycan, permitting them to thrive in harsh environments and withstand the turgor pressure exerted on the plasma membrane. Lipid II, and its modified

forms play an intermediate role in PG synthesis and mediate the attachment of proteins to the bacterial cell wall. Interestingly, the lipid molecule 'flips' between the cytoplasmic and extracellular interfaces of the cell membrane in a dynamic process (referred to as the lipid II cycle) ultimately leading to the translocation of the PG precursors which are used for construction of the cell wall (Heijenoort, 2007). The lipid II cycle is considered the rate-limiting step of PG polymer biosynthesis and is therefore, the subject of intense scrutiny in the development of novel inhibitors that target or exploit this process (Nathaniel & Breukink, 2007). It is well established that various antibiotics (ramoplanin, mersacidin, vancomycin, telavancin, nisin, epidermin), lantibiotics and other glycopeptides bind non-covalently to peptidoglycan lipid intermediates and interfere with cell wall formation (Suntharalingam et al., 2009).

Soil bacteria are the most abundant antibiotic producers (Bérdy, 2005). Antibiotics produced by bacteria can be viewed as a means of interspecies competition for survival in complex and densely populated soil habitats (D'Costa et al., 2006). In order to compete with other organisms, soil bacteria have developed reflex mechanisms that respond to antibiotic threats. These reflex mechanisms typically involve signaling systems that sense the potential threat to the microbial cell and as a result, respond by activating distinct downstream processes (Storz & Hengge-Aronis, 2000). The response of the Gram- positive soil organism *B. subtilis* to cell envelope stress (CESR) by antibiotics has been studied extensively (Wecke & Mascher, 2011). Moreover, the 'ESCAPE' (*Enterococcus faecium*, *Staphylococcus aureus*, *Klebsiella pneumoniae*, *Acinetobacter baumannii*, *Pseudomonas aeruginosa* and *Enterobacter*) group of bacteria has been the topic of intense investigation during the last decade. Their high multiple-drug resistance (MDR), has rendered entire classes of antibiotics ineffective and is threatening to bring an end to the 'antibiotic era' (Alanis, 2005).

1.2. The bacterial two-component signal transduction model

TCSs are primarily found in bacteria, playing essential roles in cellular signaling events, cell-to-cell communication, adaptation to the environment and pathogenesis thus are important for survival (Kristin Wuichet, 2012). In pathogenic bacteria, TCSs play a key role in enduring hostile conditions, as they are necessary for sensing and responding to environmental stresses. Owing to their absence in humans and other mammals, TCS proteins are considered important targets for the development of novel antibiotics. The regulatory mechanism triggered by these systems typically involves two proteins: a sensor kinase and a response regulator (RR). The integral membrane kinase protein, usually gets autophosphorylated (via ATP) at a conserved histidine residue (His) and it then transfers the phosphoryl group to a conserved aspartate residue (Asp) on the RR. In turn, the regulator binds to specific sequences on the promoter of its target genes and modulates their expression. Autophosphorylation of the sensor histidine kinase (HK) and phosphotransfer to the cognate RR are considered quintessential steps in the cascade. Transduction may be varied or amplified by incorporating additional domains to the already existing components and/or by incorporating auxiliary proteins called connector proteins (Belcheva & Golemi-Kotra, 2008; Casino et al., 2010). RRs are also subject to phosphorylation by other non-cognate sensor kinases as well as small molecular phospho-donors such as acetyl phosphate (AcPO4) or phosphoamidate (PA) (Manoharan Shankar, 2015).

An example of a complete and functional TCS would be the DesRK TCS, involved in regulating membrane fluidity in *B. subtilis*. The regulation is mediated by the cold shock-inducible expression of the *des* gene, which encodes fatty acid desaturase (Aguilar et al., 1998). Similarly, the VraSR TCS system has demonstrated its contribution to cell-wall PG synthesis, and its involvement in β-lactam and glycopeptide resistance in *S. aureus* (Kuroda et al., 2003). To date, 46 genes have been

identified to be subject to regulation by the TCS in *S. aureus*. For example, the *murZ* locus is crucial for PG synthesis whereas the *pbp2* and *sgtB* genes are required for polymerization of PG (Gardete et al., 2006).

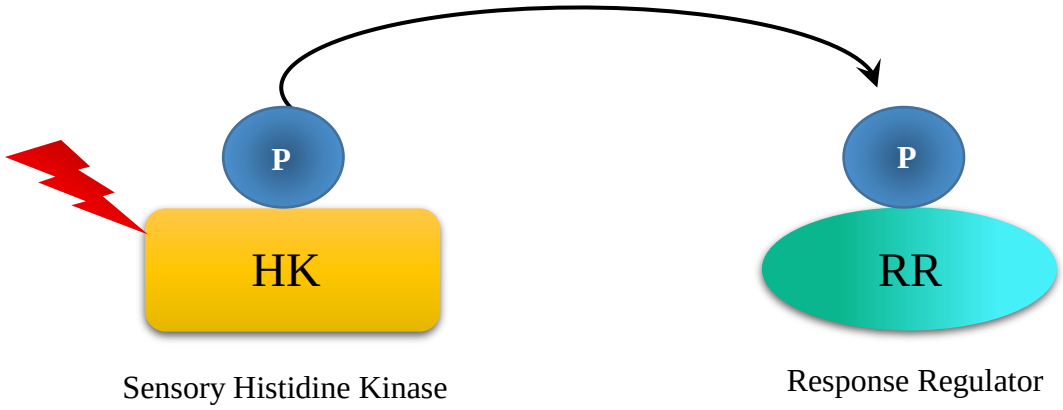

Figure 1.1.1 Schematic representation of elements of a two component system

The red bolt is indicative of an external stress stimulus/stimuli, while P denotes the phosphoryl residue being transferred from the Sensory Histidine Kinase to the Response regulator.

Besides the typical two-component organization, multistep His–Asp–His–Asp phosphorelay systems can be composed of individual phosphotransfer proteins. This modular organization of *Spo0F* has been extensively investigated in the multi-step pathway controlling sporulation in *B. subtilis* (Fabret et al., 1999).

1.3. Domain Organization and Sequence Conservation in Bacterial Histidine Kinases

The TCS includes a HK which usually contains a membrane-spanning region, and a carboxy-terminal domain consisted of approximately 250 amino acids (Pirrung, 1999). Upon receiving a stimulus, the HK typically autophosphorylates on a conserved histidine residue. These stimuli may represent external environmental conditions such as changes in osmotic pressure (EnvZ/OmpR), temperature (DesK/C), small molecules (NarX/Q, CitA/B), antimicrobial agents (PhoQ/P) and chemotaxis (CheA/Y) (Aguilar et al., 2001; Möglich et al., 2009). Although the structure of a full-length membrane-spanning HK has not yet been reported, structural studies of intracellular and extracellular sensors have elucidated how these domains bind their ligands. Accordingly, HKs form homodimers in order to facilitate autophosphorylation (Capra & Laub, 2012). While the exact mechanisms of recognition of RRs by HKs are not fully understood, there have been multiple investigations conducted using bioinformatics, protein engineering, and structural studies trying to elucidate this interaction (Cheung & Hendrickson, 2010). Many characteristic features such as the charge on the aspartate residue and sequence recognition have been identified to be the key factors responsible in the interaction of the proteins (Willett et al, 2013).

All HKs contain two highly conserved domains: a) the dimerization and histidine phosphotransfer (DHp) domain harboring the conserved histidine residue (the site of both the autophosphorylation and phosphotransfer reactions) and b) the catalytic ATP-binding (CA) domain. HKs may contain at least one, and often several, additional domains on the N-terminus. Most kinases also have at least one domain between the transmembrane (TM) and DHp domains, with PAS, HAMP, and GAF domains being by far the most common. The PAS domain was first discovered in periodic circadian proteins, aryl hydrocarbon nuclear translocator proteins, and single-minded proteins.

HAMP are present in HKs, adenylate cyclases, methyltransferases, and phosphodiesterases, whereas GAF is the main domain in cGMP-specific phosphodiesterases, adenylyl cyclases, and formate hydrogenases (Galperin et al., 2001).

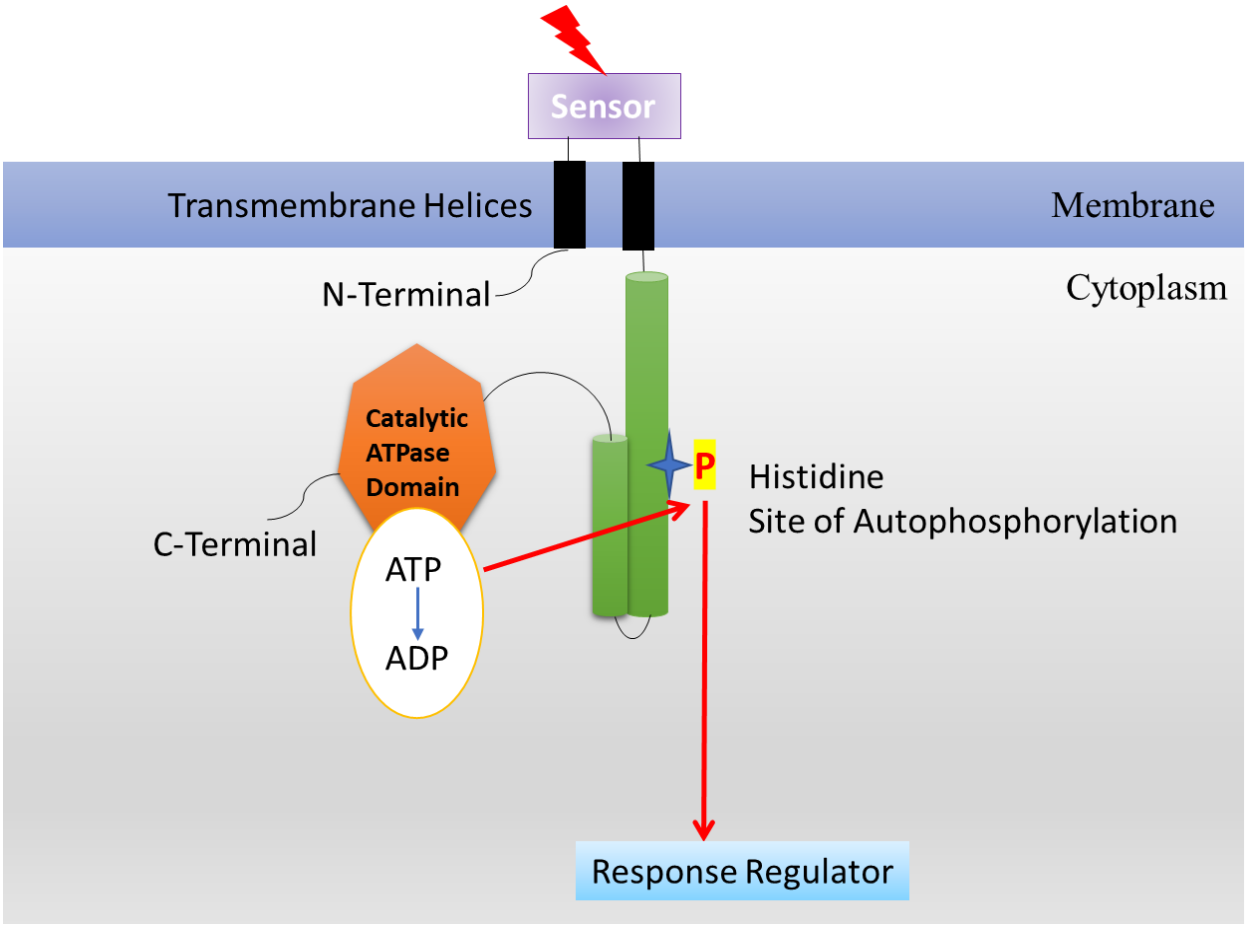

Figure 1.1.2 Representation of conserved domains in Histidine Kinases

Many of these domains are present in other protein classes. The orange structure shows the dimeric sensor interface. Anti-parallel pairs of transmembrane (TM) helices are shown in blue, followed by intracellular signal-transducing domains (White rectangle). HAMP, PAS, GAF are varying domains. DHp forms a homodimeric anti-parallel four-helical bundle with two helices connected by a hairpin loop, consisting of the phosphohistidine residue. Modified from Casino et al., 2010

Studies have shed light on a unique type of minimalistic membrane-anchored HK called intramembrane-sensing HK (IM-HK). The N-terminal 'input' domain consists of two TM sensors with a very short extracytoplasmic linker. These HKs often recruit accessory proteins as their sensors. Comparative genomics analysis has indicated such HKs are widely distributed in Gram-positive bacteria with a low G+C content (Firmicutes) and respond to cell envelope stress. Within *B. subtilis* LiaS, BceS, and YvcQ are three HKs that share a striking similarity in their domain organization with a short sensing domain consisting of two deduced TM helices with an extracytoplasmic linker of less than 25 amino acids between them. This structural similarity is suggestive of the fact that these IM-HKs sense their stimuli either on or within the membrane interface.

Some HKs stimulate the dephosphorylation of a phosphorylated RR and therefore are deemed bifunctional as they possess both kinase and phosphatase activity (Capra & Laub, 2012). Occasionally, input signals may favour dephosphorylation over phosphorylation (Raivio & Silhavy, 1997). Because the phosphatase reaction and the phosphotransfer step are mechanistically distinct, absence of the catalytic histidine in the kinase portion does not always affect the phosphatase activity of the later (Bhate et al., 2015). For example, in the CheA/Y TCS, the HK (CheA) lacks phosphatase activity towards the RR CheY. However, an independent protein, CheZ, is the designated phosphatase for phospho-CheY (Dutta et al., 1999; Perego & Hoch, 1996). Where as in the VraSR TCS of *S. aureus* phosphorylation levels of VraR, are controlled by the interplay between the histidine kinase and phosphatase activities of the bifunctional sensor protein VraS (Belcheva & Golemi-Kotra, 2008).

1.4. Domain Organization and Sequence Conservation in Bacterial Response regulator

RRs within the TCS signaling cascade control a diverse range of cellular processes. Typically, the RR receives a phosphoryl group on the aspartate residue in the N-terminal receiver domain, which then influences the properties of the C-terminal, DNA-binding domain (West & Stock, 2001) and results in a series of conformational changes that ultimately control binding to the DNA (Gao & Stock, 2009). Structural characterization of the DNA-binding domains of various response regulators has revealed several variations on the common helix-turn-helix (HTH) theme, exemplified by the NarL-type, OmpR-type "winged helix," Spo0A-type, and Fis-like structures (Martinez-Hackert & Stock, 1997; Bairoch et al., 2005).

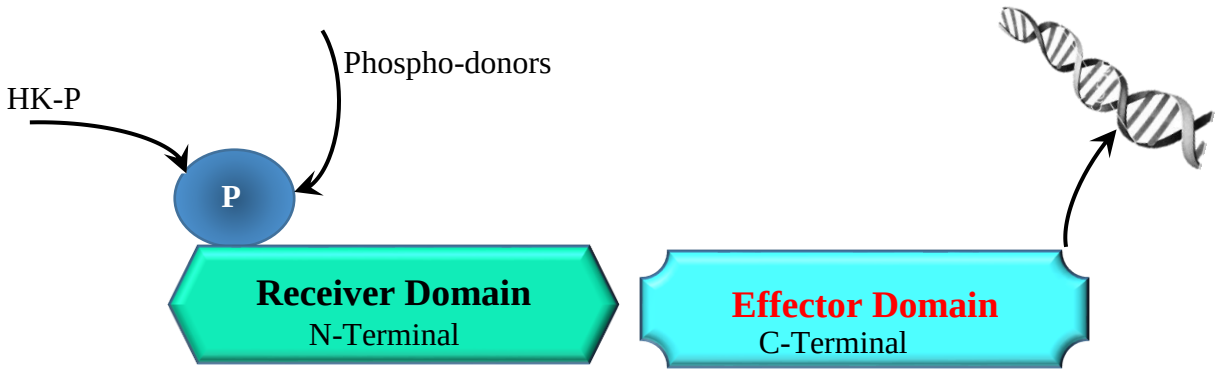

Figure 1.1.3 A prototypical Response Regulator

A typical phosphorylation event on the receiver domain (Green Hexagon) mediated by histidine kinases or small phospho-donors *in vivo*. The effector domain (Aqua Octagon) undergoes a conformational change which then affects downstream transcriptional events.

Receiver domains exist in a concentration independent equilibrium between the two predominant conformations (inactive and active). The inactive conformation is energetically favored for

unphosphorylated receiver domains and the active conformation is favored for phosphorylated receiver domains. However, sometimes receiver domains exist in the active state despite the absence of phosphorylation (Volkman et al., 2001; Nohaile et al., 1997). Inter-domain interfaces involving receiver domains can potentially influence RR activity in multiple ways. Studies have demonstrated that inter-domain interfaces can pose a barrier to RR activation, specifically by restricting the conformational dynamics required for phosphorylation by small molecule phospho-donors (Barbieri et al., 2010). In addition to forming associations with various DNA-binding domains, the receiver domain can also function as a stand-alone model (Galperin & Gomelsky, 2005).

1.5. *Bacillus subtilis*

B. subtilis is a Gram-positive, aerobic, spore-forming soil bacterium. By forming endospores, the bacterium can withstand extreme temperatures and dehydration. Bacterial endospores can survive without nutrients for a long time and are resistant to UV radiation, desiccation, extreme freezing, and most chemical disinfectants (Microbiology, 2017). *B. subtilis* also possess a flagellum which allows for faster mobility (Technology, 2009). The bacteria are able to function anaerobically in the presence of nitrates or glucose (Nakano & Zuber, 1998).

B. subtilis is typically considered non-pathogenic to humans and it is primarily found on the skin and the intestinal tract. However, because its spores are so resistant, the bacterium is easily spread and can cause opportunistic infections in humans. For instance, *B. subtilis* has been linked to liver toxicity in humans (Chen et al., 2010; Oggioni et al., 1998). In addition, *B. subtilis* has been linked to bacteremia in hospital patients treated for cancer and hematological disorders. Furthermore, the bacterium produces an extracellular toxin (subtilisin) which has been linked to allergies and

hypersensitivity reactions in humans. Lastly, this genus is also known to produce diarrheal entertoxins which cause food poisoning and are known to contaminate water and food sources (Yilmaz et al., 2006; Yassin & Ahmad, 2012).

Bacillus species of bacteria including *B. subtilis*, produce a variety of polypeptide antibiotics including bacitracin, tyrotricidin and polymaxin to name a few. These antibiotics are mostly effective against Gram-positive bacteria. However, bacteria of these species also produce large spectrum and anti-fungal antibiotics that are effective against Gram-negative bacteria (Stein, 2005).

A close relative of *B. subtilis* is *Bacillus anthracis* the etiologic agent of anthrax. Like its relative, *B. anthracis* is also a Gram-positive spore forming bacterium with proven devastating health consequences to humans. Inhalation of anthrax spores is typically lethal and its use as a biological weapon in bioterrorism has been well documented. This coupled with antibiotic resistance renders *B. anthracis* a potentially important human pathogen (Nicholson et al., 2000; Yassin & Ahmad, 2012).

Although *B. subtilis* is non-pathogenic, one cannot dismiss the possibility that its virulence characteristics might increase with time. Also, it is well established that cell-to-cell communication and signaling between microorganisms in the wild can influence bacterial behaviour and in particular lead to alteration in factors contributing to virulence (Howell et al., 2006). One can therefore envision that antibiotic susceptible strains can potentially acquire new resistance mechanisms from antibiotic resistant bacteria as a result of interspecies signaling (Ryan & Dow, 2008).

1.6. LiaSR TCS

The regulatory network of the model organism *B. subtilis* possesses over 30 HKs and RRs. It also comprises of at least two ECF σ factors and four important TCSs dealing with cell envelope stress response (CESR) (Cheung & Hendrickson, 2010; Mascher et al., 2003). One such signaling system is LiaSR of *B. subtilis*, which was identified as a result of investigations of the bacitracin stimulon (Mascher et al., 2003). LiaSR (formerly YvqCE) also known as **l**ipid II cycle **i**nterfering **a**ntibiotic **s**ensor and **r**esponse regulator (Mascher, 2006) mainly responds to the presence of cell wall antibiotics such as bacitracin, ramoplanin, vancomycin or cationic antimicrobial peptides (CAMPs) all of which interfere with the lipid II cycle (Mascher et al., 2004; Pietiäinen et al., 2005). LiaSR also responds to detergents, organic solvents (e.g. ethanol, phenol), and nonspecific stimuli such as secretion stress, alkaline shock, and filamentous phage infection, albeit to a weaker degree (Mascher et al., 2004; Pietiäinen et al., 2005; Petersohn et al., 2001; Tam et al., 2006; Wiegert et al., 2001). The LiaSR is a damage sensing TCS that is responsible for maintaining cell envelope integrity under conditions of stress. The *lia* locus consists of six genes (*liaIH-liaGFSR)*. LiaG is a putative membrane-anchored protein, whose expression is believed to be controlled by a weak promoter upstream of the *liaG* locus. Expression of the promoter (P_{liaSR}) is induced by phosphorylated LiaR (Jordan Sina, 2006; Mascher, 2006). The LiaSR TCS is functionally and genetically linked to a third protein (LiaF) forming a three-component system known as LiaFSR. LiaF acts as a strong suppressor of LiaR-dependent gene expression thereby inactivating the TCS (Jordan Sina, 2006; Mascher, 2006).

In- depth studies of the transcriptional profile of the homologous system of YvqFEC in *B. licheniformis*, demonstrated strong induction in the presence of bacitracin and to a weaker degree, by vancomycin and D- cycloserine (Wecke & Mascher, 2011). Growing and isolating deletion

mutants for *liaF* in *L. monocytogenes* has proven to be difficult indicating uncontrolled HK activity of LiaS leading to highly elevated levels of LiaR~P. This lethality is most likely attributed to the remodelling of the cellular envelop and the substantial upregulation of membrane-associated and

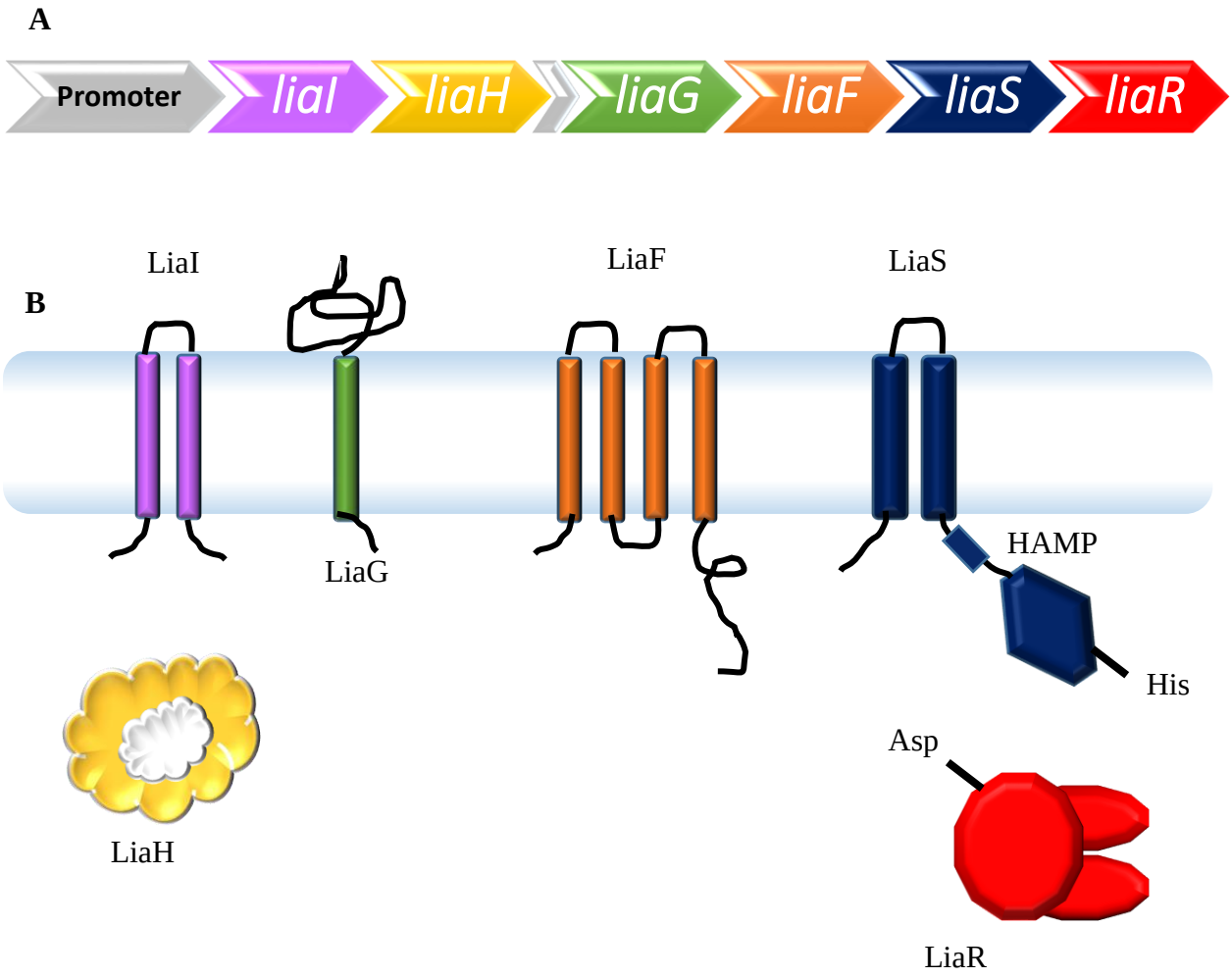

Figure 1.1.4 Organization of the *liaSR* genetic operon in *B. subtilis*

A: The *lia* locus consists of six genes. Grey coloured arrows indicate the promoter upstream of liaIH and a putative promoter upstream of liaG. **B:** Cellular distribution of the Lia proteins. Images adopted from (Jordan Sina, 2006).

extracytoplasmic proteins (Frederike et al., 2011). Other orthologs of the LiaSR TCS have been characterized in the foodborne pathogens *Enterococcus* species and *S. aureus* where multi-drug resistance is rapidly evolving. Overall the role of the LiaSR TCS has been implicated in acid, osmotic, detergent and antibiotic stress responses (Pöntinena et al., 2017; Munita et al., 2014; Belcheva & Golemi-Kotra, 2008). Lastly, the physiological role of the LiaFSR system in *Listeria monocytogenes* is presently unclear, since no resistance against inducing compounds has been detected (Frederike et al., 2011; Bisicchia et al., 2007).

1.6.1. LiaS the Histidine Kinase and LiaR the Response Regulator

It is proposed that *B. subtilis* LiaS is an ideal IM-HK that acts as a stimulus sensor in the cytosolic portion of the cytoplasmic membrane (Mascher, Margulis et al., 2003). Its second transmembrane helix is connected to a cytoplasmic HAMP domain, while the conserved HK core of LiaS contains a DHp domain as well as an ATP- binding domain. The phosphohistidine residue is located within the DHp domain (Toymentseva et al., 2012; Inouye, 2006).

VraS from *S. aureus* is a homologous HK involved in sensing cell wall stress and antibiotics (Belcheva & Golemi-Kotra, 2008). Remarkably, LiaS from *L. monocytogenes* causes a repression of the LiaSR regulon indicating its bifunctional HK/phosphatase role (Pöntinena et al., 2017). LiaS from *Streptococcus mutans,* has been demonstrated to control a large regulon consisting of 174 genes involved in biofilm formation and acid tolerance, but it lacks phosphatase activity towards its cognate RR (Manoharan Shankar, 2015).

B. subtilis LiaR is a typical two- domain RR protein with a conserved N- terminal receiver domain that contains an aspartate residue and a variable C- terminal DNA- binding domain. LiaR belongs to the NarL/LuxR family of response regulators, which possesses a characteristic helix- turn- helix motif responsible for binding to DNA (Galperin M. , 2010). Examination of LiaR from *E.*

faecium, *E. faecalis* and its homolog from *S. aureus*, VraR, suggests a remarkable flexibility in its quaternary structure. *E. faecium* LiaR and VraR are largely monomeric and both form dimers upon phosphorylation. In contrast, *E. faecalis* LiaR exists predominately as a dimer that oligomerizes to an active tetramer upon phosphorylation in order to mediate the cellular membrane stress responses (Davlieva et al., 2016; Davlieva et al., 2015). DNase I footprinting analysis of the promoters for all three organisms has revealed additional DNA binding sites (secondary binding sites) following phosphorylation.

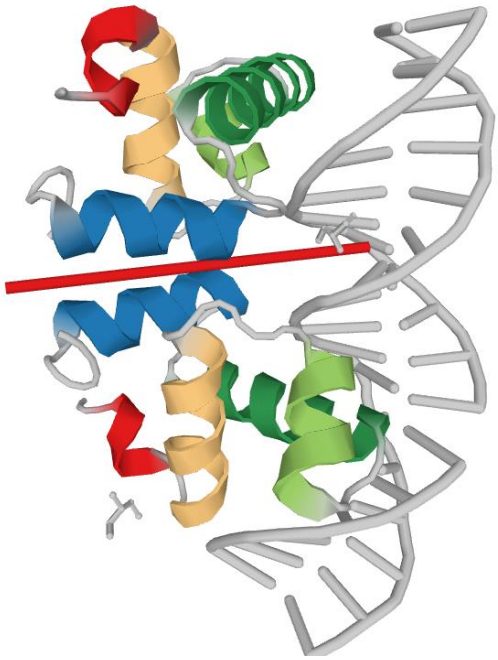

Figure 1.1.5 Crystal structure of the DNA-binding domain of LiaR from *Enterococcus faecalis* (Davlieva et. al, 2015, PDBID: 4WSZ).

This model represents the binding of the LiaR DNA binding domain to a 22 bp DNA sequence. DNA is shown in grey. The red bar represents the interaction surface for the monomers.

Furthermore, the crystal structure of the beryllofluoride-activated LiaR from *E. faecium* and the DNA binding domains of wild-type LiaR from *E. faecalis* has elucidated the molecular

architecture of the dimerization interface and revealed identity of the DNA binding sequence **(Figure 1.1.5)**.

Deletion of *liaR* in *E. faecalis* renders the cells susceptible to daptomycin and other antimicrobial peptides (Reyes et al., 2014). In group B *Streptococcus* bacteria, deletion of *liaR* confers susceptibility to cell wall-active antibiotics and antimicrobial peptides (Klinzing et al., 2013) suggesting that LiaR is a good target for the development of novel therapeutic agents that would effectively target antibiotic resistance.

1.6.2. Physiological role of acetyl phosphate in two- component signal transduction pathways

Acetyl phosphate is a highly energetic molecule ($\Delta G° = 43.3$ kJ/mol) able to store greater amount of energy and can be used as a substrate for the production of ATP via, substrate level phosphorylation (Madigan et al., 2003). Acetyl phosphate levels are regulated by first glycolysis in order to break down glucose and other carbon sources followed by phosphotransacetylase - acetate kinase (Pta- AckA) pathway. Accordingly, acetyl phosphate levels are directly correlated to the energy state of the cell. For example, when nutrients are abundant and cellular growth is exponential, acetyl phosphate levels are high in the cell. Similarly, acetyl phosphate levels are low during the stationary growth phase of the cell (nutrients are depleted) (Gueriri et al., 2008). Several RR proteins, such as CheY, NRI, PhoB, or OmpR, are able to use acetyl phosphate as the phosphoryl group- donor *in vitro* (Howell et al., 2006). Therefore, it has been hypothesized that acetyl phosphate may be able to act as a global signal producer *in vivo* as it is able to phosphorylate RRs of TCSs *in vitro* (Wolfe, 2005).

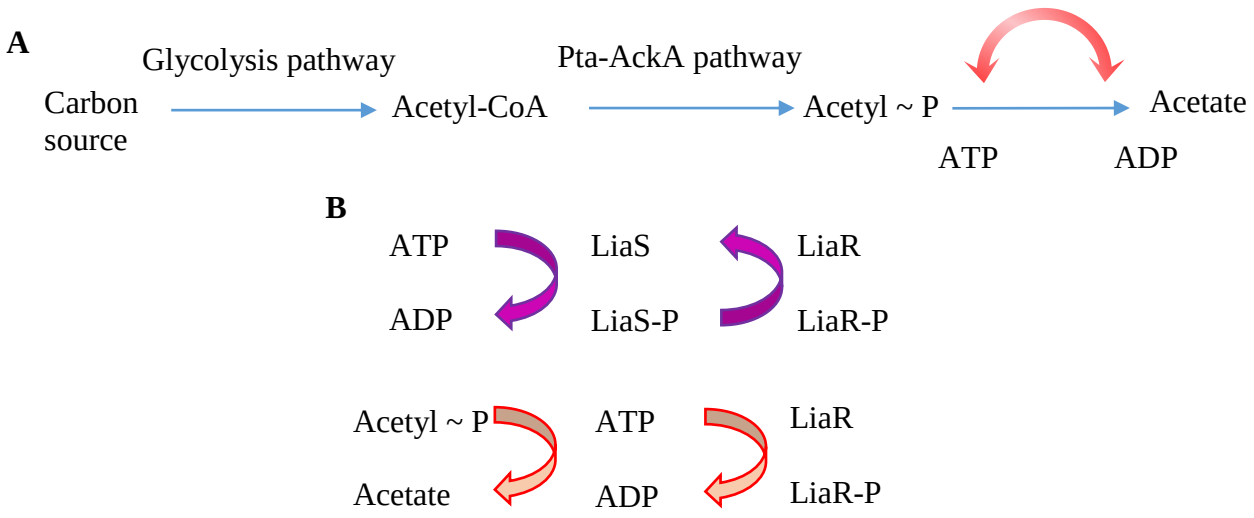

Figure 1.1.6 A schematic of the Pta-AckA pathway that converts acetyl-CoA to acetate and LiaSR phosphorelay

A: A representation of the phosphotransacetylase (Pta) acetate kinase (AckA) pathway that converts acetyl-coenzyme A (acetyl-CoA) to acetate via an acetyl phosphate (acetyl ~ P) intermediate. Image adapted from (Fredericks, et al., 2006). **B**: Shows the possible mechanisms by which *B. subtilis* LiaR can get phosphorylated via LiaS or Acetyl phosphate.

RRs that are acetyl phosphate- sensitive under physiologically relevant conditions can be divided into three major groups: (i) RRs that do not possess a cognate HK (e.g. RssB), (ii) RRs that are present in excess of their cognate HK (e.g. OmpR), or (iii) RRs whose cognate HK mainly acts as a phosphatase (e.g. RcsB, NRI) (Haijun Xu, 2010). Nonetheless, the *in vivo* relevance of the phosphotransfer reaction is still debated as phosphorylation induced by acetyl phosphate is only observed after deletion of the cognate HKs (Wolfe, 2005).

1.7. TCS and Drug designing

Attractive pharmacological targets of TCSs could include but are not limited to: a) the autophosphorylation site of the sensor-kinase, b) the physical interphase between the sensor~P and the response regulator (RR), c) the signal transfer of sensor-kinase~P to RR (phosphotransfer or dephosphorylation), and d) the binding of the RR to the regulatory gene promoter (Stock et al., 1995). It has been reported that oleic acid inhibits the formation of KinA~P in a concentration-dependent manner in the presence or absence of the cognate RR KinB (Strauch et al., 1992). Interestingly, another natural compound, bromoacetosyringone completely inhibits the expression of *vir* genes required for crown-gall tumour formation in the pathogenic *Agrobacterium tumefaciens*. (Lee et al., 1995; Barret & Hoch, 1998). A multitude of chemicals have also been demonstrated to inhibit TCSs in Gram-positive organisms. These include benzoxazines, benzimidazoles, bis-phenols, cyclohexenes, trityls, salicylanilides and others (Frechette et al., 1997; Licata et al., 1998; Macielag et al., 1997). Many of these synthetic chemicals were shown to temporarily inhibit growth of vancomycin resistant *E. faecium* and penicillin-resistant *S. pneumoniae* (Macielag et al., 1997).

However, the aforementioned natural and chemical agents are generally inhibitory to Gram-positive bacteria and seem to target the ATP-binding site of histidine protein kinases. It is noteworthy that, at higher concentrations, many of these compounds could potentially affect the integrity of the bacterial cell membrane. Since the structure of the cellular membrane in Gram-negative bacteria is more robust there is a need to discover drugs that are able to permeate these cells and specifically attack the TCS. Several known inhibitors are unfortunately very hydrophobic and thus not suitable for use as therapeutic agents (Barret & Hoch, 1998; Pawelczyk et al., 2012;

Procaccini et al., 2011; Sonja et al., 2012). Nevertheless, hopefully by using the mechanisms and techniques used by these inhibitors, it would be easier to decipher ideal target sites on the TCS. Because TCSs are ubiquitous in bacteria, interrupting phosphotransfer and cross talk between proteins may perhaps disrupt their ability to develop resistance against antibiotics. Offering us the potential for developing a new class of antibacterial agents (Bassler, 1999).

Chapter 2 : Understanding the Signaling Mechanism in LiaSR Two Component System

1. Aim of the Thesis

To date, there is very limited information regarding TCSs in *B. subtilis* (strain 168), particularly with respect to the mechanisms of stimulus perception and the actual signaling cascades governing cell envelope stress- sensing system. Therefore, the main objective of this thesis was to gain deeper insight into the underlying molecular/signaling mechanisms governing the LiaSR TCS. We hypothesised that the LiaSR TCS behaves identical to other well-characterized, homologous TCSs. In order to achieve this, my work focused on the biochemical characterization of the LiaSR system in *B. subtilis* and set out to address three main aspects.

The first objective aimed at describing and characterizing LiaS with respect to its autokinase and phosphatase activity. In addition, the ability of LiaS to phosphorylate its cognate RR, LiaR, was investigated. My second objective aimed at: a) investigating whether LiaR is subject to phosphorylation by acetyl phosphate *in vitro*, b) describing the oligomeric state of LiaR and determining the reaction rate constant governing the phosphorylation event, c) determining the exact location of the DNA biding sites and the affinity of the binding of LiaR to its target gene promoter, d) determining the nature of the interaction between the receiver and effector domains of LiaR, and e) determining the identity of the amino acids involved in maintaining the dimerization interface of LiaR by studying the crystal structure of the homologous protein from *E. faecalis*. My third objective aimed at determining whether there is functional cross-talk between interspecies TCSs. Accordingly, the ability of LiaSR to cross-talk with its homologous TCS VraSR, from *S. aureus*, was investigated.

2. Experimental Procedures

2.1. Materials and Chemical Reagents

All chemicals and antibiotics were from Sigma Aldrich (Oakville, Canada) and Thermo-Fisher (Whitby, Canada), unless otherwise indicated. Oligonucleotides were ordered from Sigma Aldrich (Oakville, Canada). The *Escherichia coli* strains, NovaBlue and BL21 (DE3), and cloning materials were purchased from EMD4 Biosciences (New Jersey, USA) unless otherwise stated. The GST-Tag pGEX-4T vector was acquired from GE Health Care (Quebec, Canada). Restriction enzymes were either from New England Biolabs (Pickering, Canada) or Thermo-Fisher. Chromatography reagents and columns were from GE Health Care (Quebec, Canada). Bacterial growth media were from Thermo-Fisher (Whitby, Canada). The γ labelled ATP was purchased from Perkin Elmer LAS Canada Inc. (Toronto, Canada). The *Pfu Turbo*® High Fidelity DNA polymerase enzyme was ordered from Agilent Technologies (Mississauga, Canada). The Proteo Extract All-in-One Trypsin Digestion Kit was from EMD4 Bioscience was used. Plasmid extraction and Gel extraction kits were ordered from Qiagen (Canada). The *B. subtilis* strain 168 genome was attained from ATCC (Burlington, Canada).

2.2. Cloning of the cytosolic portion of LiaS (GST-LiaS)

2.2.1. GST-LiaS (GST-LiaS^{Ala126})

The following primers were used to amplify the DNA sequence that encoded the *B. subtilis liaS* cytoplasmic region (amino acids 126-360): Forward, 5´-CATGGATCCCGATTGGCCAGAGAT CTTC-3´ and Reverse, 5´-ACGCCCGGGTTATCAATCAATAATACTCGAATC-3´. The primers contained the restriction sites *BamH*I and *Sma*I (underlined sequences), respectively. The

amplified gene is referred to as *liaS*^{Ala126}. The amplicon (708 bp) was digested and subsequently cloned into the corresponding restriction sites of the vector pGEX-4T-1 resulting in *liaS*^{Ala126} fused to the C-terminus of GST tag. The inserted sequence was verified by DNA sequencing at TCAG sequencing services (Sick Kids Hospital, Toronto). The verified construct pGEX-4T-1:: *liaS* ^{Ala126} (hereon referred to as GST-LiaS) was transformed into *E. coli* BL21 (DE3).

2.2.2. GST-LiaS Arginine 153 (GST-LiaS^{Arg153})

The nucleic acid sequence of *liaS* encoding the cytoplasmic histidine kinase domain of LiaS, (amino acid residues 153 to 360), was cloned into the pGEX-4T-1vector, for subsequent GST affinity purification. *BamH*I and *Sma*I restriction sites (underlined sequences) were incorporated in the forward and reverse primers: Forward, 5´- CATGGATCCGCATCCCTCCAGAAACTTTC -3´ and Reverse, 5´-ACGCCCGGGTTATCAATCAATAATACTCGAATC-3´. The verified (sequenced) construct (hereon referred to as GST-LiaS^{R153}) pGEX-4T-1::*liaS*^{R153} was transformed into *E. coli* BL21 (DE3).

2.3. Mutation of Histidine 159 to Alanine (GST-LiaS H159A)

Mutagenesis was carried out using *Pfu Turbo*® DNA polymerase, the pGEX-4T1::*liaS* ^{Ala126} vector and the following primers: Forward, 5´-CCAGAGATCTTGCTGATGCGGTCAG-3´ and Reverse, 5´-CTGACCGCATCAGCAAGATCTCTGG-3´. Successful mutation of the histidine to alanine was confirmed by DNA sequencing. The mutagenized pGEX-4T1::*liaSH159A* construct (hereon referred to as GST-LiaS H159A) was subsequently transformed into E. *coli* BL21 (DE3) for protein expression.

2.4. Cloning of LiaR

Cloning of LiaR was carried out by Dr. Karen Schrecke under the supervision of Dr. Thorsten Mascher in Germany by using the same strategy as VraR in Belcheva & Golemi-Kotra, 2008. The construct was then brought to our lab in 2009.

2.5. Mutation of Aspartate 54 to Alanine in LiaR (LiaR D54A)

Aspartate 54 of LiaR (GAT) was mutated to Alanine (GCC) using Pfu *Turbo*® DNA polymerase and the following primers: Forward, 5′- GATGTCATTTTAATGGCCCTTGTCATGG-3′ and Reverse, 5′-CCATGACAAGGGCCATTAAAATGACATC -3′. The pET26b::*liaR* vector was used as the template for site directed mutagenesis. Successful mutation of the aspartate to alanine was confirmed by DNA sequencing and the resulting pET26b::*liaRD54A* construct was used for transforming *E. coli* BL21 (DE3) cells.

2.6. Cloning of the *liaR*^{N} gene into an expression plasmid (LiaR^{N})

Glycine 131 of LiaR (GGA) was mutated to a stop codon (TGA). For site directed mutagenesis, Pfu *Turbo*® DNA polymerase and the following primers were used: Forward, 5′-AAAGTGGCGTGAAAAGTATTATCCAGGCT-3′ and Reverse, 5′-AGCCTGGATAATACTTTTCACGCCACTTT -3′. The pET26b::*liaR* vector was used as the template. Successful introduction of a stop codon was verified by DNA sequencing and the resulting pET26b::*liaR*^{N} construct was used for transformation of *E. coli* BL21 (DE3) cells.

2.7. Cloning of the *liaR*^{C} gene into an expression plasmid (LiaR^{C})

The cloning strategy for *liaR*^{C} did not result in the introduction of tags or extra amino acid residues and was similar to the strategy employed for cloning of full-length LiaR. The C-terminal domain

of *liaR*, spanning residues 139–211 (sequence was designed by using ExPASy), was amplified using pET26b::*liaR* and the following primers: Forward, 5′-ACGCATATGTCAGGTGAAAACGC-3′ and Reverse, 5′-ACGAAGCTTCTAATTCACGAGATGATTT-3′ (the restriction sites *Nde*I and *Hind*III are underlined). The PCR product was digested with *Hind*III and subsequently ligated into the pET26b vector between the *Msc*I and *Hind*III cloning sites. The resulting construct was used for transformation of *E. coli* NovaBlue. The purified pET26b::*liaR*^{C} plasmid was then treated with *Nde*I to remove the DNA stretch between *Nde*I sites. Correct cloning of *liaR*^{C} was verified by DNA sequencing analyses. The ensuing construct was then pET26b::*liaR*^{C} transformed into *E. coli* BL21 (DE3) competent cells.

2.8 Mutation of Threonine 198 to Alanine in LiaR (LiaR T198A), LiaR^{C} (LiaR ^{C}T198A), LiaR (LiaR V202A), LiaR^{C} (LiaR^{C} V202A) LiaR (LiaR H205A) and LiaR^{C} (LiaR ^{C} H205A)

Threonine 198 residue of LiaR (ACG) was mutated to Alanine (GCG), Valine 202 residue of LiaR (encoded by GTG) was mutated to Alanine (encoded by GCG) and the Histidine 205 residue of LiaR (CAC) was mutated to Alanine (encoded by GCC) on both the full length and C-terminus. Site directed mutagenesis was carried out by using pET26b::*liaR and* pET26b::*liaR*^{C} as template DNA, *Pfu Turbo*® DNA polymerase and forward and reverse primers (List of Primers in Appendix). DNA sequencing was used to verify the successful mutation and the confirmed construct was then used to transform *E. coli* BL21 (DE3) cells competent cells.

2.9 Cloning of *liaSR* promoter in pT7Blue-3 vector

The amplified gene is referred to as *liaSR* promoter was amplified using genomic DNA of *Bacillus subtilis* 168 from ATCC. The following forward and reverse primers were used to amplify the nucleic acid sequence that encodes the *B. subtilis liaSR* promoter sequence (P_{liaSR}, -161 to +31): Forward 5´- GAAAGGGAAGCAAGTGTTCATCTGTAAAG-3´ and Reverse, 5´- TTCATGCAGATCCTCCTTTCGTTTT - 3´. The amplified gene (192 bp) was gel extracted and ligated with pT7blue vector. The resulting construct pT7Blue-3::*liaSR* was introduced into NovaBlue cells via transformation. The inserted sequence was confirmed by DNA sequencing.

2.10 Expression and Purification of Target Proteins

2.10.1 Protein expression of wild-type GST-LiaS and GST-LiaS H159A.

Expression of wild-type LiaS and its mutant was carried as follows: An overnight seed culture of *E. coli* BL21 (DE3) hosting the pGEX-4T-1::$liaS^{Ala126}$ plasmid was prepared in 5 ml Luria Bertani (LB) media containing 100 µg/ml ampicillin at 37°C. A 500 µl aliquot from the seed culture was used to inoculate 350 ml Terrific Broth medium (TB) supplemented with 100 µg/ml ampicillin. The growth of bacteria was allowed to continue up to an optical density ($OD_{600\ nm}$) of ~0.6. Induction of protein expression was initiated with the addition of 1 mM isopropyl β-D-thiogalactopyranoside (IPTG) at 17°C for 17 h. The culture was harvested by centrifugation (6300g for 20 min at 4°C) and stored at -80°C.

Protein was purified using Glutathione Sepharose affinity resin chromatography. The target protein was eluted with 10 mM reduced glutathione in 50 mM Tris buffer, pH 8.0. Fractions were analysed on a 12.5% SDS-PAGE gel and subsequently concentrated using an Amicon Ultra-10 kDa concentrator (Millipore, Toronto). Dialysis was carried out overnight (4°C) to exchange the

buffer into 50 mM Tris pH 7.4, supplemented with 100 mM KCl and 5 mM $MgCl_2$. The purity of protein was assessed by electrophoresis using a 12.5% SDS-PAGE which was then stained with Coomassie Blue. Similar growth, expression and purification techniques were used for GST-LiaS H159A and GST-LiaS ^{R153}.

2.10.2 Wild-type LiaR, LiaR D54A, LiaR T198A, LiaR V202A, LiaR H205A LiaR^C, LiaR^C T198A, LiaR^C V202A and LiaR^C H205A

Expression of wild-type LiaR and its variants was carried out as follows: an overnight seed culture of *E. coli* BL21 (DE3) hosting either pET26b::*liaR* wild-type or the variant vectors, was prepared in 5 ml LB medium, supplemented with 50 μg/ml kanamycin. A 500 μl aliquot from the seed culture was used to inoculate 350 ml TB supplemented with 50 μg/ml kanamycin. Cells were grown to an optical density (OD_{600nm}) of ~0.6, and protein expression was induced by adding 0.5 mM IPTG. The cell culture was incubated for 17 hr at 17°C with gentle shaking at 120 rpm. Cells were harvested by centrifugation at 6300 g, for 20 min at 4°C and stored at -80°C.

Purification of LiaR was performed by two steps on a Fast Protein Liquid Chromatography (FPLC) (AKTA Purifier 10, GE Health Care) as previously described (Belcheva & Golemi-Kotra, 2008) with a few modifications. Briefly, the cell pellet was resuspended in the 50 mM Tris, pH 7.0, supplemented with 5 mM $MgCl_2$, and sonicated to liberate soluble proteins. Cell debris was removed by centrifugation at 13000 rpm for 1 hr at 4°C. The resulting supernatant was loaded onto a DEAE-Sepharose column and the protein was eluted using a linear gradient of 500 mM Tris, pH 7.0, supplemented with 5 mM $MgCl_2$. The protein containing fractions were examined using a 15% SDS polyacrylamide gel. LiaR containing fractions were concentrated using an Amicon stirred cell (MWCO, 5 kDa). The protein was loaded onto the Heparin-Sepharose column, equilibrated with 50 mM Tris, pH 7.0, supplemented with 5 mM $MgCl_2$. The protein was eluted

using a linear gradient up to 500 mM Tris, pH 7.0, buffer, supplemented with 5 mM $MgCl_2$. Protein containing fractions were analyzed using 15% SDS-PAGE. The fractions containing LiaR were combined and concentrated using Amicon centrifugal filter tubes (MWCO 3 kDa). Expression and purification of $LiaR^C$ wild-type and its variants was carried out in a similar fashion to LiaR full-length protein.

2.10.3 $LiaR^N$

Expression and purification of $LiaR^N$ wild-type and its variants was carried out like $VraR^N$ in Belcheva & Golemi-Kotra, 2008. To briefly state, the cells were grown to an OD_{600} of 0.6 and allowed to express with 0.5 mM IPTG for 17 hrs at 17ºC. Purification of the protein was carried out using FPLC with DEAE and Size exclusion column (Sephacryl S-200 HiPrep 26-60) after sonication and concentration. The concentration of the protein was verified ech time by using nanodrop and BSA standards.

2.10.4 Wild-type GST-VraS and wild-type VraR

Expression and purification of GST-VraS was carried out very similar to GST-LiaS, the only differences were with respect to the induction temperature being 25 ºC in comparison to LiaS. The purification involved the GST affinity chromatography with the help of 10 mM reduced glutathione in 50 mM Tris buffer, pH 8.0. VraR expression was carried out with the same parameters as the LiaR protein. Purification was carried out as previously described for LiaR with 20 mM Tris and 5 mM $MgCl_2$ equilibration buffer, hence allowing for quicker elution of the buffer while using FPLC (DEAE and Heparin Sepharose column) (Belcheva & Golemi-Kotra, 2008)

2.10.5 Wild-type His-VraS

Bacterial growth and expression of VraS was done as previously described (Uzma Muzamal, 2014) with some modifications. The modifications include sonication buffer 20 mM Sodium phosphate,

300 mM NaCl, 20 mM imidazole, pH 7.4, sonication cycle of total 8 minutes, 15 secs on, 30 secs rest, at 30% power, 60% pulse. Buffer exchange was performed using dialysis buffer (50 mM Tris, 50 mM KCl, 5 mM $MgCl_2$, pH 7.4) overnight at 4°C.

2.11 Circular Dichroism (CD) spectroscopy and Thermal melting of purified proteins

CD measurement of the target proteins were carried out by preparing a protein solution of 20 µM in an equilibration buffer. The CD spectrum was recorded from 200 to 260 nm using a Jasco J-810 instrument (path length of cuvette 0.1 cm). Phosphorylation was carried out using acetyl phosphate (50 mM). The buffer contribution was subtracted and the corrected data were plotted using Microsoft Excel. Thermal melting curves were acquired for wild-type LiaR, its mutants (T198A, V202A and H205A) and $LiaR^N$ proteins and have also been shown in Henry Le's undergraduate thesis, 2017 (Le, 2017). Each of the respective proteins (20 µM) were buffer exchanged with 50 mM Tris and 5 mM $MgCl_2$ buffer at pH 7.0. The melting spectrum was recorded by monitoring the change in CD signal at 222 nm by ramping the temperature from 25 °C to 90 °C at a rate of 5 °C/min. Buffer correction was performed in order to gauge the melting temperature.

2.12 *In vitro* Autophosphorylation of GST-LiaS and its variants

5 µM GST-LiaS was equilibrated in phosphorylation buffer (PB: 50 mM Tris, pH 7.4, 50 mM KCl, 5 mM $MgCl_2$) supplemented with 10 mM $CaCl_2$. The reaction was initiated by the addition of [γ- 32P]-ATP at 25 °C. The reactions were quenched by the addition of 5X SDS sample buffer at various time intervals. Samples were analyzed by 12.5% SDS-PAGE. The gel was incubated on a phosphor screen for 2 hr. The screen was scanned using Typhoon Trio+ variable-mode imager.

The band intensities were plotted to obtain progress curves. Phosphorylation was quantified by using the NIH ImageJ software (Version 1.45s) (Belcheva & Golemi-Kotra, 2008). ATP concentrations ranging from 10 µM to 250 µM were used by mixing hot and cold ATP (a 1:9 ratio was used).

We calculated the pseudo first order equation for phosphorylated GST-LiaS, I = A(1-e -kt), where I was the average band intensity, k the rate constant, t was the time and A was the proportionality constant relating intensity with concentration.

In addition, a graph of rate versus ATP concentration was also plotted and fitted to the Mechalis-Menten equation to calculate binding efficiency, Km and catalytic efficiency, kcat (Belcheva & Golemi-Kotra, 2008).

$$v = Vmax \times \frac{[S]}{Km + [S]}$$

Similar experiments were carried out for GST-LiaS H159A and GST-LiaS ^{R153}.

2.13 Phosphotransfer reaction from wild-type GST-LiaS to wild-type LiaR and its variants

Phosphorylation of GST-LiaS was carried out as previously described (Belcheva & Golemi-Kotra, 2008). Excess [γ-32P] ATP was removed with the use of a desalting column (Zeba^{TM}, Pierce). GST-LiaS-phosphate (4 µM) was added to WT-LiaR (20 µM) in the PB buffer. 20 µl reactions were carried out at different time intervals and quenched by adding 5 µl of 5X SDS-PAGE sample buffer. Samples were loaded onto a 15% SDS-PAGE. The radioactive gels were exposed to a phosphor screen (GE Health Care) for 2 hr and imaged using a Typhoon Trio+ variable-mode imager (GE Health Care). The radioactive gels were stained with Coomassie Blue dye. The

phosphor images of the radioactive gels were quantified using the NIH ImageJ software (Version 1.45s). Similar experiments were conducted for GST-LiaS to LiaR D54A and GST-LiaS to $LiaR^N$.

2.14 Phosphorylation of LiaR and its variants by the small phosphor-donor, lithium potassium acetyl phosphate.

To investigate phosphorylation of LiaR by small molecule phosphate donors, lithium potassium acetyl phosphate was used as previously described (Belcheva & Golemi-Kotra, 2008). Briefly, various concentrations of LiaR and its variants were equilibrated in PB 20 buffer (50 mM Tris, pH 7.4, 50 mM KCl, 20 mM $MgCl_2$) and phosphorylation was initiated by the addition of lithium potassium acetyl phosphate to a final concentration of 50 mM. The reaction mixture was incubated at 37°C for 1 hr. Phosphorylation experiments on LiaR T198A, V202A and H205A were conducted by Henry Le (Le, 2017).

2.15 Observing change in the oligomeric structure of LiaR and its variants post phosphorylation via Native- Poly Acrylamide Gel Electrophoresis (PAGE)

The oligomerization state of LiaR prior to and following phosphorylation were examined by native-PAGE gel electrophoresis. Protein solutions of 10, 20 and 30 μM in PB 20 were supplemented with 50 mM acetyl phosphate and incubated for 1 hr at 37°C to facilitate phosphorylation of LiaR and its variants. 20 μl aliquots were removed and quenched by adding 5X native sample buffer. The SDS free native-PAGE gel was run at a voltage of 90 V and the internal temperature of the buffer during the gel electrophoresis was maintained at 4°C. The gels were stained with Coomassie Blue to visualize the protein bands. $LiaR^C$ was analyzed on an acidic

native gel to check the protein based on its isoelectric point rather than its molecular weight in its native state.

2.16 Analysis of phosphorylation of the target proteins by small molecule phospho-donors using Phos-tag ™ gel

The phosphorylated species were separated from unphosphorylated species on 15% Phosphate Affinity SDS-PAGE containing Acrylamide-pendant Phos-tag™ AAL-107 (50 µmol/l) as the active chemical (Wako chemical USA, Inc., Cedarlane) (Kinoshita, et al., 2006). From here this gel will be referred to as Phos-tag ™ gel. Wild-type LiaR, LiaR D54A and $LiaR^N$ samples of 20 µM in phosphorylation buffer (P20B) were supplemented with 50 mM acetyl phosphate and incubated for 1 hr at 37°C. 10µl of samples were quenched with 5 X SDS sample buffer at various time intervals. The gels were run at 120 V and stained by Coomassie Blue dye for visualization of the separation. Intensities of the phosphorylated species were quantified using ImageJ software and averaged. A graph of intensity versus time was plotted and data were fitted to non-linear fitting curve using the pseudo first order equation on Erithacus GraFit software (version 5.0.10) and the rate of phosphorylation was determined.

2.17 Identification of LiaR, LiaR D54A and $LiaR^C$ by mass spectrometry

After purifying the proteins, the homogeneity of the protein was determined by Coomassie Blue staining of the SDS polyacrylamide gels. The band corresponding to the protein of interest was cut from the gel and was subject to in-gel trypsin digestion carried out using the Trypsin Profile IGD kits (Sigma). Proteins identities were confirmed by liquid chromatography-mass spectrometry (LC-MS/MS) at the Advanced Protein Technology Centre at The Hospital for Sick Children (Toronto, Canada).

2.18 Sample preparation for mass spectrometry analysis

The masses of $LiaR^N$ and $LiaR^N$-P were analyzed by ESI-MS at Dr. Wilson's lab (York University). 40µM $LiaR^N$ was prepared in 50 mM sodium acetate pH 7.0 buffer. Phosphorylated sample of 40µM $LiaR^N$ was prepared by incubating the protein and 50 mM acetyl phosphate for 1 hr at 37°C, followed by desalting.

2.19 Analytical Ultracentrifugation analysis of $LiaR^N$

Sedimentation equilibrium experiments on $LiaR^N$ (MW:14.029 kDa and partial volume/MW :0.753) were carried out at the Ultracentrifugation Service Facility in the Department of Biochemistry at the University of Toronto by Ms. Elisa Leung. Briefly, 0.25 mg/ml, 0.50 mg/ml and 1 mg/ml $LiaR^N$ samples were spun at 20000 and 24000 and 28000 rpm at 20^o C. Absorbance was recorded at 280 nm and 60-Ti Rotor in a Beckman Optima XL- A analytical ultracentrifuge was used.

2.20 DNA binding ability of LiaR and its variants

2.20.1 Electromobility Shift Assays for wild-type LiaR, $LiaR^C$ and LiaR mutants (D54A, T198A, V202A and H205A)

Binding of wild-type LiaR and phosphorylated LiaR to the promoter region of *liaSR* (P_{liaSR}), was assessed by electrophoretic mobility shift assay (EMSA) as described in Belcheva & Golemi-Kotra, 2008. To perform EMSA experiments, the gel purified *liaSR* promoter (2 ng/µl) was 5' end labeled with [γ- 32P]-ATP (3000 Ci/mmol) and LiaR (phosphorylated and unphosphorylated) samples ranging from 0 to 10 µM concentration. Similar studied were done for LiaR D54A, $LiaR^C$ and LiaR mutants (T198A, V202A and H205A).

2.20.2 DNase I footprinting experiments with *liaSR* promoter for LiaR and its variants

The DNase I footprinting was carried out as previously described with a few changes (Belcheva & Golemi-Kotra, 2008). Briefly, the *liaSR* promoter region spanning -161 to +31 was amplified using the following primers Forward 5′- GAAAGGGAAGCAAGTGTTCATCTGTAAAG-3′ and Reverse 5′- TTCATGCAGATCCTCCTTTCGTTTT-3′. Prior to amplification, the forward primer was 5′ end-labeled with [γ- 32P]-ATP (3000 Ci/mmol) using T4 polynucleotide kinase (NEB). The end-labeled and purified DNA (8 ng/µl) was mixed with LiaR/LiaR~P at concentrations ranging from 0 to 20 µM. Similar reactions were done for LiaR D54A, and $LiaR^{C}$.

2.21 Investigation of cross-communication between LiaSR and VraSR TCS

2.21.1 Phosphotransfer reaction between GST-LiaS and VraR

Phosphorylation of GST-LiaS followed by phosphotransfer to VraR was carried out as described in Belcheva & Golemi-Kotra, 2008 as well as the method used for LiaS to LiaR phosphotransfer experiments. That is using the HK and the RR in a 1:4 ratio with first autophosphorylating the HK and then co-incubating the protein with the RR for varying time intervals. Followed by analysing the gels using autoradiography and ImageJ (version 1.5) software.

2.21.2 Phosphotransfer reaction between GST-VraS and LiaR

Phosphorylation of GST-VraS followed by phosphotransfer to LiaR was carried out as described Belcheva & Golemi-Kotra, 2008.

2.21.3 DNase I footprinting experiments with *vraSR* promoter for LiaR and VraR

The DNase I footprinting was carried out as described previously (Belcheva & Golemi-Kotra, 2008). Briefly, the *vraSR* promoter region spanning -121 to +150 was amplified using the following forward and reverse primers. Prior to amplification, the forward primer was 5′ end-labeled with [γ- 32P]-ATP (3000 Ci/mmol) using T4 polynucleotide kinase (NEB). The end-labeled and purified DNA (8 ng/µl) was mixed with LiaR/LiaR~P and VraR/VraR~P at concentrations ranging from 0 to 20 µM.

2.21.4 Investigation of protein-protein interactions by pull-down assays of GST-LiaS: LiaR, GST-VraS: LiaR, GST-LiaS: VraR and GST-LiaS: His-VraS

Pull down assays ere conducted as describes in Fridman, et al., 2013 with a few modifications. Glutathione-Sepharose affinity resin (75 µl) was equilibrated in PB buffer. GST-LiaS was incubated with the resin for 30 min at room temperature. The flow-through was collected, and the resin was washed with 1 × PB buffer until no protein eluted. At this point, GST-LiaS-bound resin was incubated with LiaR with a 1:4 ratio for 30 min at room temperature. Subsequently, the resins were washed fifteen times with 200 µl of 1 × PB buffer. The proteins were eluted with 100 µl aliquots of 10 mM reduced glutathione in 50 mM Tris (pH 8.0). Flow-through fractions, wash fractions, and elution fractions were analyzed by 12.5% SDS-PAGE. In addition, the resin itself µwas incubated with the prey proteins LiaR to investigate for non-specific interactions of these proteins with resin. A similar protocol was used to investigate the interaction between GST-VraS and LiaR (ratio 1:4), GST-LiaS and VraR and GST-LiaS (ratio 1:4). In the case of GST-LiaS and His-VraS, His –VraS was also immobilized onto Ni-NTA agarose resin, and GST-LiaS was added. The elution fractions were collected using 100 µl 500 mM Sodium phosphate, 300 mM NaCl, 300 mM imidazole, and pH 7.4 for 5 min each time and then analyzed by 15% SDS-PAGE (Uzma Muzamal, 2014).

3 Results

3.1 Cloning, Expression and purification of proteins

3.1.1 GST-LiaS

Initially, the *B. subtilis* (strain 168) full-length *liaS* gene had been cloned into a pGEX-4T1 vector but protein expression was not optimal due to solubility issues. In order to circumvent this, the cytosolic domain of LiaS (residues126-360) was amplified from the pre-cloned *liaS* full-length gene and fused at the COOH-terminus of GST in the pGEX-4T-1 vector (GST-LiaS). An additional construct (residues 153-360) was also fused with the GST tag in the pGEX4T-1 vector (GST-LiaS^{Arg153}).

Induction of protein expression was attempted at various temperatures and concentrations of IPTG in order to maximize the production of soluble protein. Optimal expression was achieved by induction with 1 mM IPTG for 17 hr at 17 °C. Purification of GST-LiaS (theoretical molecular weight of 52431 Da) was carried out with the use of Glutathione Sepharose 4B affinity resin. We tried using PBS buffer as well as a range of pH levels in order to optimize protein yield and purity **(Figure 2.1.1)**. Use of GST-LiaS^{Arg153} was discontinued after a few initial experiments, as GST-LiaS (residues126-360) yielded higher phosphorylation (band intensity with radiolabelled ATP) in comparison and consisted of the longer sequence altogether.

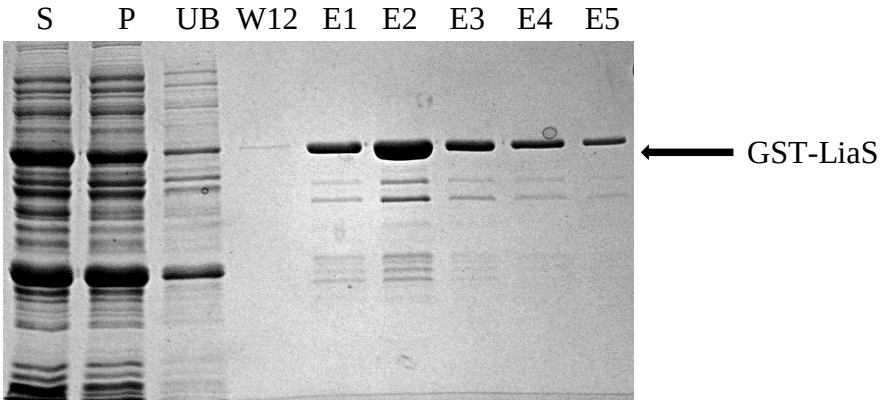

Figure 2.1.1 GST-LiaS purification with glutathione resin

12.5% SDS-PAGE analysis of fractions collected during purification. Lane S (supernatant); Lane P, (cell pellet following sonication); Lane UB (unbound protein); Lane W12 (fraction collected following 12 washes with sonication buffer); Lanes E1 to E5 represent fractions collected during elution with 10 mM reduced glutathione in 50 mM Tris (pH 8.0).

3.1.2 GST-LiaS H159A

To verify the importance of the histidine residue for autophosphorylation, site directed mutagenesis was carried out. The phosphohistidine (159^{th} residue) was mutated to an alanine. The overexpression and the purification of the protein was carried out as previously described (section 3.1.1). The supernatant, pellet and elution fractions containing the protein were analyzed on a 12.5% SDS gel, as seen in **Figure 2.1.2.** GST-VraS, and His-VraS have previously been cloned in the laboratory (Belcheva & Golemi-Kotra, 2008; Uzma Muzamal, 2014)

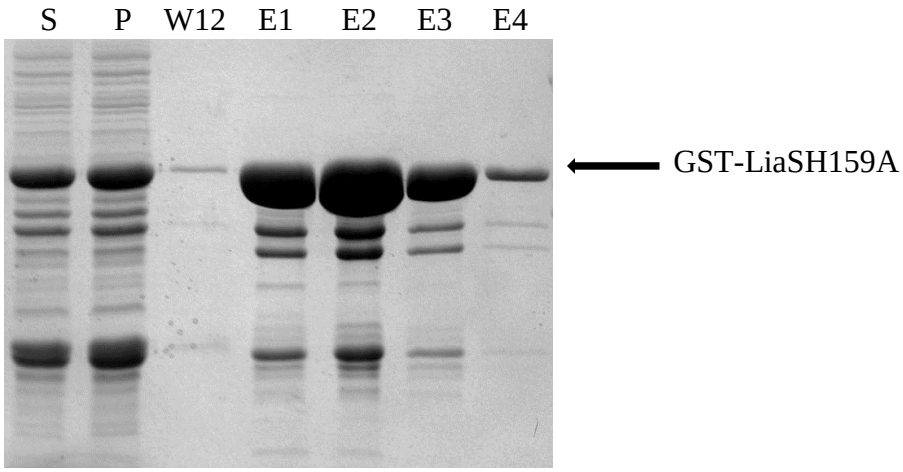

Figure 2.1.2 GST-LiaSH159A purification with glutathione resin

12.5% SDS-PAGE analysis of fractions collected during purification. Lane S (supernatant); Lane P, (cell pellet following sonication); Lane W12 (fraction collected following 12 washes with sonication buffer); Lanes E1 to E4 represent fractions collected during elution with 10 mM reduced glutathione in 50 mM Tris (pH 8.0).

3.1.3 WT-LiaR, LiaR D54A, Li aR T198A, LiaRV202A and LiaR H205A

LiaR mutants (LiaR D54A, LiaR T198A, LiaRV202A and LiaR H205A) were all generated by mutating the full-length wild-type gene, using site directed mutagenesis. Growth and expression of all mutant strains was carried out under identical conditions to those used for the wild-type. Optimal expression was achieved by inoculating a single colony and adding 0.5 mM IPTG for 17 hr at 17°C. The calculated molecular weight of LiaR was determined to equal 23124.76 Da with a theoretical pI of 5.13. The mutations did not have an effect on either the molecular weight or pI of the proteins as compared to those of the wild-type. Wild-type VraR was previously cloned in the laboratory (Antonetta Belcheva, 2009).

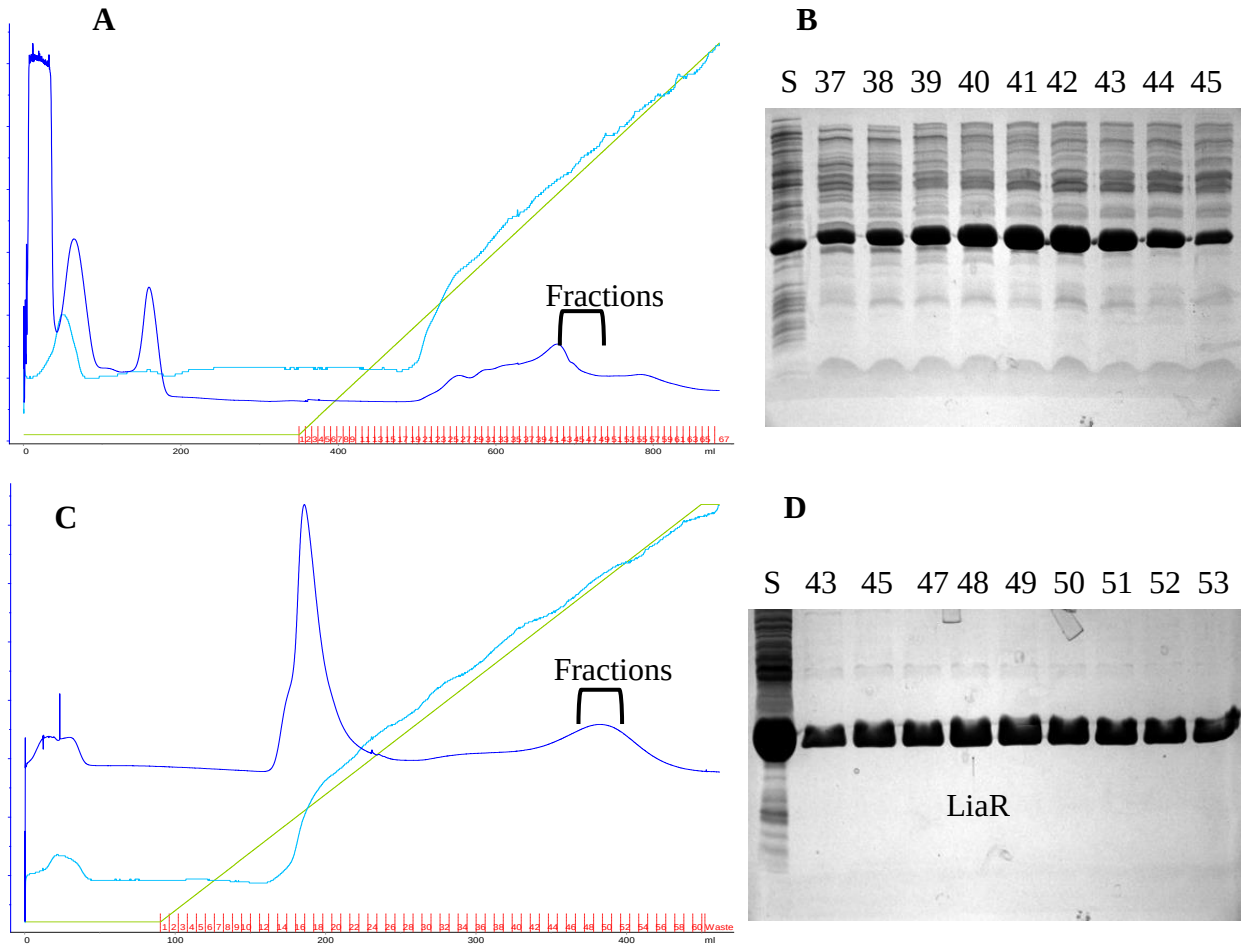

Figure 2.1.3 Purification of wild-type full-length LiaR and its mutants using FPLC

A: FPLC UV (280 nm)-chromatogram showing proteins eluted from a Diethylaminomethyl (DEAE) Sepharose column and the fractions selected for further analysis. **B**: 15% SDS-PAGE of fractions 37 to 45. Lane 1 represents the supernatant collected following cell lysis. **C**: FPLC UV (280 nm)-chromatogram of the eluted proteins from a heparin sepharose column. The fractions selected for further analysis by SDS-PAGE are shown. **D**: 15% SDS-PAGE of different fractions collected from the heparin sepharose column. Lane 1 represents the supernatant prior to the heparin column elution, while lanes 2-9 represent fractions 43-53 corresponding to the peak observed on the chromatogram.

Purification of WT-LiaR and its mutants was carried out using FPLC at 4°C. A DEAE column was used to elute the protein based on charge. As shown in the chromatogram in **Figure 2.1.3 A**,

the resulting fractions were analyzed using a 15% SDS-PAGE **(Figure 2.1.3. B)**. Subsequent step of purification was carried out by keeping in mind the properties of a transcriptional regulatory protein that binds to the DNA. Heparin-Sepharose formulation exhibits excellent binding capacity for proteins due to its similar structure to the DNA backbone. LiaR was eluted from the heparin column at a 40-60% concentration of the elution buffer **(Figure 2.1.3 C)**. Analysis of the elution fractions by electrophoresis **(Figure 2.1.3 D)** indicated that the purified protein contained some impurities despite using a wide range of experimental protocols.

3.1.4 C-terminal LiaR and its mutants (LiaR^{C} T198A, LiaR^{C} V202A, LiaR^{C} H205A)

The calculated theoretical weight and the pI of the C-terminal domain of LiaR was determined to be 7466.58 Da and 7.09 respectively. The mutations {(T198A: MW-7436.56 Da; pI- 7.09), (V202A: MW-7438.53 Da; pI- 7.09) and (H205A: MW-7400.52 Da; pI- 7.03)} did not cause a major change in the molecular weight or pI of the resulting proteins compared to the wild-type C-Terminal LiaR by using ExPASy ProtParam for the theoretical estimation.

Purification of WT-LiaR^{C} was carried out at 4°C using DEAE and Heparin Sepharose columns. The overall concentration and yield of purified protein was almost half compared to full-length WT-LiaR, with a few contaminants present, as indicated in **Figure 2.1.4.** This could potentially be attributed to the fact that the actual pI of the proteins was in fact much higher than the predicted values. Accordingly, a range of pH values ranging from 7.0 to 9.0 was tested for the buffers in order to maximize the purity of the isolated proteins. The purity and stability was highest at a pH of 8.5 **(Figure 2.1.4)**.

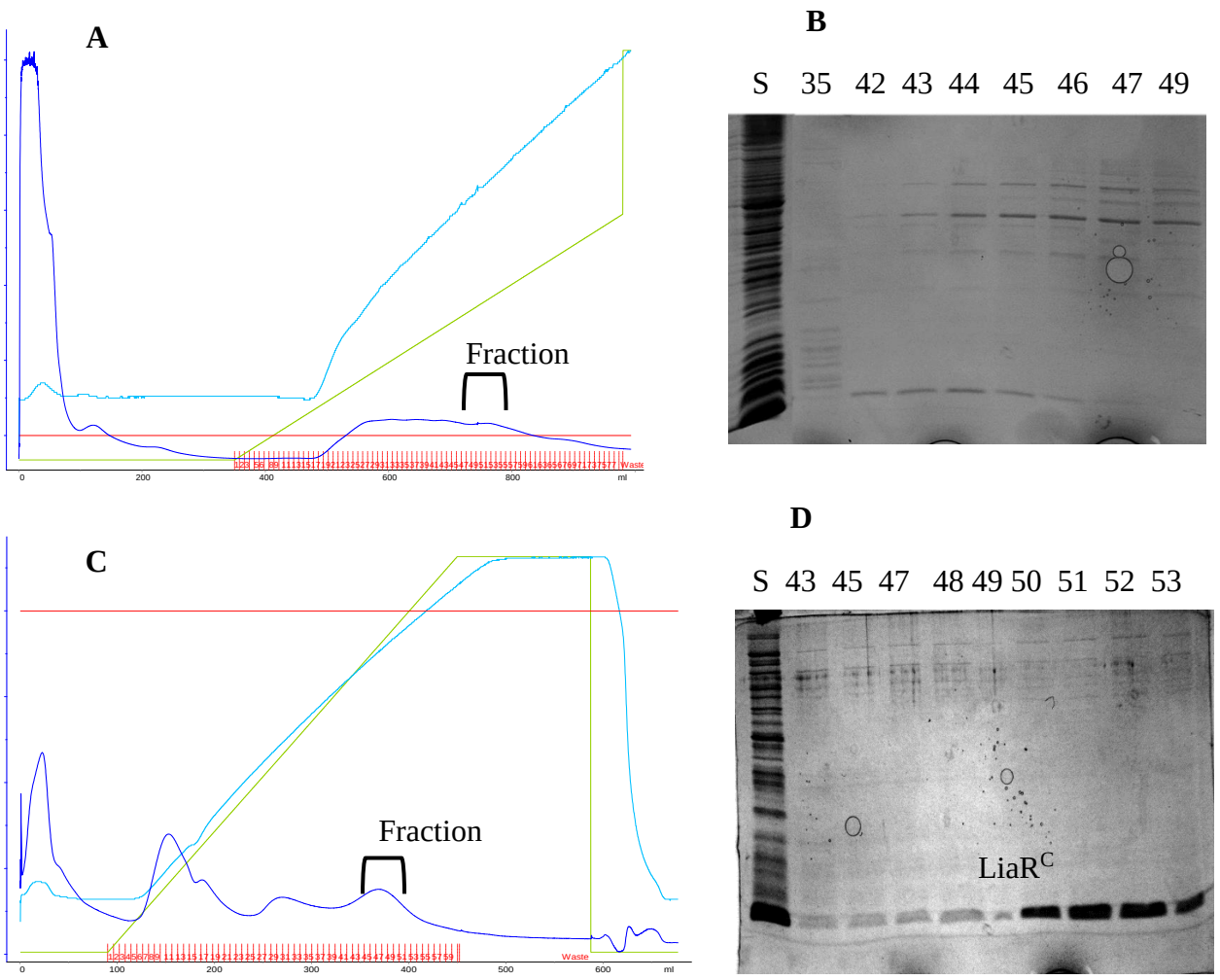

Figure 2.1.4 Purification of WT-LiaR^C and its mutants using FPLC

A: FPLC UV (280 nm)-chromatogram showing proteins eluted from a DEAE Sepharose column and the fractions selected for further analysis. **B**: 20% SDS-PAGE of fractions 35 to 49. Lane 1 represents the supernatant collected following sonication of cells. **C**: FPLC UV (280 nm)-chromatogram of the eluted proteins from the Heparin sepharose column. The fractions selected for further analysis by SDS-PAGE are indicated. **D**: 20% SDS-PAGE of different fractions collected from the Heparin sepharose column. Lane 1 represents the supernatant after sonication, while lanes 2-9 represent fractions 43-53 corresponding to the peak observed on the chromatogram.

3.1.5 N-terminal LiaR

The receiver domain, LiaR^N was analysed separately by introducing a stop codon on the 131st residue. LiaR^N was purified at 4 °C using FPLC, the cellular lysate was first passed through a

DEAE column and the resulting fractions were verified using SDS-PAGE. Subsequently, the fractions were concentrated and loaded onto a size exclusion column (Sephacryl S-200 HiPrep 26-60) as opposed to a heparin column because the protein lacked the DNA binding domain. The calculated molecular weight of N-terminal LiaR was determined to equal 14029.27 Da with a theoretical pI of 4.38. The isolated target protein was homogeneous as seen on **Figure 2.1.5.**

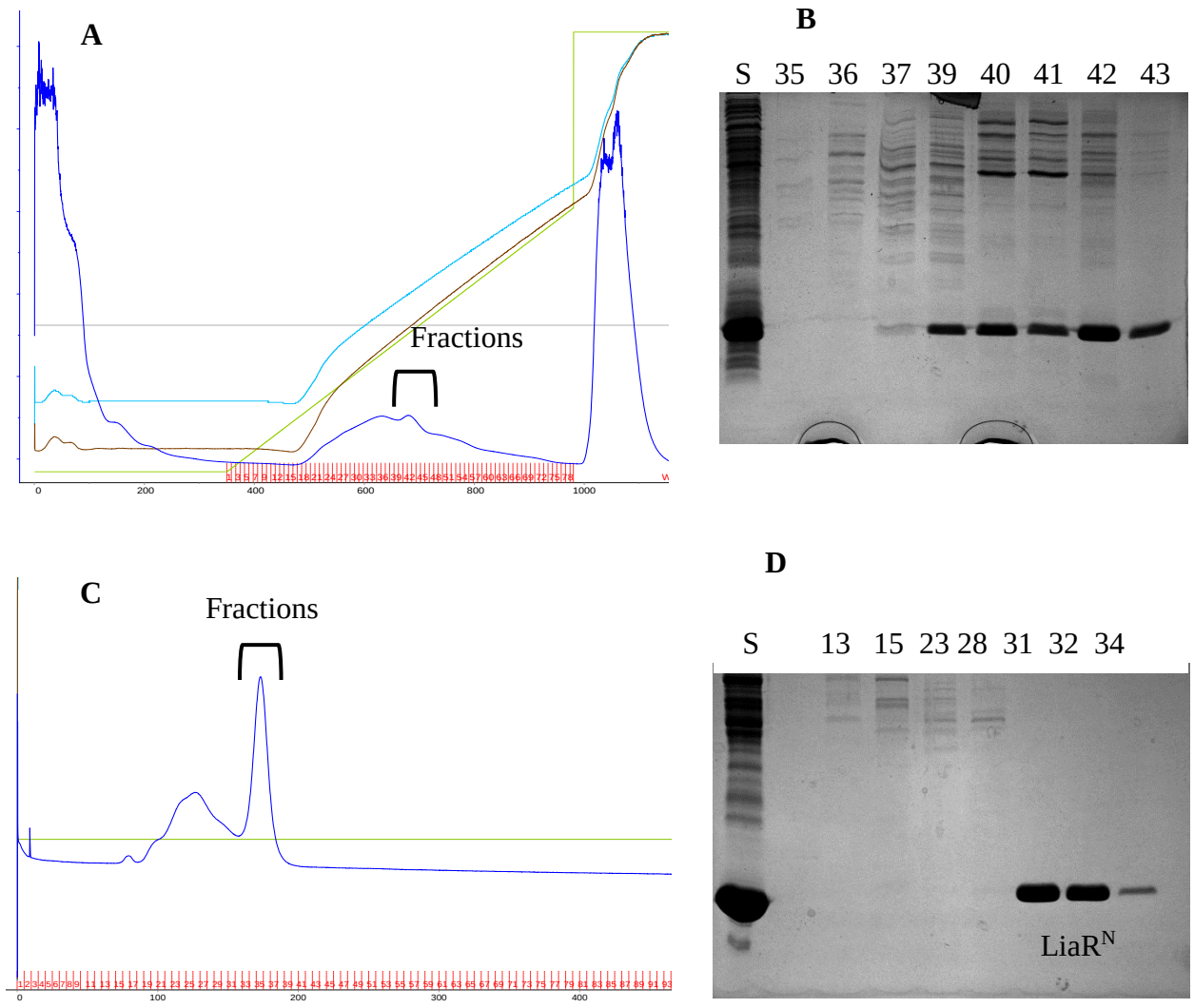

Figure 2.1.5 Purification of wild-type N-terminal LiaR using FPLC

A: FPLC UV (280 nm)-chromatogram displaying proteins eluted from a DEAE Sepharose column and the fractions selected for further analysis. **B**: 20% SDS-PAGE of fractions 35 to 43. Lane 1 represents the supernatant collected following sonication. **C**: FPLC UV (280 nm)-chromatogram of the eluted proteins from the Sephacryl S-200 HiPrep column. The fractions selected for further analysis by SDS-PAGE are indicated. **D**: 20% SDS-PAGE of various fractions collected from the size exclusion column. Lane 1 represents the supernatant obtained following sonication, while lanes 3-10 represent fractions 13-34 corresponding to the peak observed on the chromatogram.

3.2 Circular Dichroism and thermal melting curves of the isolated proteins

Circular dichroism (CD) is an important tool used for analysis of the structural properties of proteins. This technique is based on the principal that optically active biomolecules, including proteins, reveal different absorption of left and right circularly polarized light over a range of wavelengths (200-260nm). Here, CD was used for analyzing proper folding of the purified proteins. The thermal melting (TM) spectrum was recorded by monitoring the change in CD signal at 222 nm by ramping the temperature from 25 °C to 90 °C at a rate of 5 °C /min. The CD spectrum suggested that GST-LiaS has a stronger α-helical component, indicated by the negative absorbance near 210 nm and 220 nm. Mutation of the histidine residue demonstrated a slight variation in secondary structure with respect to α-helices and β-sheets. The CD spectrum of LiaR and its mutant LiaR D54A and $LiaR^{C}$ all resembled that of a well folded protein with similar CD spectrums to other DNA binding proteins (helix-turn-helix motif). Similar studies were conducted on LiaR T198A, LiaR V202A and LiaR H205A (Le, 2017). However, the observed CD spectrum of the N terminal of LiaR was different in comparison to its full-length protein **(Figures 2.1.6 A and B)**. In addition, phosphorylation-induced conformational changes were further confirmed by CD for the wild-type protein and all full-length mutants (LiaR T198A, LiaR V202A, LiaR H205A) **(Figure 2.1.7)**. These results were similar to a study done on VraR by Belcheva & Golemi-Kotra, 2008. In addition, structural analysis was carried out using thermal melting. The melting temperature of $LiaR^{N}$ was rather unique in comparison to the classical two step mode seen in full-length protein or its mutants **(Figure 2.1.8)**.

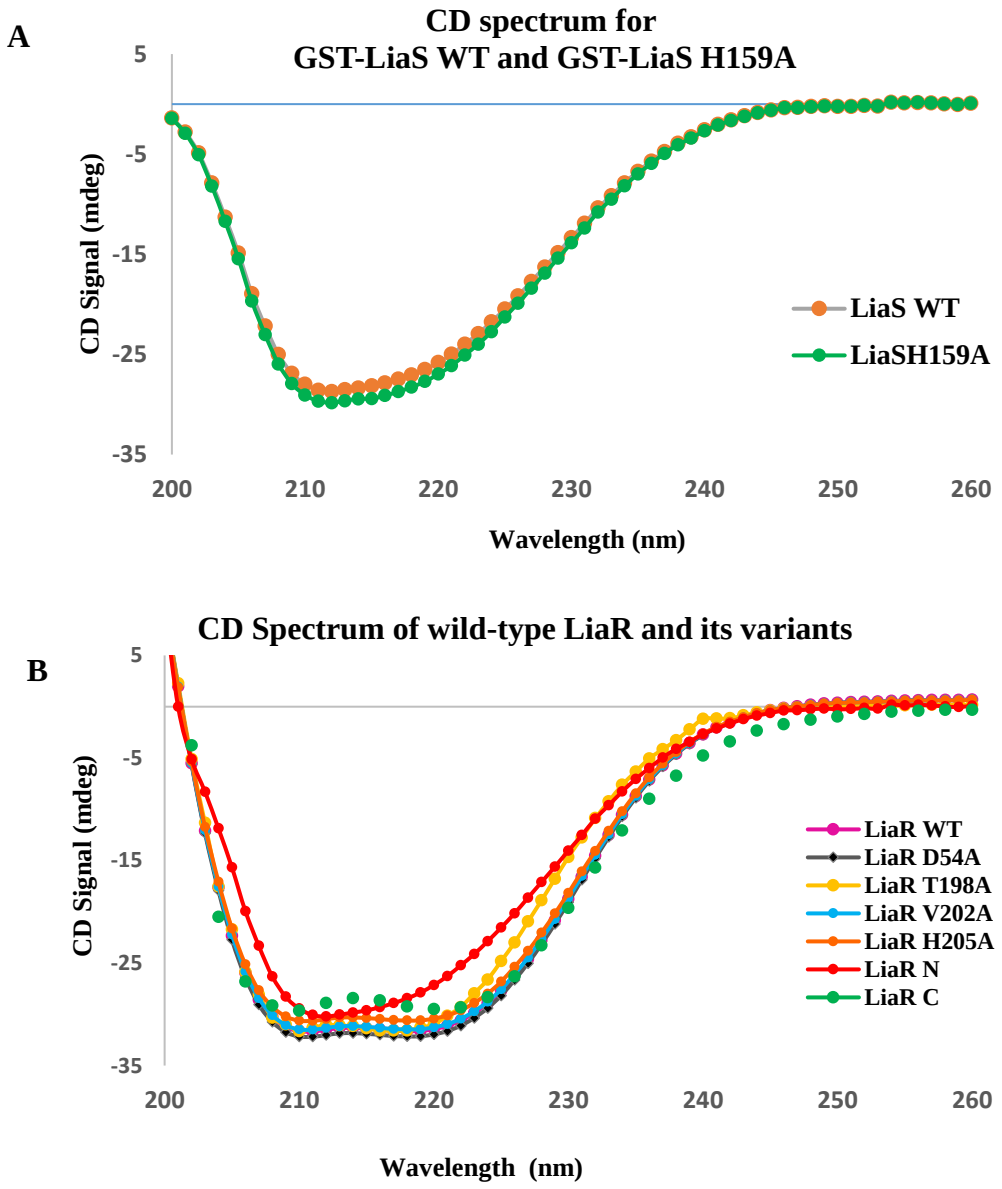

Figure 2.1.6 The CD spectrum (200-260nm) of the purified proteins (Data shown from Le, 2017 and used with permission)

A: Displays the CD spectrum corresponding to GST-LiaS and GST-LiaS H159A indicating no substantial changes in secondary structure **B**: Displays of the spectrum corresponding to WT-LiaR and its variants. The N-terminus is structurally different from the wild-type full-length protein and the mutants.

Table 1: Analysis of the secondary structure component of LiaS Wild-Type and its mutant, in WT-LiaR and its mutants when analysed using CD analysis and plotting Tool (CAPITO).

CD spectra of all proteins (30µM) were first plotted on Excel indicating folding pattern.

Protein	**α-Helical component**	**β-Strand component**	**Irregular coils**
LiaS Wild-Type	16%	30%	54%
LiaS H159A	16%	30%	54%
LiaR Wild-Type	7%	44%	49%
Phosphorylated LiaR Wild-Type	9%	41%	49%
LiaR T198A	7%	44%	49%
Phosphorylated T198AA	8%	41%	51%
LiaR V202A	7%	44%	49%
Phosphorylated V202A	7%	44%	49%
LiaR H205A	7%	44%	49%
Phosphorylated H205A	10%	41%	49%
LiaR N	15%	29%	55%
LiaR C	7%	45%	48%

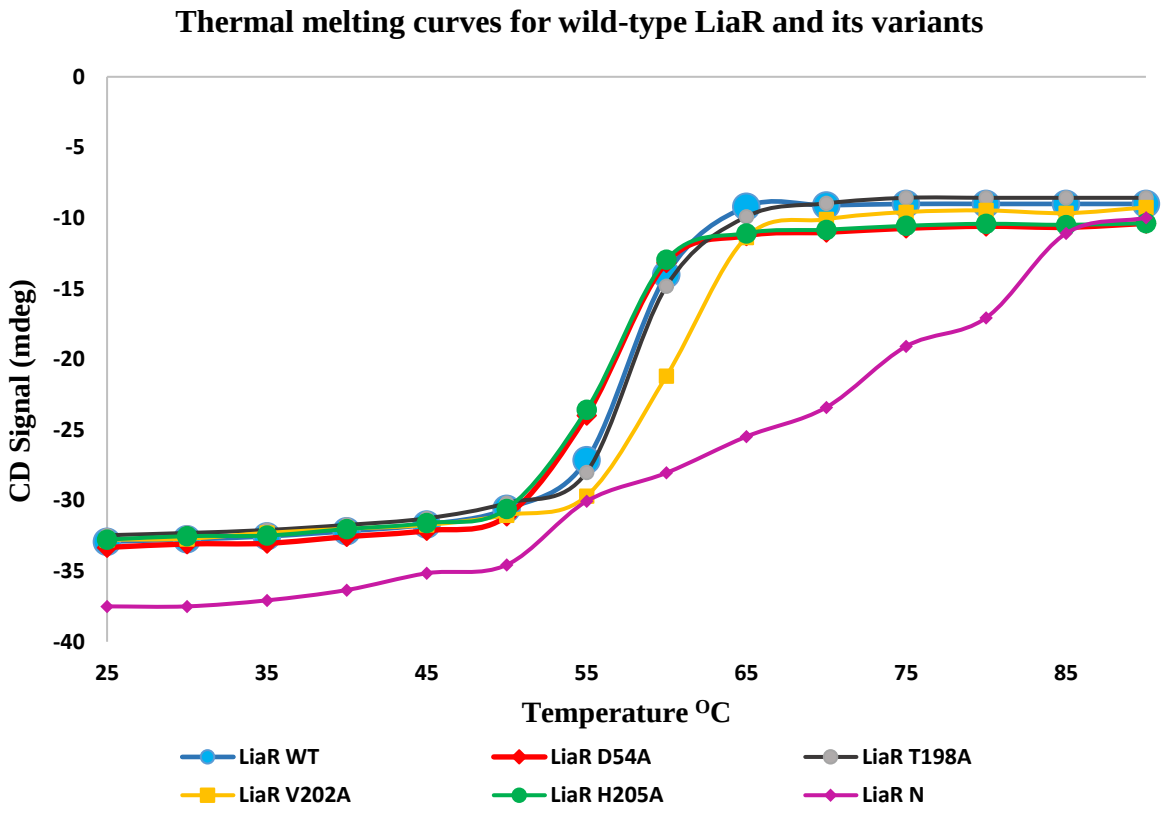

Figure 2.1.7 Thermal melting curve for LiaR and its variants (Data shown from Le, 2017 and used with permission)

Thermal melting curves of wild-type full-length LiaR, N-terminal LiaR and mutants (10 µM) acquired by monitoring the change in ellipticity at 222 nM by ramping the temperature from 25 °C to 90 °C at a rate of 5 °C/min in equilibration buffer, pH 7.0

3.3 *In vitro* Autophosphorylation of GST-LiaS and LiaS H159A

Studies of several HKs have demonstrated that autophosphorylation is involved in the regulation of catalytic activity and signaling *in vivo*. Autophosphorylation of GST-LiaS in the presence of [γ - 32P]-ATP at room temperature, indicated a progressive increase in phosphorylation with maximal saturation at 60 min. The rate of phosphorylation of GST-LiaS was determined for a concentration of ATP ranging from 5 mM to 250 mM **(Figure 2.1.10)**. Km and Vmax values were

calculated using the GraFit software (K_m of 3.3186 ± 0.7006 µM and Vmax of 0.0667 ± 0.0032 s^{-1}) for ATP concentrations ranging from 5 µM to 25 µM and were based on the Mechalis Menten equation **(Figure 2.1.9)**. Such a low Km value would mean that the *in vivo* ATP requirements for the system are rather low. As expected the mutation of the phosphohistidine residue at position 159 abolished the kinase activity of the protein **(Figure 2.1.10).** These results are indicative of the key role played by the histidine residue in autophosphoryation and hence making it one of plausible the drug target sites

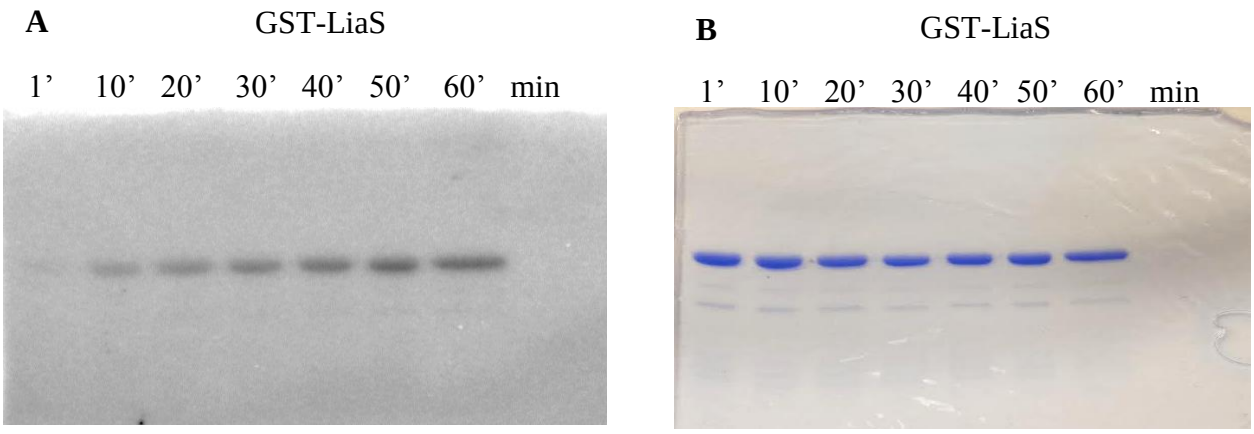

Figure 2.1.8 *In vitro* autophosphorylation of GST-LiaS using radioactive ATP

A: Autophosphorylation of 5 µM GST-LiaS in the presence of [γ - 32P]-ATP indicates a progressive increase in phosphorylation saturating over a span of 60 min. 10 µl samples were quenched with 5X SDS dye every 10 min **B**: GST-LiaS mixed with [γ - 32P]-ATP. 10 µl samples were quenched with 5X SDS dye every 10 min and loaded onto a 12.5% SDS-PAGE, stained with Coomassie Blue, to ensure equal loading.

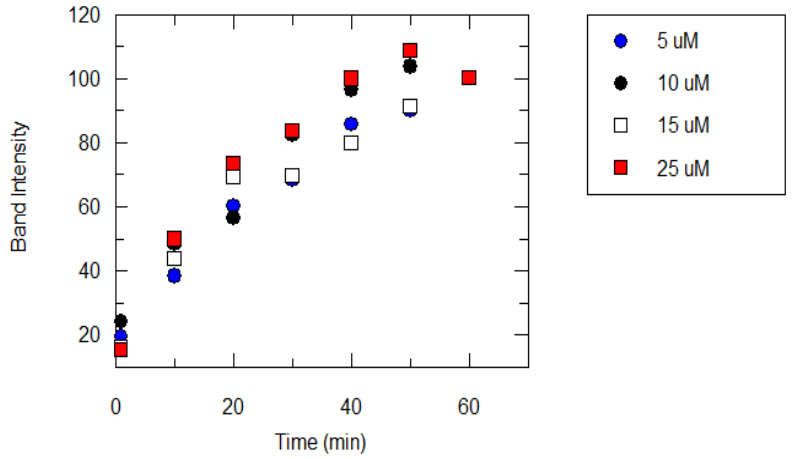

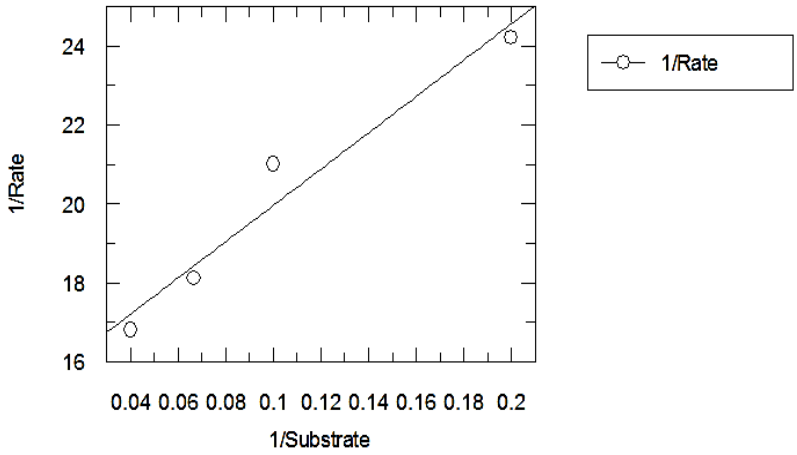

Equation: Enzyme Kinetics

Parameter	Value	Std. Error
Vmax	0.0667	0.0032
Km	3.3186	0.7006

Figure 2.1.9 Band intensity of phosphorylated GST-LiaS quantified using ImageJ and plotted against time. The data were fitted using GraFit software to pseudo first order equation to calculate rate constant.

Progress curve of autophosphorylation reaction. The quantified band intensities of phosphorylation were plotted against time and the standard deviation represented as errors is averaged over three different trials.

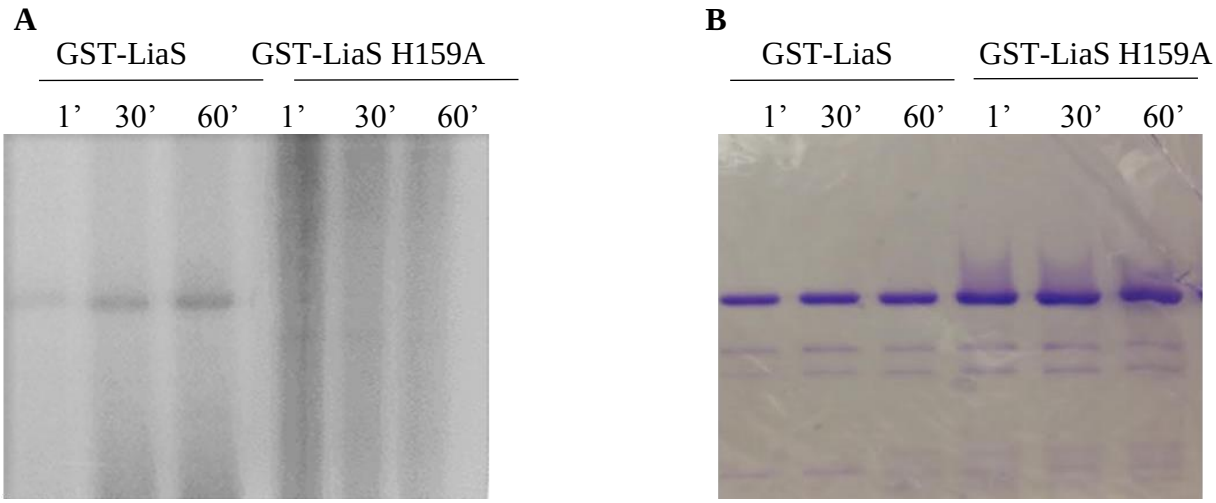

Figure 2.1.10 *In vitro* autophosphorylation of GST-LiaS H159A using radioactive ATP

A: Autophosphorylation of 5 µM wild-type GST-LiaS in the presence of [γ - 32P]-ATP. GST-LiaS H159A demonstrates lack of phosphorylation over a span of 60 min (phosphor image of 12.5% SDS-PAGE). **B**: 12.5% SDS-PAGE from same trial, stained with Coomassie Blue displaying equal protein loading.

3.4 Phosphotransfer reaction from GST LiaS to WT-LiaR and its variants (LiaR D54A and LiaR^{N})

In vitro phosphotransfer occurs when a radioactively labelled group is transferred from the HK to the RR. Having established the autokinase activity of GST-LiaS, its ability to transfer phosphoryl groups inter molecularly to its cognate RR, LiaR was examined. **Figure 2.1.11** demonstrates that GST-LiaS is capable of transferring a phosphoryl group to LiaR. It was observed that almost 50% of the phosphate associated with GST-LiaS was transferred to the RR within the first 30 secs. The estimated pseudo first order rate constant for the phosphotransfer reaction was 0.0609 ± 0.0288 s^{-1}. Past 1 minute, the signal for LiaR begins to fade. This is most likely attributed to the phosphatase

activity displayed by LiaS towards WT-LiaR. Moreover, the rate of dephosphorylation from the phosphotransfer experiments was determined to be 0.1042 ± 0.0060 s^{-1} **Figure 2.1.12**. Because of its ability to phosphorylate and dephosphorylate substrates, LiaS, has a bifunctional role in signal transduction. The relevance of Asp54 as the predicted site of phosphorylation on LiaR was investigated by performing a phosphotransfer reaction between LiaS and LiaR D54A. As illustrated in **Figure 2.1.13**, and as expected, LiaS, was able to successfully phosphorylate WT-LiaR. |On the other hand, mutant form LiaR D54A, demonstrated little if any phosphorylation by LiaS. It is thus evident that the two versions of LiaR are distinctly different as far as their ability to receive a phosphate from LiaS.

The receiver domain of LiaR ($LiaR^N$) was also able to get phosphorylated by LiaS, albeit to a lesser extend than WT-LiaR. Interestingly, the rate of phosphorylation of $LiaR^N$ was much slower than that of full-length LiaR. As seen in **Figure 2.1.14**, only about 30% of the phosphate on LiaS was transferred to the N terminal domain of LiaR, with a calculated phosphorylation rate of 0.0828 ± 0.0325 s^{-1}. Additionally, LiaS does not display any phosphatase activity towards $LiaR^N$, as indicated by a negative rate of dephosphorylation **(Figure 2.1.15)**. These observations with respect to the low phosphorylation and lack of phosphatase activity suggested the role of the C-terminal for complete phosphorylation as well as for a physical interaction between LiaS and the C-terminal to aid in dephosphorylation of LiaR.

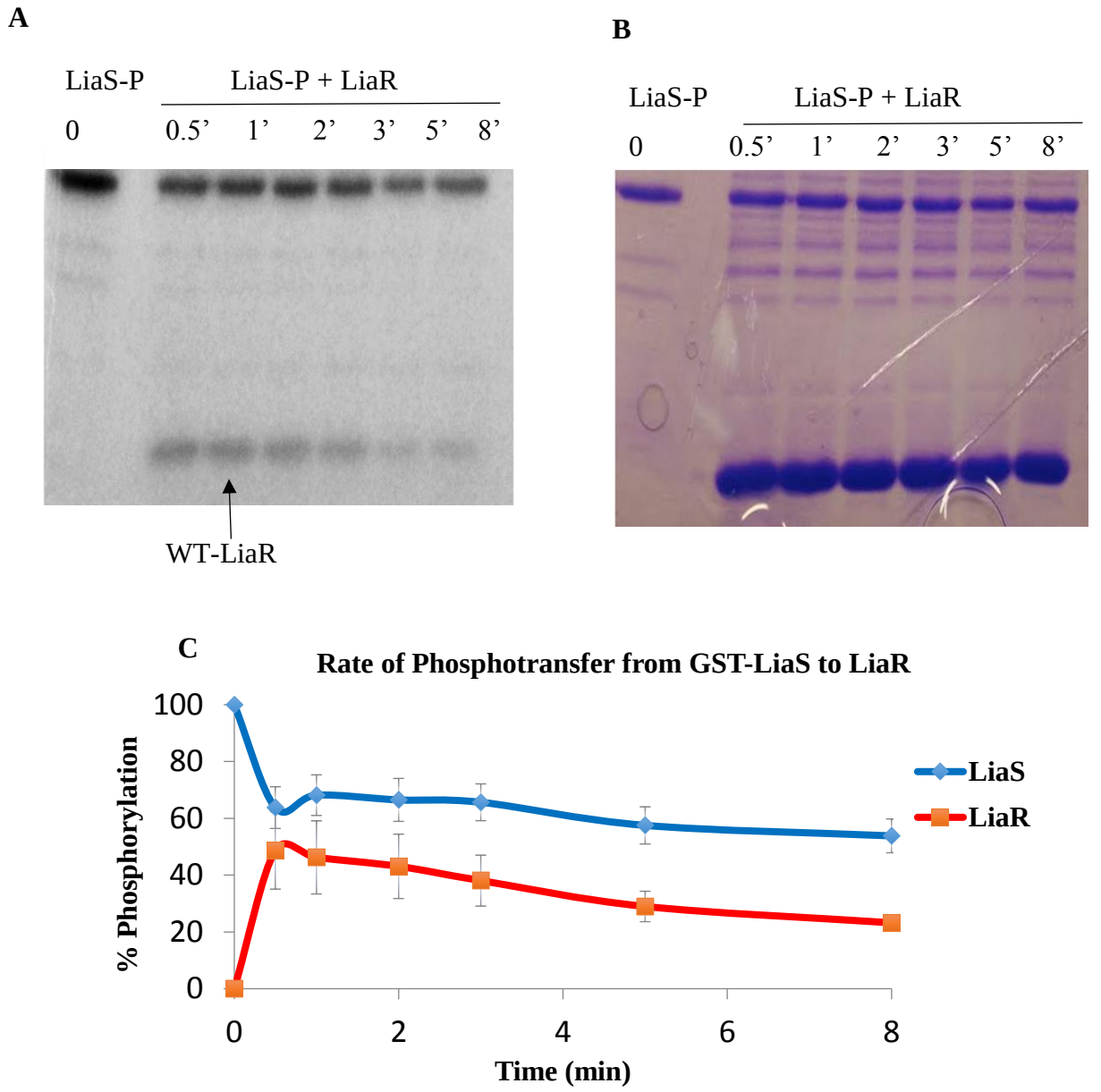

Figure 2.1.11 *In vitro* Phosphotransfer between GST-LiaS and LiaR using radioactive ATP at room temperature

A: 5 µM of [γ - 32P]-ATP phosphorylated LiaS was used as the control. Phosphorylated GST-LiaS was added to LiaR samples in a concentration ratio of 1:5. The samples were quenched with 5X SDS dye at time intervals ranging from 0.5 min to 8 min for the phosphotransfer to occur and was analysed using 15% SDS-PAGE. The gel was exposed to a phosphoscreen for 2 h and scanned with a Typhoon scanner. **B**: Phosphorylated GST- LiaS mixed with LiaR at room temperature. 15% SDS-PAGE gel stained with Coomassie Blue demonstrating loading concentrations **C**: Quantified data using the ImageJ software showing the rate of phosphotransfer.

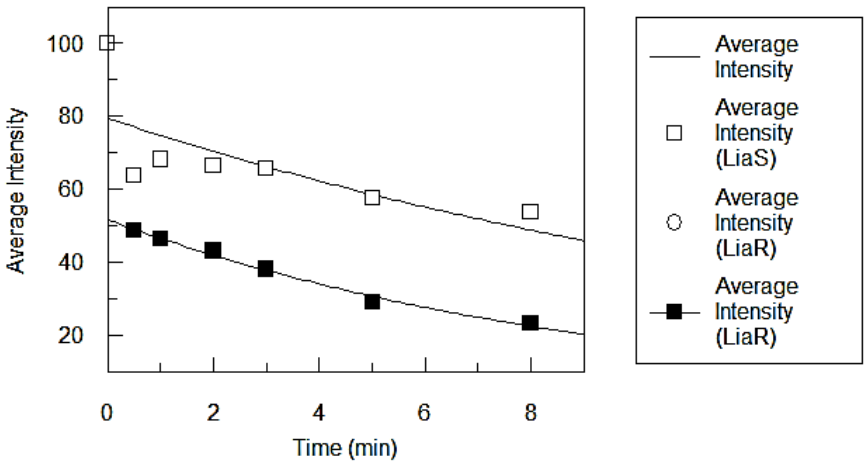

Parameter	Value	Std. Error
rate constant	0.0609	0.0288
proportionality constant	79.4203	6.9527

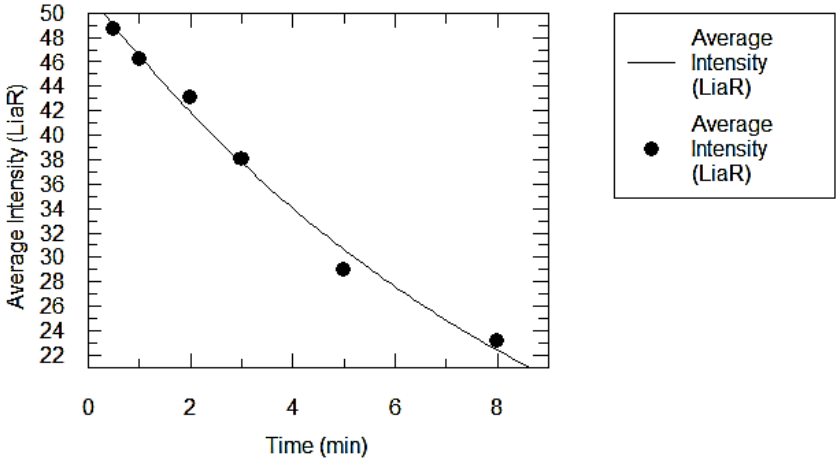

Parameter	Value	Std. Error
rate constant for dephosphorylation	0.1042	0.0060
proportionality parameter	51.6023	0.9082

Figure 2.1.12 Band intensity of phosphorylated LiaR, via phosphotransfer reactions between GST-LiaS and LiaR using radioactive ATP.

Quantified using ImageJ and plotted against time. The data were fitted using GraFit software to pseudo first order equation to calculate rate constant.

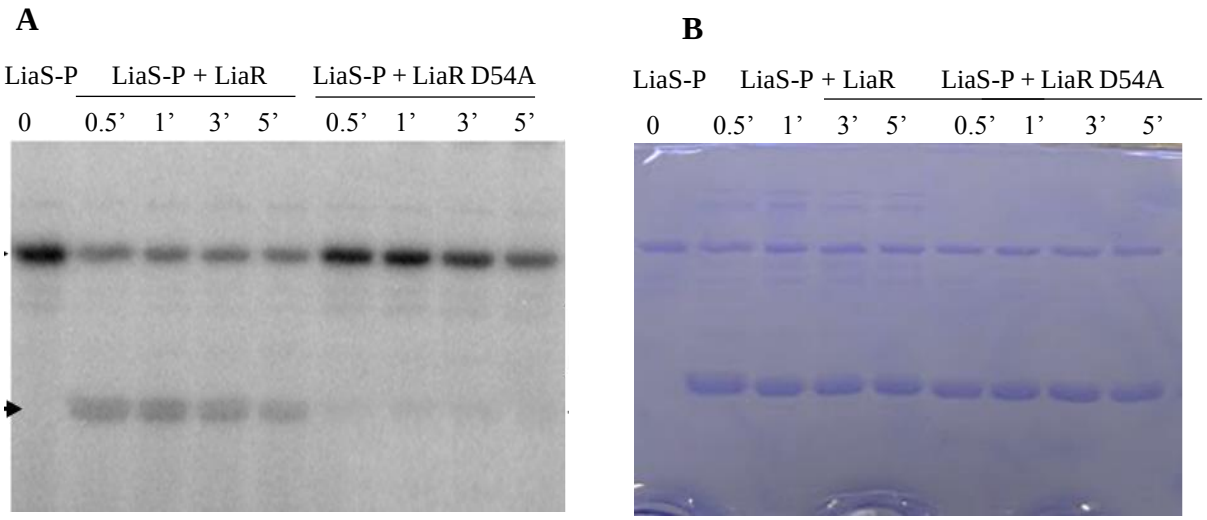

Figure 2.1.13 *In vitro* Phosphotransfer between GST-LiaS and WT-LiaR and LiaR D54A using radioactive ATP at room temperature

A: 5 µM of phosphorylated GST- LiaS was added to WT-LiaR and LiaR D54A samples in a concentration ratio of 1:5. The samples were quenched with 5X SDS dye at time intervals ranging from 0.5 min to 5 min. Samples were analyzed using gel electrophoresis (15% SDS-PAGE gel). The exposed gel shows that mutation of the aspartate residue at position 54 renders the protein incapable of receiving a phosphate group from its cognate histidine kinase, LiaS. **B**: Phosphorylated GST- LiaS mixed with WT and mutant LiaR at room temperature. 15% SDS-PAGE gel, stained with Coomassie Blue, demonstrating loading concentrations.

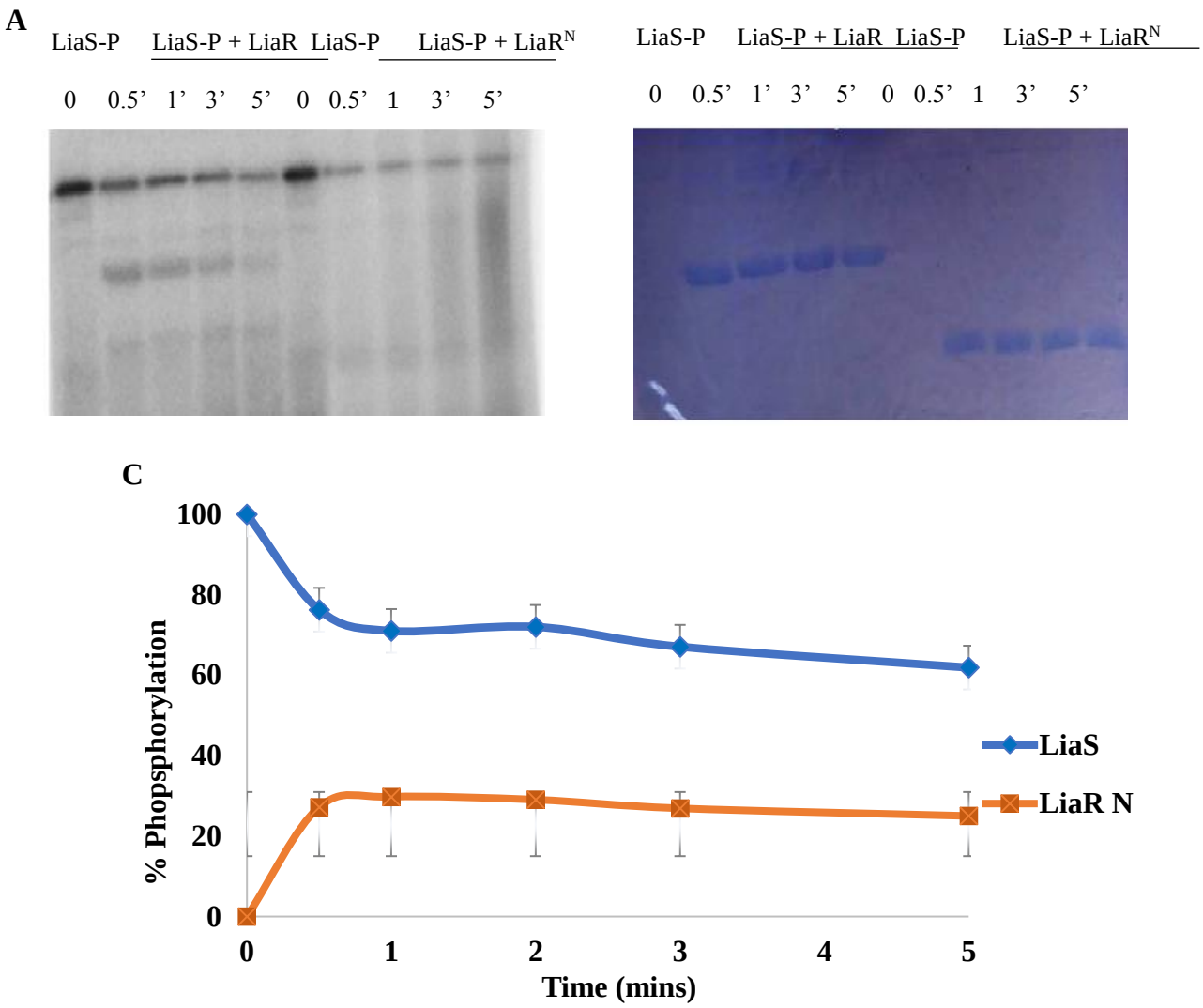

Figure 2.1.14 *In vitro* Phosphotransfer between GST-LiaS and LiaR^N using radioactive ATP at room temperature

A: 5 µM of phosphorylated GST-LiaS serving as the control was added to WT-LiaR and LiaR^N samples in a concentration ratio of 1:5. The samples were quenched with 5X SDS dye at time intervals ranging from 0.5 min to 5 min for the phosphotransfer to occur and were analysed using a 20% SDS-PAGE gel. The gel was exposed to a phosphoscreen for 2 hr and scanned with a Typhoon scanner. **B**: Image of the 20% SDS-PAGE gel, stained with Coomassie Blue, displaying loading concentrations. **C**: Quantified data using the ImageJ software displaying a slower rate of phosphotransfer for LiaR^N compared to WT-LiaR.

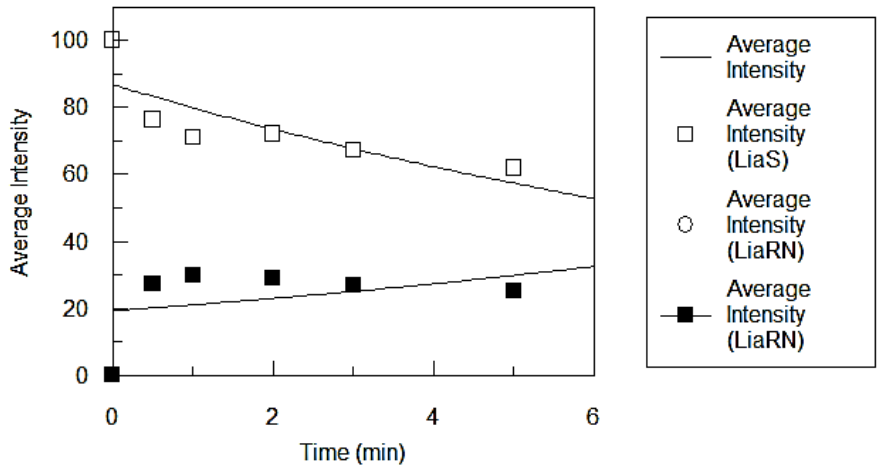

Parameter	Value	Std. Error
rate constant	0.0828	0.0325
proportionality constant	86.6791	5.9637

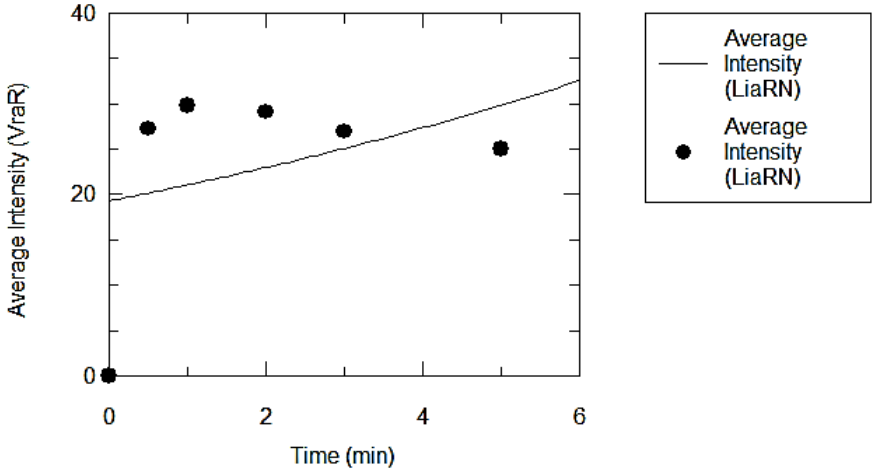

Parameter	Value	Std. Error
rate constant for dephosphorylation	-0.0871	0.1181
proportionality parameter	19.2799	6.8245

Figure 2.1.15 Band intensity of phosphorylated LiaR, via phosphotransfer reactions between GST-LiaS and LiaR^N using radioactive ATP. Quantified using ImageJ and plotted against time. The data were fitted using GraFit software to pseudo first order equation to calculate rate constant.

3.5 Determination of effect of phosphorylation of LiaR and its variants upon by a small phosphor-donor.

Homologous RR from other species when subjected to phosphorylation with acetyl phosphate are said to undergo a change from monomeric to a dimeric species**.** LiaR and its variants were all examined using various techniques such as Native PAGE, Phos-tag ^{TM} gel, Mass spectrometry and Analytical ultracentrifugation for $LiaR^{N}$ in particular to help with studying the importance of the C-terminal for phosphorylation and also the conformational implications.

3.5.1 Oligomeric structure changes of LiaR and its variants following phosphorylation as revealed by Native-PAGE

Addition of 50 mM lithium potassium acetyl phosphate (37 °C for 1 hr) to LiaR resulted in phosphorylation.

The use of Native-PAGE ensured that the protein would not denature as the gels lack SDS.

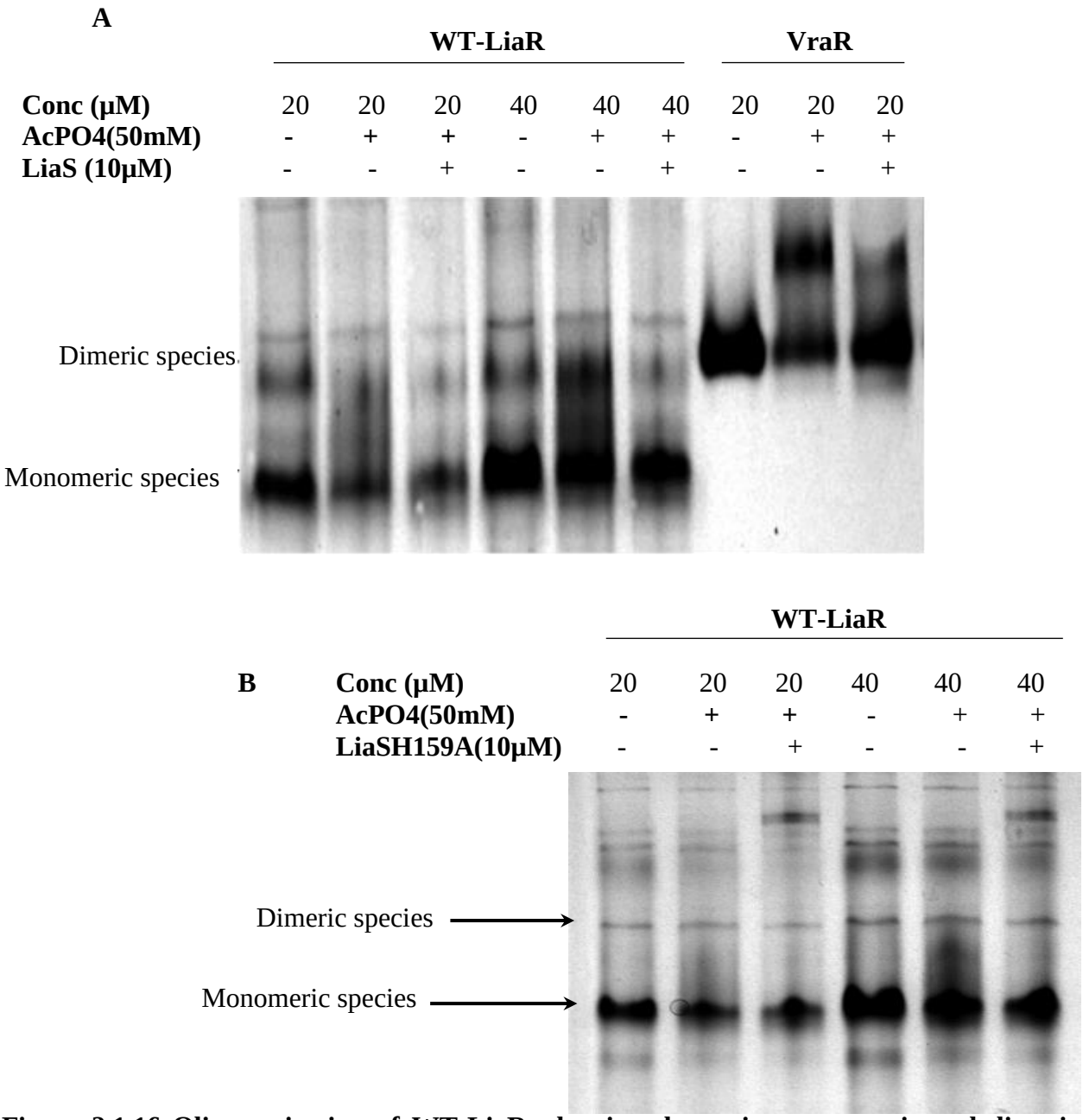

Figure 2.1.16 Oligomerization of WT-LiaR, showing the native monomeric and dimeric states and an equilibrium shift upon phosphorylation with the small phospho-donor, acetyl phosphate

A: A 10% Native-PAGE gel used to analyse the oligomeric properties of LiaR with VraR serving as a positive control. Samples were phosphorylated by acetyl phosphate (37 °C for 1 hr) and 10 µM WT- LiaS was subsequently added to phosphorylated samples and incubated for an additional 10 min to investigate its phosphatase activity. **B:** A 10% Native - PAGE gel was used for the analysis of the oligomeric properties of LiaR in its native and phosphorylated state. 10 µM LiaSH159A was added to phosphorylated samples and incubated for an additional 10 min in order to detect its phosphatase activity.

The results obtained from Native-PAGE indicated that WT-LiaR exists primarily as a monomeric and dimeric mixture. Following phosphorylation of LiaR, a shift in the equilibrium between the dimeric and monomeric state was observed with the monomeric state being the predominant form (quantified using Image J software version 1.4s) **(Figure 2.1.16)**.

In order to gain additional insight into the structural determinants responsible for the assembly of the dimerization interface, 3 distinct mutants of WT-LiaR were constructed (LiaR T198A, LiaR V202A and LiaR H205A). These mutants behave similarly to WT-LiaR in their native state as they appear to exist as a mixture of monomeric and dimeric species. Following phosphorylation, there appears to be a slight shift in equilibrium between monomeric and dimeric species although this is not clearly visible in the native gels shown in **Figure 2.1.17 A-C**. This is further corroborated by changes observed in the CD spectra following phosphorylation **Table 1**. Finally, as seen in **Figure 2.1.17 D** the oligomeric state of $LiaR^{N}$ does not change pre or post phosphorylation with the latter existing as a monomeric and dimeric mixture. These results are helped us understand that the dimerization interface was not present on Threonine (198), Valine (202) or Histidine (205). Additionally, the results obtained for N terminals oligomeric state were particularly intriguing, which were followed up with further studies like Mass spectrometry and Analytical ultracentrifugation.

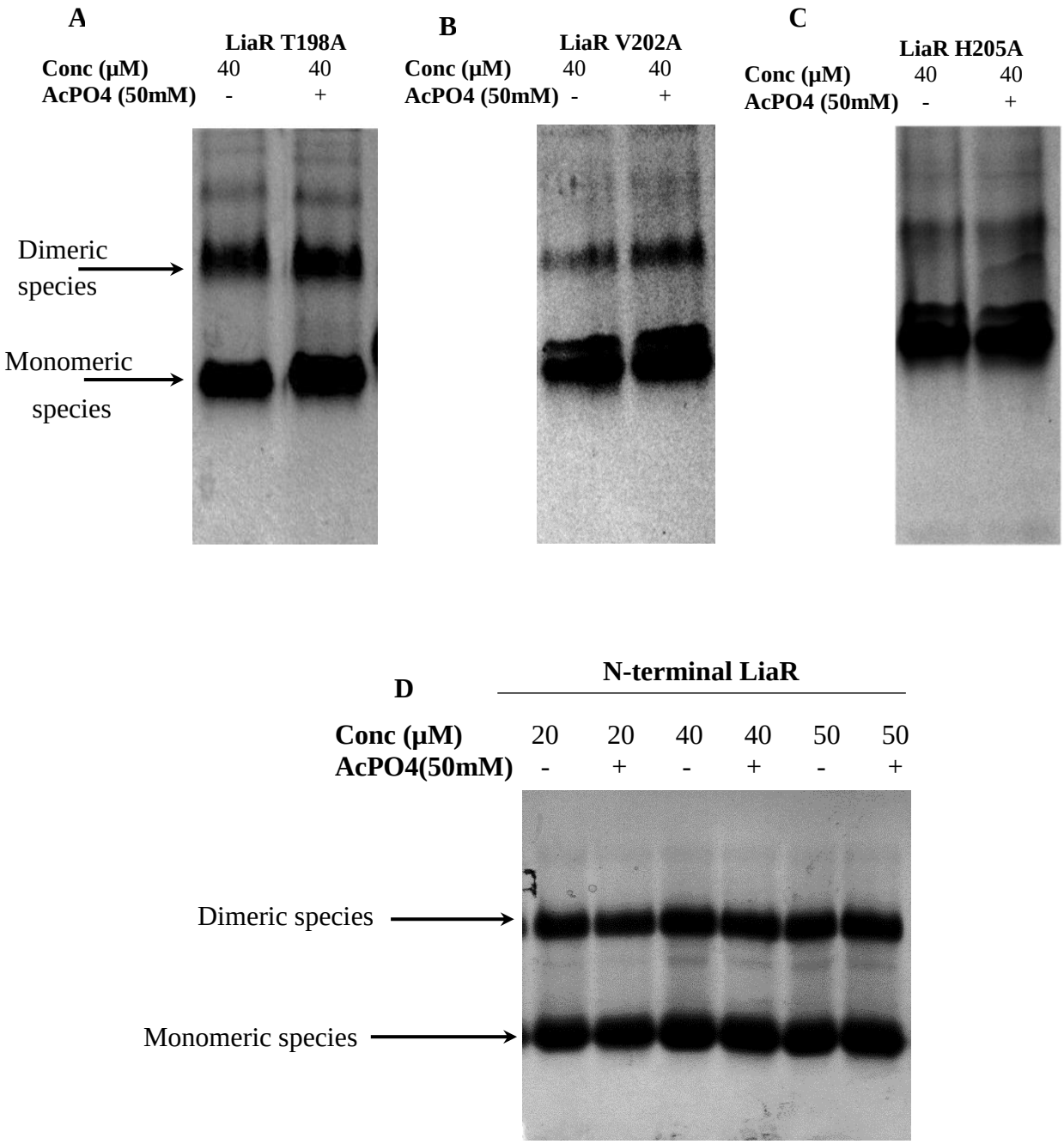

Figure 2.1.17 Oligomerization states of LiaR variants, showing pre and post phosphorylation dimeric and monomeric states {A- C Data shown from Le, 2017 and used with permission}

A, B, C: 10% Native - PAGE gel was used to analyse the oligomeric properties of LiaR T198A, LiaR V202A and LiaR H205A pre and post phosphorylation D:15% Native - PAGE gel was used to analyse the oligomeric properties of $LiaR^N$ with or without the addition of acetyl phosphate.

3.5.2 Analysis of phosphorylation WT-LiaR, LiaR^{N}, LiaR D54A by acetyl phosphate using Phos-tag ™ analysis

Phos-tag SDS-PAGE is used for the separation and detection of large phosphoproteins. In brief, the gel separates phosphorylated species from non-phosphorylated species based on the principle that the phosphorylated species migrate slower due to charge interactions between the negatively charged $PO4^{-}$ and the positively charged Mn2+ ions chelated on the Phos-tag chemical (Kinoshita, et al;, 2006). In this series of experiments, Phos-tag ™ analysis was used to describe the rate of phosphorylation of WT-LiaR, LiaR D54A and LiaR^{N} **(Figures 2.1.18 and 2.1.19)**. More than half (53%) of WT-LiaR is phosphorylated within an hour of incubation with acetyl phosphate and the rate constant for the reaction was calculated to be 0.0325 ± 0.0055 s^{-1} **(Figures 2.1.20)**. As expected LiaR D54A was not subject to phosphorylation, indicating a key role for the aspartate residue in the phosphate transfer. Lastly, the rate of phosphorylation of LiaR^{N} was significantly slower when compared to WT-LiaR with the extent of phosphorylation remaining constant from 5 min to 60 min unlike the full-length protein where there is a steady increase seen.

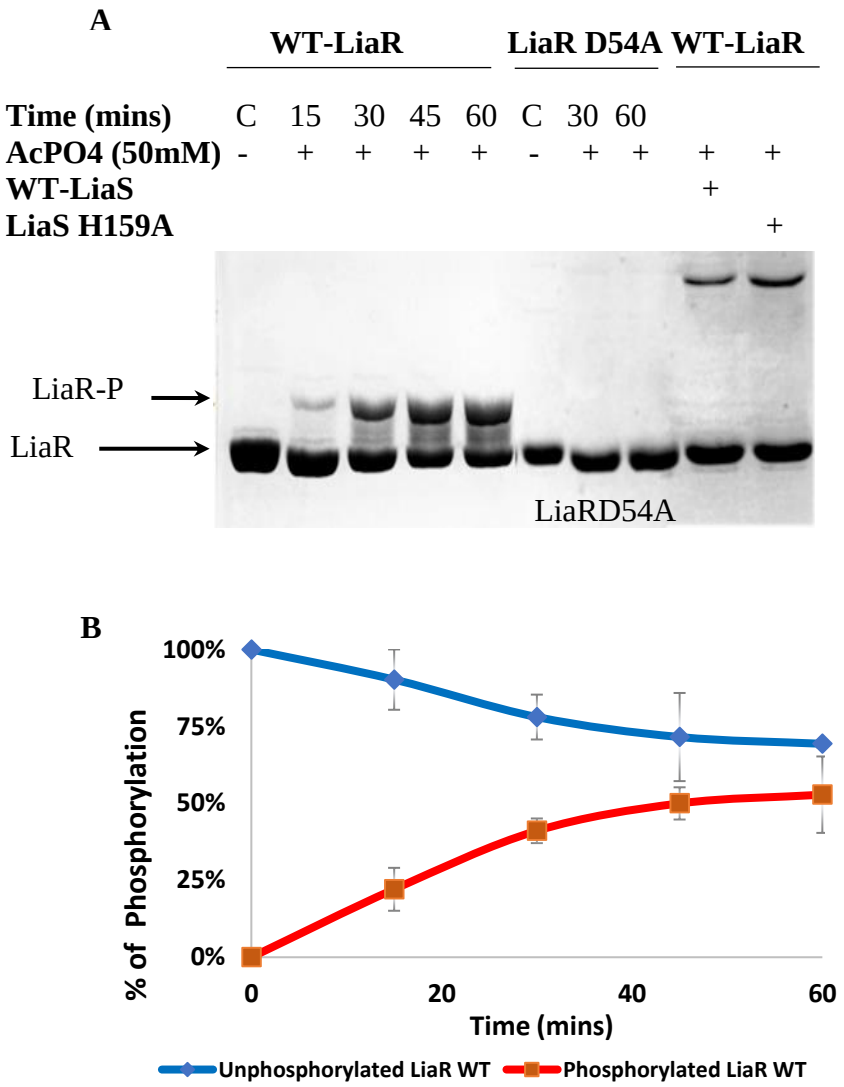

Figure 2.1.18 Phos-tag ™ gel analysis of WT-LiaR and LiaR D54A

A: A 12.5% SDS-PAGE gel was used to analyse WT-LiaR and LiaR D54A samples phosphorylated using acetyl phosphate. Lane C shows the control LiaR samples prior to the addition of acetyl phosphate, while 15, 30, 45 and 60 min display a steady increase in the rate of phosphorylation over time. WT-LiaS and LiaS H159A were used for dephosphorylation WT-LiaR. **B**: Graph displaying quantification of the data obtained using for Phos-tag ™ gel analysis for WT-LiaR.

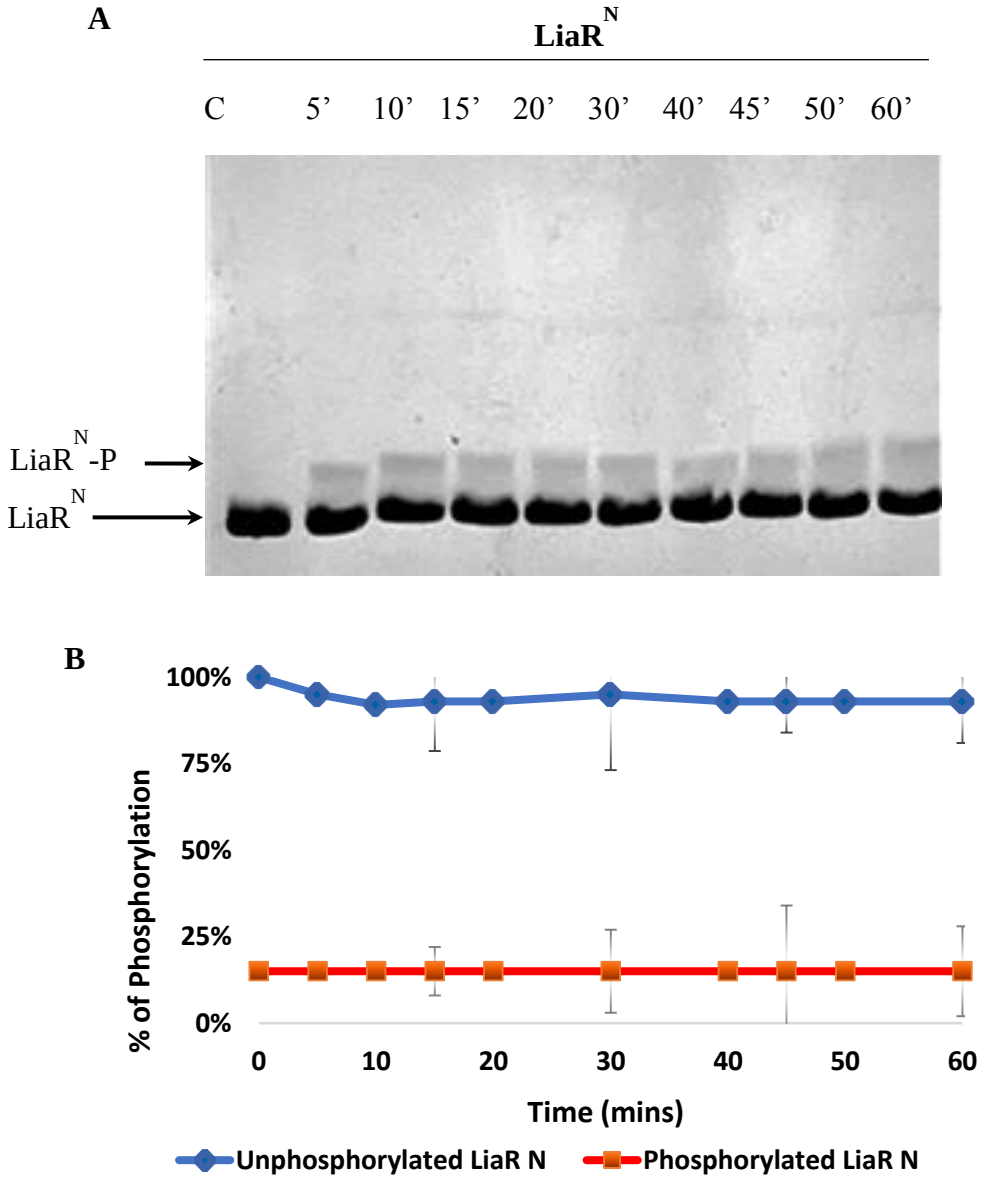

Figure 2.1.19 Phos-tag analysis of LiaR^N

A: An 18% SDS-PAGE gel was used to analyze phosphorylation of LiaR^N. Lane C shows control LiaR samples without acetyl phosphate. **B**: Graph quantifying phosphorylation data for LiaR^N.

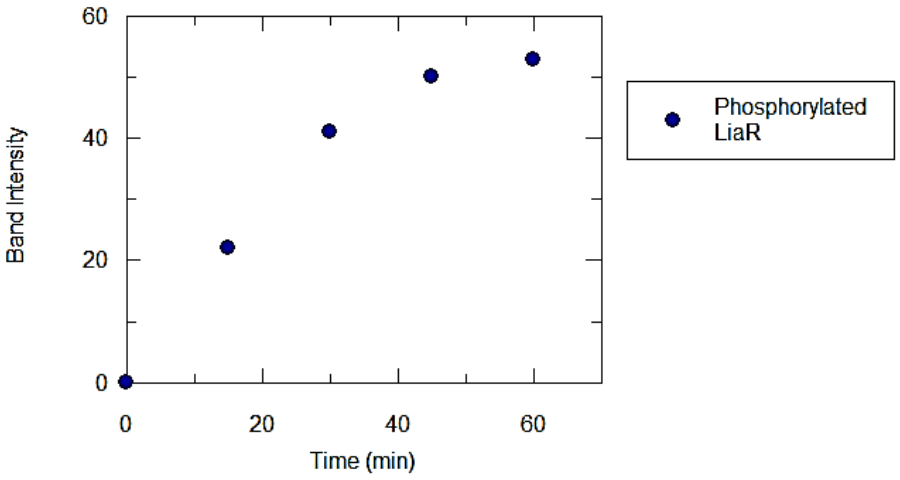

Parameter	Value	Std. Error
rate constant	0.0325	0.0055
proportionality constant	63.2475	5.0822

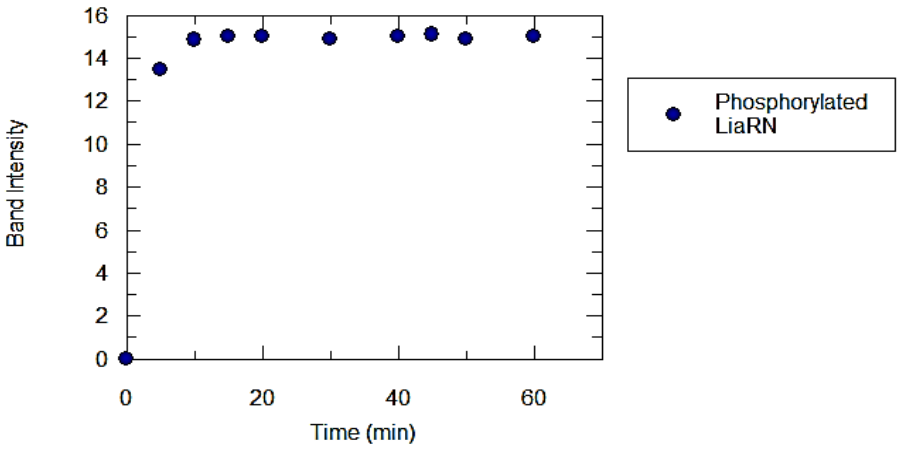

Parameter	Value	Std. Error
rate constant	-0.0079	0.0037
proportionality constant	-35.7531	16.5548

Figure 2.1.20 Band intensity of LiaR and LiaR^{N} phosphorylated by acetyl phosphate were quantified using ImageJ and plotted against time. The data were fitted using GraFit software to pseudo first order equation to calculate rate constant.

3.5.3 Mass spectrometry analysis for $LiaR^N$

Mass spectrometry (MS) allows us to study signaling by allowing rapid identification of phosphorylation sites with precision and sensitivity. Upon phosphorylation, a protein shows an additional mass of 80 Da corresponding to the phosphate group $PO4^-$ (Noah Dephourea, 2013). In order to confirm the ability of $LiaR^N$ to be phosphorylated, we used mass spectrometry. As seen in **Figure 2.1.21** no change in the spectrum was observed following the addition of acetyl phosphate as the molecular weight of the protein remained unchanged (~14028 Da) pre and post the addition of acetyl phosphate. This result was unexpected as the primary role of the receiver domain is to be phosphorylated on the aspartate reside. Two possible justifications can be given for the same, one being incorrect sample preparations, i.e. the centrifugation was breaking the phosphate bond and hence was not detected by the machine. The second reason being a detection limit which makes the low rate of phosphorylation difficult to be caught by the machine. Thus showing negative results.

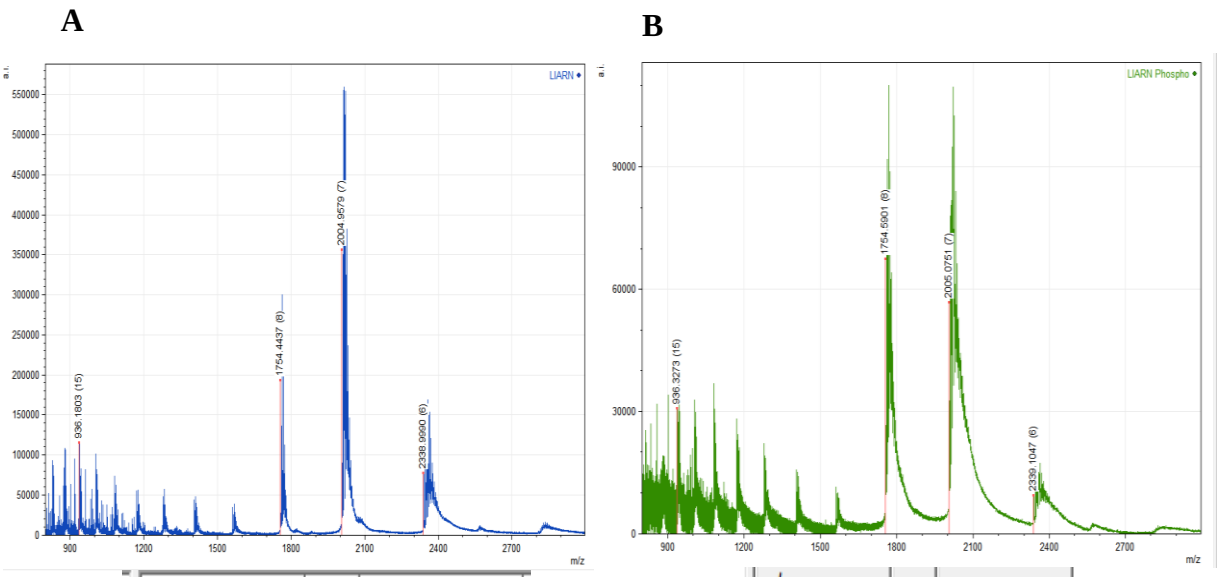

m/z	z	mass
936.1803	15	14027.5954
1754.4437	8	14027.4914
2004.9579	7	14027.6544
2338.9990	6	14027.9503

m/z	z	mass
936.3273	15	14029.8004
1754.5901	8	14028.6626
2005.0751	7	14028.4748
2339.1047	6	14028.5845

Figure 2.1.21 Mass Spectrometry studies for LiaR^N for assessment of phosphorylation

LiaR^N was phosphorylated using acetyl phosphate and then subjected to mass spectrometry for molecular weight assessment. There were no quantifiable changes in the weight for unphosphorylated **A** and phosphorylated **B** sample seen in the spectra. Here m stands for mass and m/z signifies the mass to charge ratio.

3.5.4 Analytical ultracentrifugation studies for LiaR^N

Analytical ultracentrifugation (AUC) permits real-time observation of sedimentation behavior of proteins. Information from the shape of the sedimentation profiles permits the identification and determination of the equilibrium between different oligomeric states. AUC sedimentation studies were conducted in the Department of Biochemistry at the University of Toronto.

AUC experiments for 0.25 mg/ml, 0.50 mg/ml and 1 mg/ml of LiaR^N indicated that LiaR^N the monomer-dimer model was fit for LiaR^N. 1.1:1 was the ratio attained after fixing the molecular

weight (MW) to the theoretical MW of the monomer, and the deduced association constant Ka was 0.074 μM **(Figure 2.1.22)**.

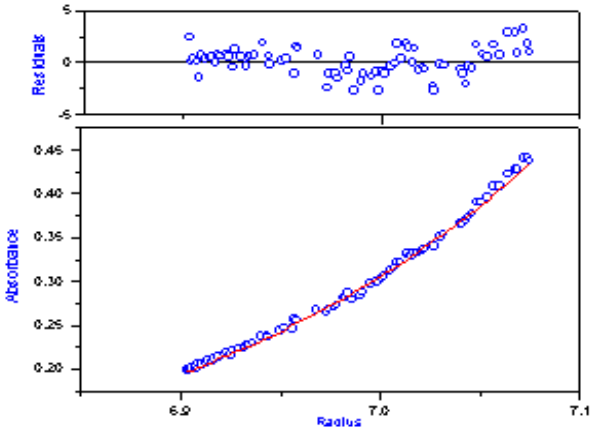

Model	Monomer-Dimer
Ka	0.074
Variance	6.47

Figure 2.1.22 Analytical ultracentrifugation run of LiaR^N samples

Fitting of the absorbance values at 280 nm against radius of the protein (bottom panel) and the plot of the residuals (top panel). Experimental data were obtained at 0.25 mg/ml, 0.5 mg/ml and 1 mg/ml LiaR^N sample. The obtained data was found to be fit for a monomer-dimer model.

3.6 DNA binding ability of WT-LiaR and its variants

3.6.1 Electrophoretic Mobility shift assay (EMSA)

In order to study the DNA-binding properties of LiaR and its variants, the end-labeled P_{liaSR} DNA fragment was incubated with increasing concentrations of LiaR and its variants. The promoter sequence was determined by studying the primer extension analysis and the full-length sequence provided by Jordan Sina, et al; 2006. The resulting DNA-protein complexes were separated from free DNA on 9% non-denaturing polyacrylamide gels. EMSA experiments conducted using WT-LiaR demonstrated a high binding affinity towards the promoter region of *liaSR*. In addition,

phosphorylation of WT-LiaR had very little impact on its ability to bind to the DNA. The K_D values for phosphorylated and unphosphorylated WT-LiaR samples were 0.3006 ± 0.005 µM and 0.337 ± 0.027 µM respectively **(Figure 2.1.23)**. LiaR D54A was also able to bind to the promoter region of *liaSR* as demonstrated by the K_D values (0.355 ± 0.4242 µM and 0.333 ± 009) pre and post phosphorylation **(Figure 2.1.24)**.

Similar studies were also conducted for the full-length LiaR mutants (LiaR T198A, LiaR V202A and LiaR H205A). All mutants exhibited binding patterns similar to the WT protein under both phosphorylated and unphosphorylated conditions suggesting that the mutations had no effect on the DNA binding ability of the response regulator **(Figure 2.1.25 and 2.1.26)**. This is also apparent by the K_D values calculated for the mutants pre and post phosphorylation (Table 1). These values are also very similar to the ones obtained for the WT protein. This suggested that the mutations had no effect on the proteins ability to bind to the DNA.

Finally, EMSA demonstrated that the effector domain of LiaR ($LiaR^C$) is unable to bind to the promoter region of *liaSR*. Increasing the protein concentration or phosphorylating the protein did not modify its ability to bind to the DNA as seen in **Figure 2.1.27**.

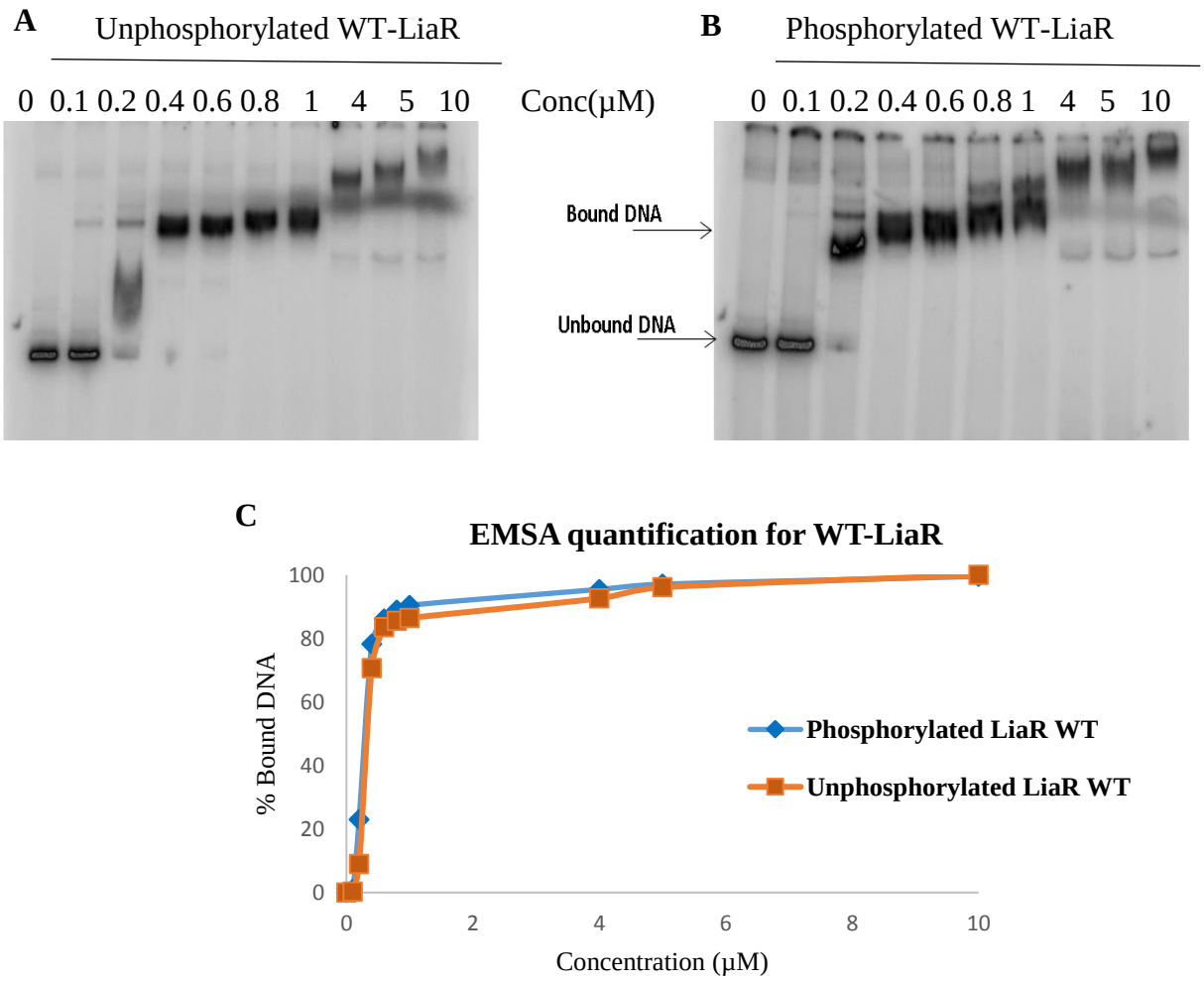

Figure 2.1.23 DNA binding affinity of WT-LiaR for the *liaSR* promoter

A: DNA binding affinity of WT-LiaR to the *liaSR* promoter under unphosphorylated conditions. **B:** DNA binding affinity of WT-LiaR-P the *liaSR* promoter post phosphorylation. **C:** Percentage of bound DNA plotted against protein concentration for both the experimental conditions.

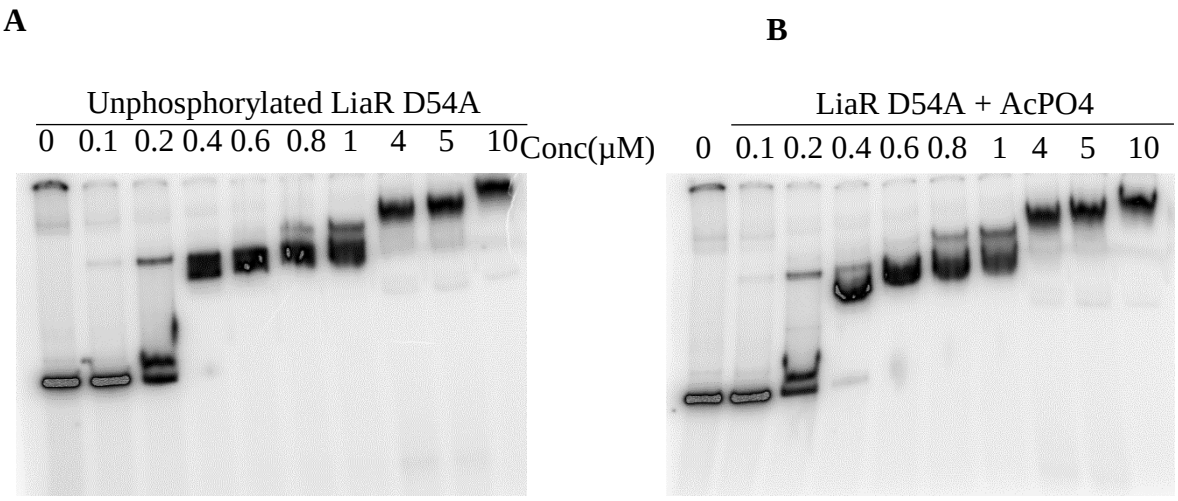

Figure 2.1.24 DNA binding affinity of LiaR D54A on the *liaSR* promoter

A: DNA binding ability of LiaRD54A to the *liaSR* promoter under unphosphorylated conditions.
B: DNA binding ability of LiaRD54A incubated with acetyl phosphate.

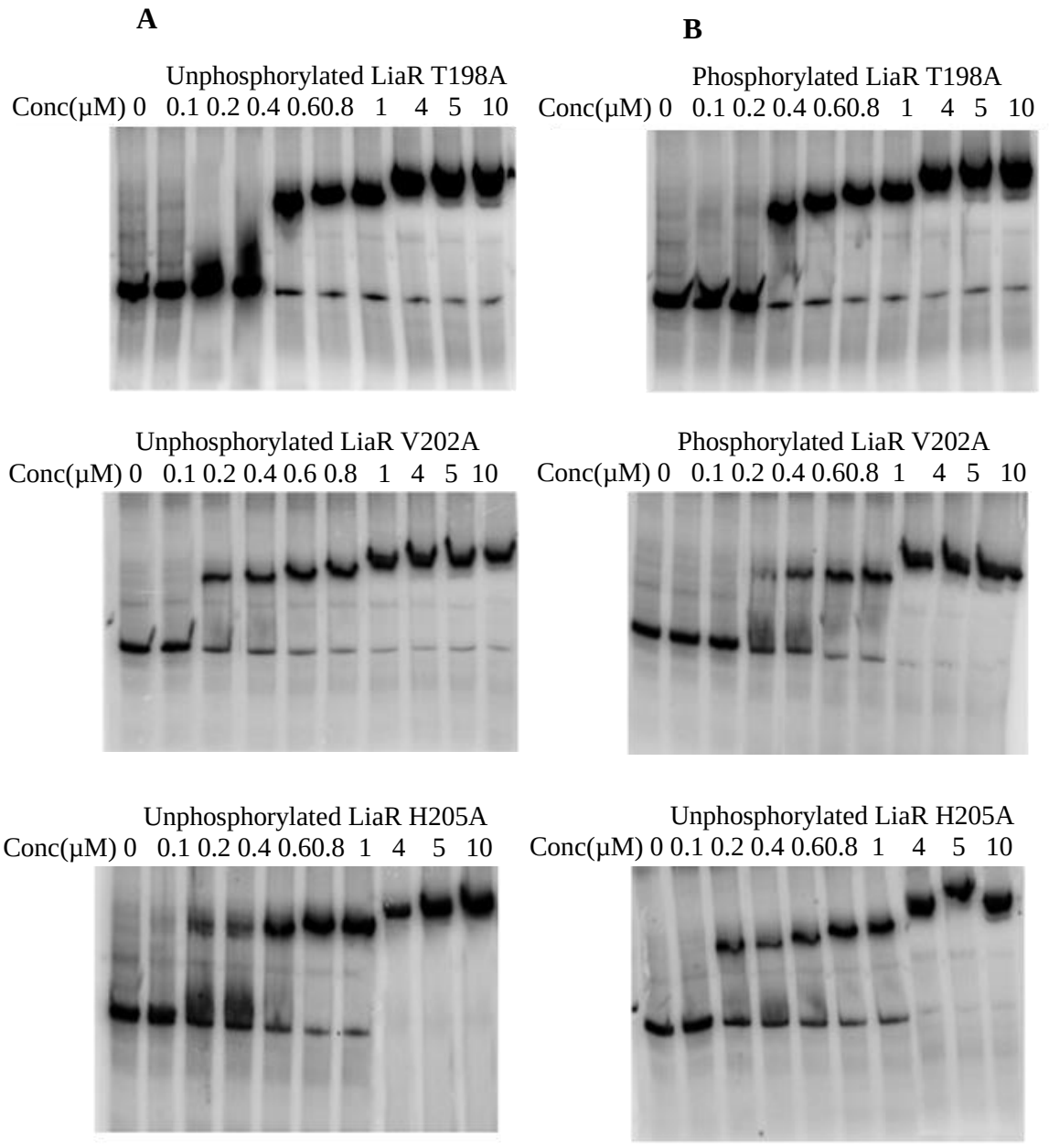

Figure 2.1.25 DNA binding affinity of LiaR mutants (T198A, V202A and H205A) for the *liaSR* promoter

A: DNA binding affinity of LiaR T198A, LiaR V202A and LiaR H205A to the *liaSR* promoter under unphosphorylated conditions. **B:** DNA binding ability of LiaR T198A, LiaR V202A and LiaR H205A to the *liaSR* promoter following phosphorylation.

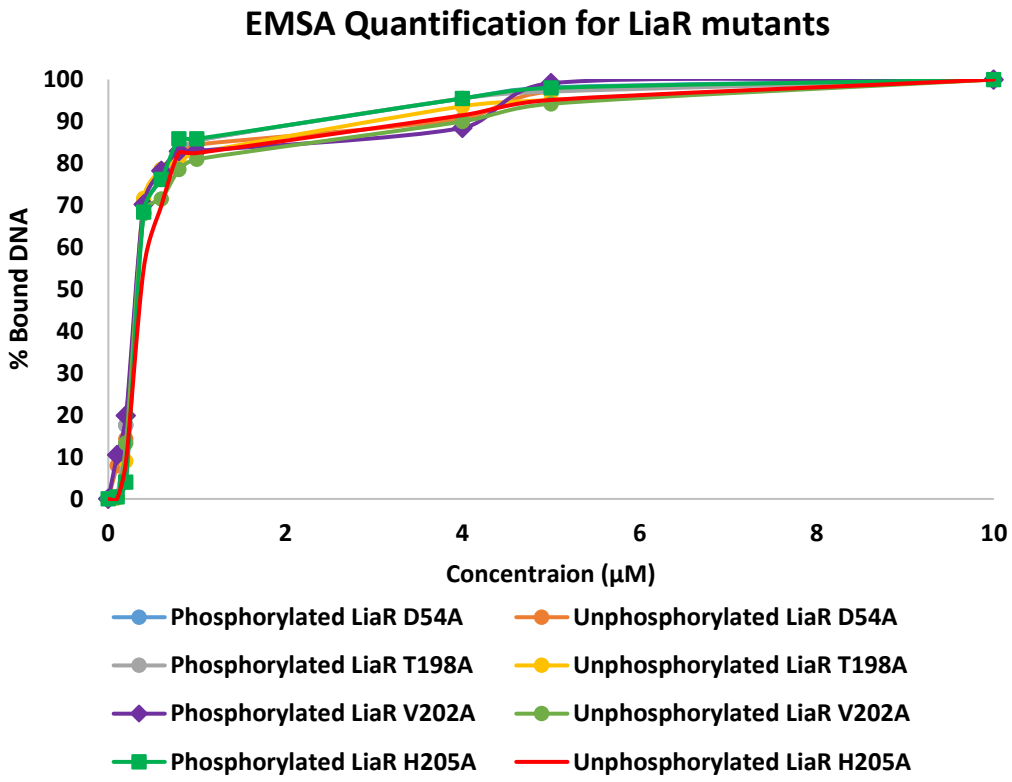

Figure 2.1.26 EMSA quantification of the binding affinity of LiaR mutants towards the *liaSR* promoter

The affinity of LiaR mutants (LiaR D54A, LiaR T198A, LiaR V202A and LiaR H205A) towards the promoter. The percentage of bound DNA pre and post phosphorylation was plotted against the protein concentration.

Table 2: K_D values determined for WT-LiaR and its variants

Protein	Unphosphorylated	Phosphorylated
WT-LiaR	0.3006 ± 0.0050	0.3370 ± 0.7220
LiaR D54A	0.3550 ± 0.4242	0.3330 ± 0090
LiaR T198A	0.3669 ± 0.456	0.3733 ± 0.2781
LiaR V202A	0.4001 ± 0.9121	0.3788 ± 0.576
LiaR H205A	0.4220 ± 0.1000	0.4169 ± 0.016

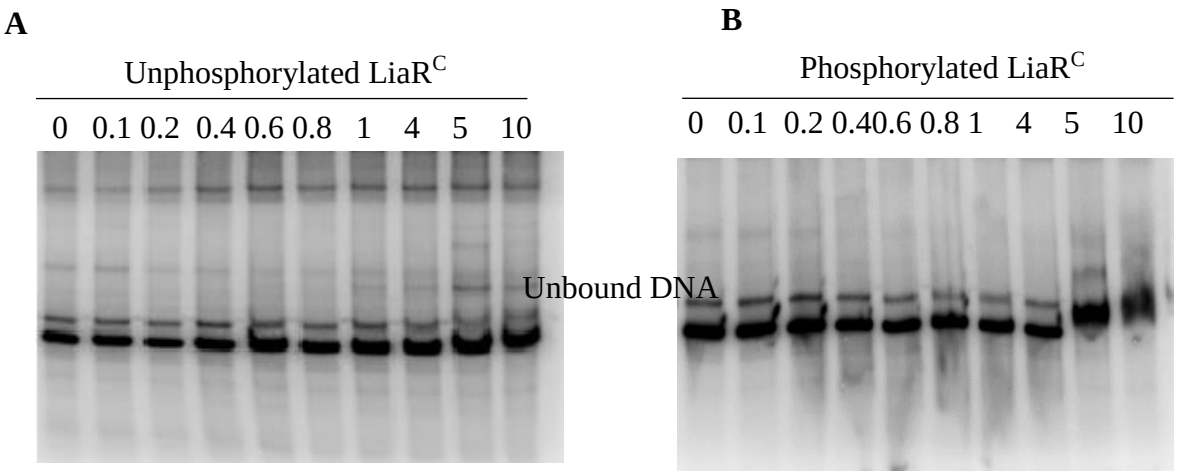

Figure 2.1.27 DNA binding of LiaR^C to the *liaSR* promoter

A: Unphosphorylated LiaR^C **B:** Phosphorylated LiaR^C. LiaR^C is unable to bind to the promoter of *liaSR* pre or post phosphorylation at varying concentrations.

3.6.2 DNase-I footprinting analysis

Having established that LiaR is able to bind to the promoter of *liaSR*, the next step was to map in detail the exact nucleotide sequence of the binding site using DNase I footprinting assay. WT-LiaR, LiaRD54A and LiaR^C were used for the assays displayed in **Figure 2.1.28 and 2.1.29**.

Interestingly, in the presence of unphosphorylated WT and LiaR D54A one common region of protection is evident (designated as R1). Remarkably, in addition to the first area of protection (consensus), upon phosphorylation a secondary region of protection is readily observed for WT-LiaR (designated as R2). The absence of the secondary protection site in the mutant protein is indicative of the importance of phosphorylation in inducing structural changes in the protein thus altering DNA binding. As far as LiaR^C is concerned, and as expected, there was no protection observed from DNase I cleavage. The primary site of protection was also lacking, additionally representing the importance of the N-terminus in the instrumental role of LiaR for DNA binding **(Figure 2.1.29)**.

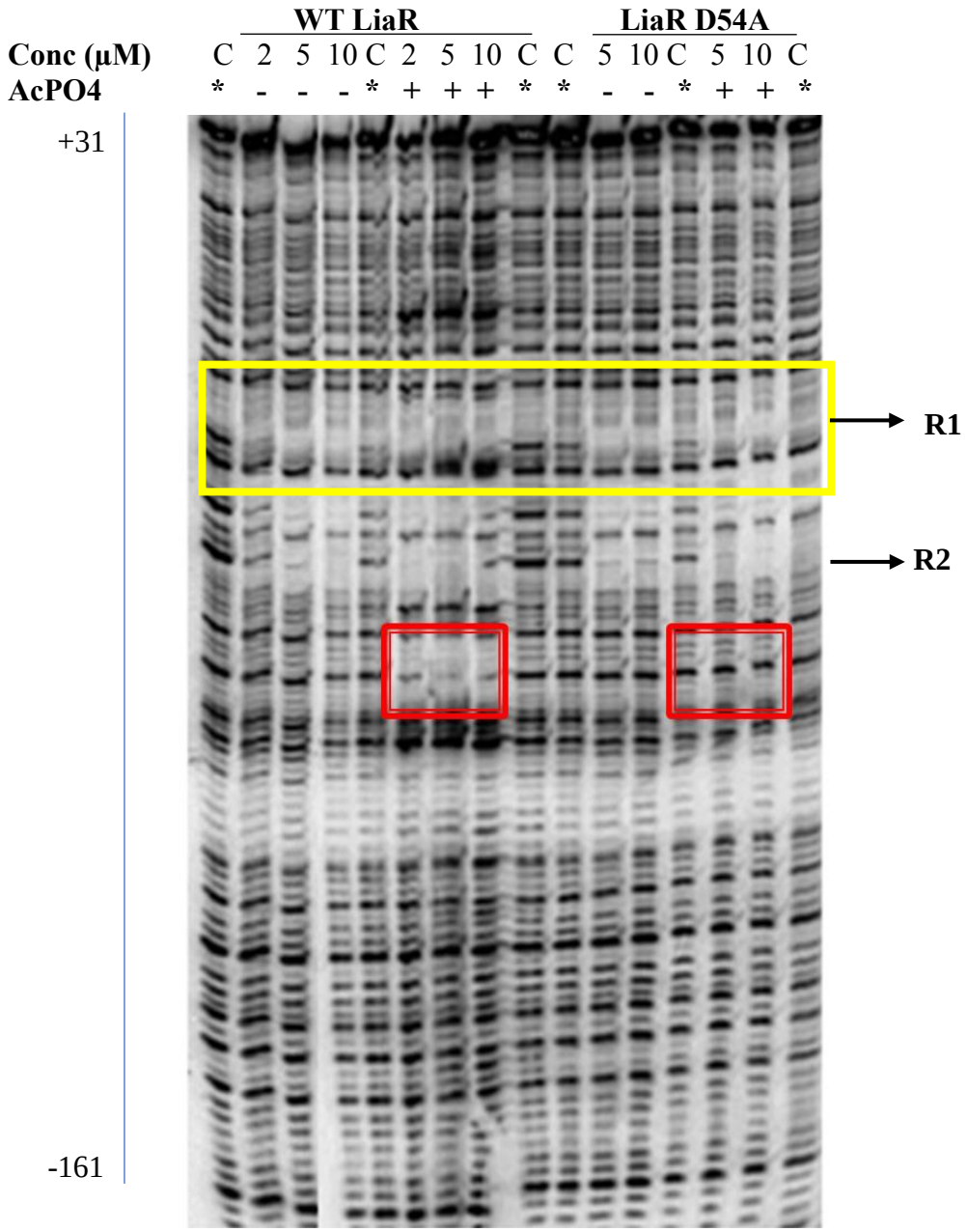

Figure 2.1.28 WT-LiaR and LiaR D54A DNase-I footprinting on the labelled top strand of the *liaSR* promoter

Lanes 1, 5, 9, 10, and 16 represent the controls having no protein. Lanes 2-4 represent different protein concentrations of unphosphorylated WT-LiaR. Lanes 6-8 represent phosphorylated WT-LiaR. Lanes 11-12 represent unphosphorylated LiaR D54A samples in concentrations 5 and 10 µM. Lanes 14-15 represent phosphorylated LiaRD54A. The secondary binding site appears when WT-LiaR is phosphorylated, demonstrating extra protection from DNase I cleavage.

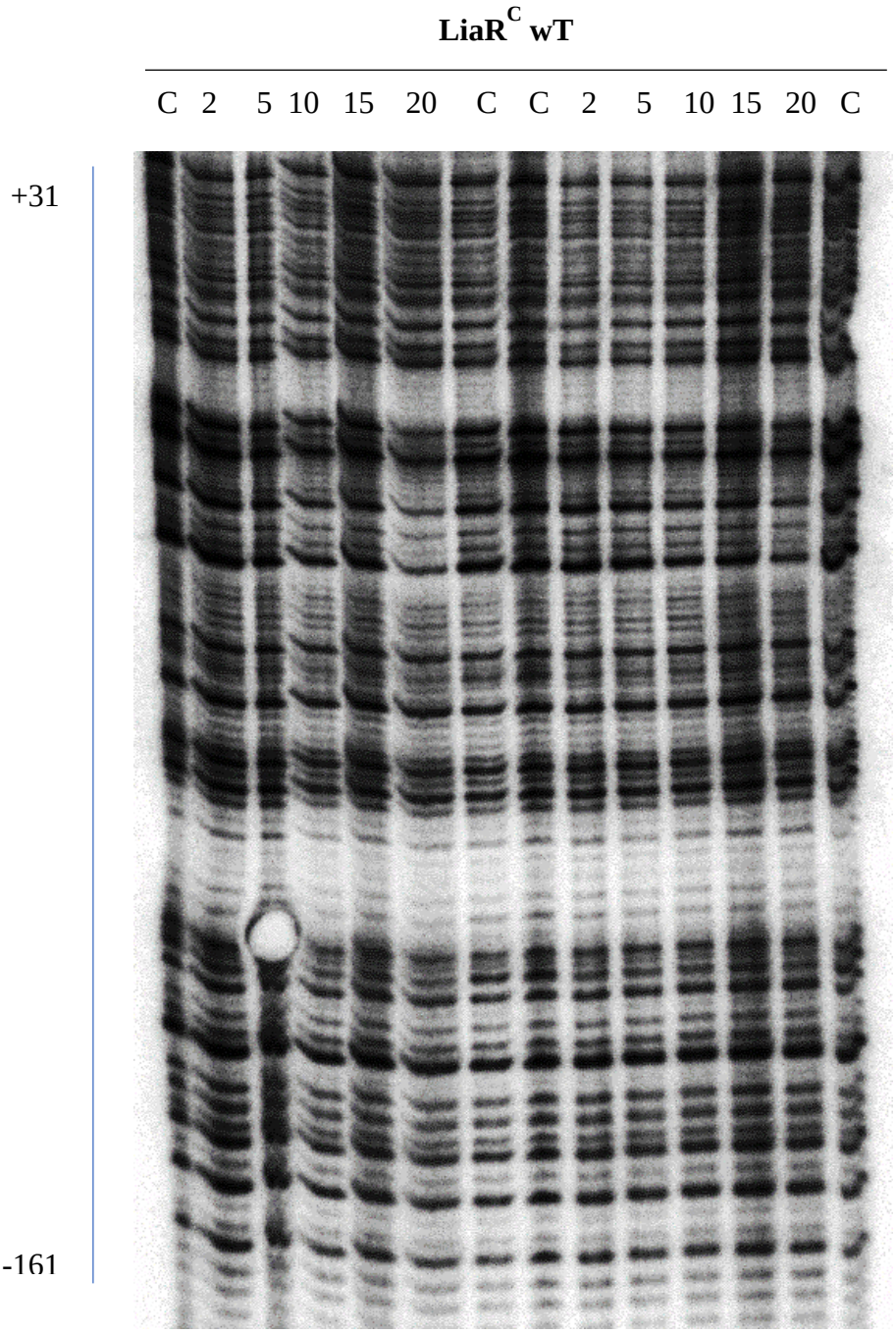

Figure 2.1.29 LiaR^C DNase-I footprinting on labelled top strand of the *liaSR* promoter

Lanes 1, 7, 8 and 13 represent the controls having no protein. Lanes 2-6 represent different concentrations of unphosphorylated LiaR^C. Lanes 9-12 represent varying concentrations of phosphorylated LiaR^C.

3.7 Investigation of cross-communication between the LiaSR and VraSR TCSs

LiaSR from *B. subtilis* and VraSR TCS from *S. aureus* share a high sequence similarity. Considering the high sequence resemblance, one can not help but wonder if the two distinct TCSs are capable of cross talk. In order to address this possibility additional phosphotransfer as well as DNase I footprinting experiments were conducted.

As seen in **Figure 2.1.30**, autophosphorylated GST-VraS (P^{32}) was able to transfer its phosphoryl groups onto LiaR, when the two proteins were co-incubated. LiaR was able to extract 90% of the phosphoryl groups from GST-VraS within a span of less than 30 seconds. In addition, the observed drop in the phosphorylation signal from 2-12 min is indicative of the phosphatase activity that VraS is exhibiting towards its non-cognate response regulator LiaR. The estimated pseudo first order rate constant for the phosphotransfer reaction was calculated to be $3.2129 \pm 0.7339\ s^{-1}$, while the rate of dephosphorylation was established to be $0.3604 \pm 0.0336\ s^{-1}$ by using GraFit software.

On the contrary, when autophosphorylated LiaS was co-incubated with VraR, phosphotransfer was still occurred albeit to a much weaker extent. Only 25% of the phosphoryl groups successfully transferred from LiaS to VraR in the first 30 sec all the way up to 5 min **(Figure 2.1.31)**. Furthermore, LiaS did not exhibit any phosphatase activity towards VraR an observation that is further corroborated by previous Native-PAGE experiments **(Figure 2.1.16 A)**.

Lastly, in order to investigate the ability of LiaR to bind to the promoter of VraSR, DNase I footprinting experiments were conducted. Accordingly, when the P_{vraSR} locus was exposed to DNase I cleavage, LiaR and VraR both demonstrated protection. However, the protection intensities were different for both the proteins **(Figure 2.1.32)**. These results cumulatively help us show how the two component systems can cross talk using signal transduction. Possibly how a

non pathogenic bacterium can learn how to combat antibiotics and gain resistance from a resistant strain. Through this study we can predict that *in vivo* VraS from *S. aureus* can signal LiaR from *B. subtilis*, eventually causing gene expression to aid in cell wall synthesis and perhaps even resistance from antibiotics. Further the DNase 1 footprinting assay also corroborates that LiaR can bind to the *vraSR* gene promoter to carry out further downstream actions in *S. aureus*.

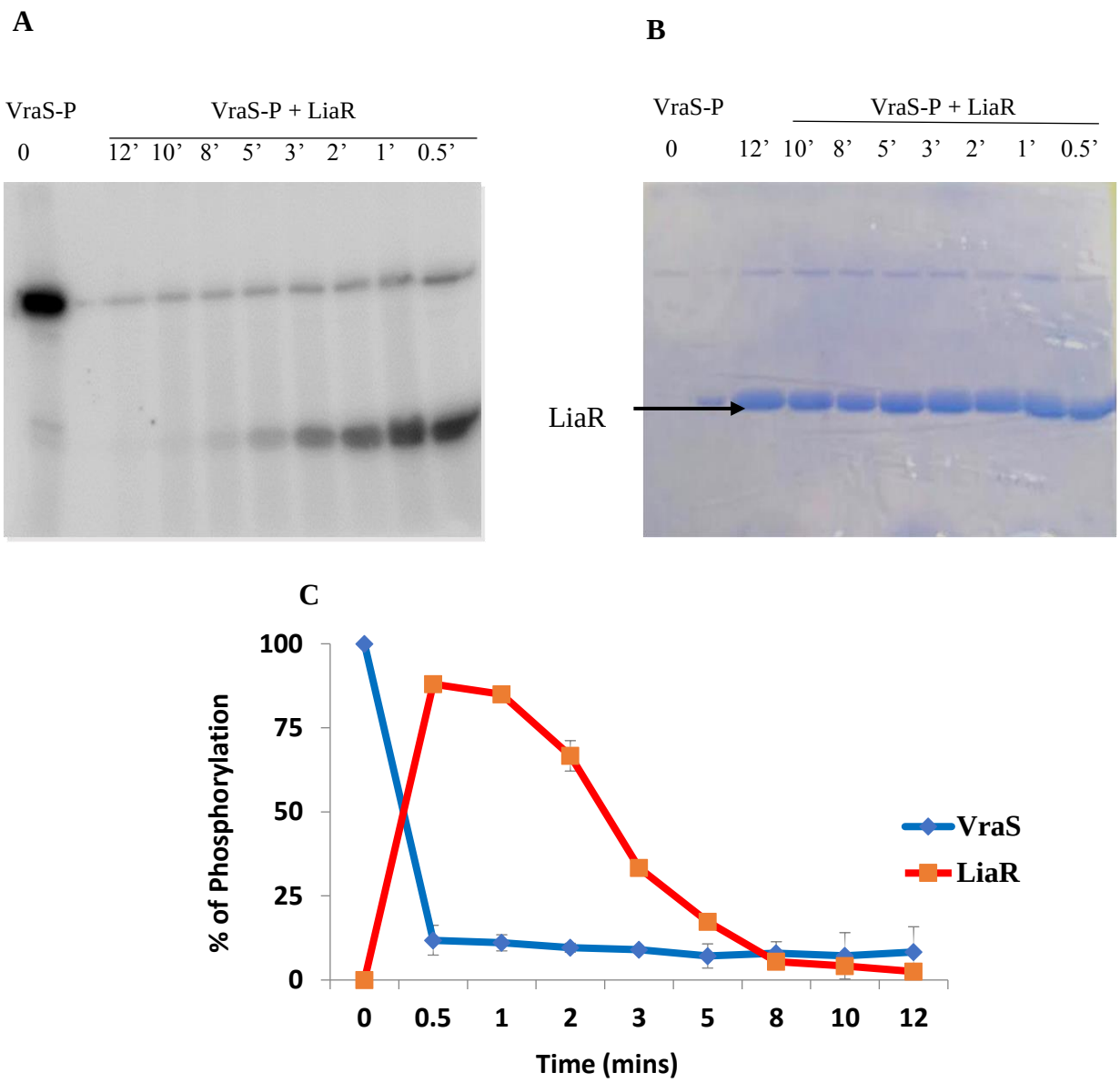

Figure 2.1.30 : *In vitro* Phosphotransfer between GST-VraS and LiaR using radioactive ATP at room temperature

A: 5 µM of [γ - 32P]-ATP phosphorylated VraS was used as the control. Phosphorylated GST-VraS was added to LiaR samples in a concentration ratio of 1:5. The samples were quenched with 5X SDS dye at time intervals ranging from 0.5 min to 12 min for the phosphotransfer to occur and was analysed using 15% SDS-PAGE. The gel was exposed to a phosphoscreen for 2 hr and scanned with a Typhoon scanner. **B**: Phosphorylated GST- VraS mixed with LiaR at room temperature. 15% SDS-PAGE gel stained with Coomassie Blue demonstrating loading concentrations **C**: Quantified data using the ImageJ software showing the rate of phosphotransfer.

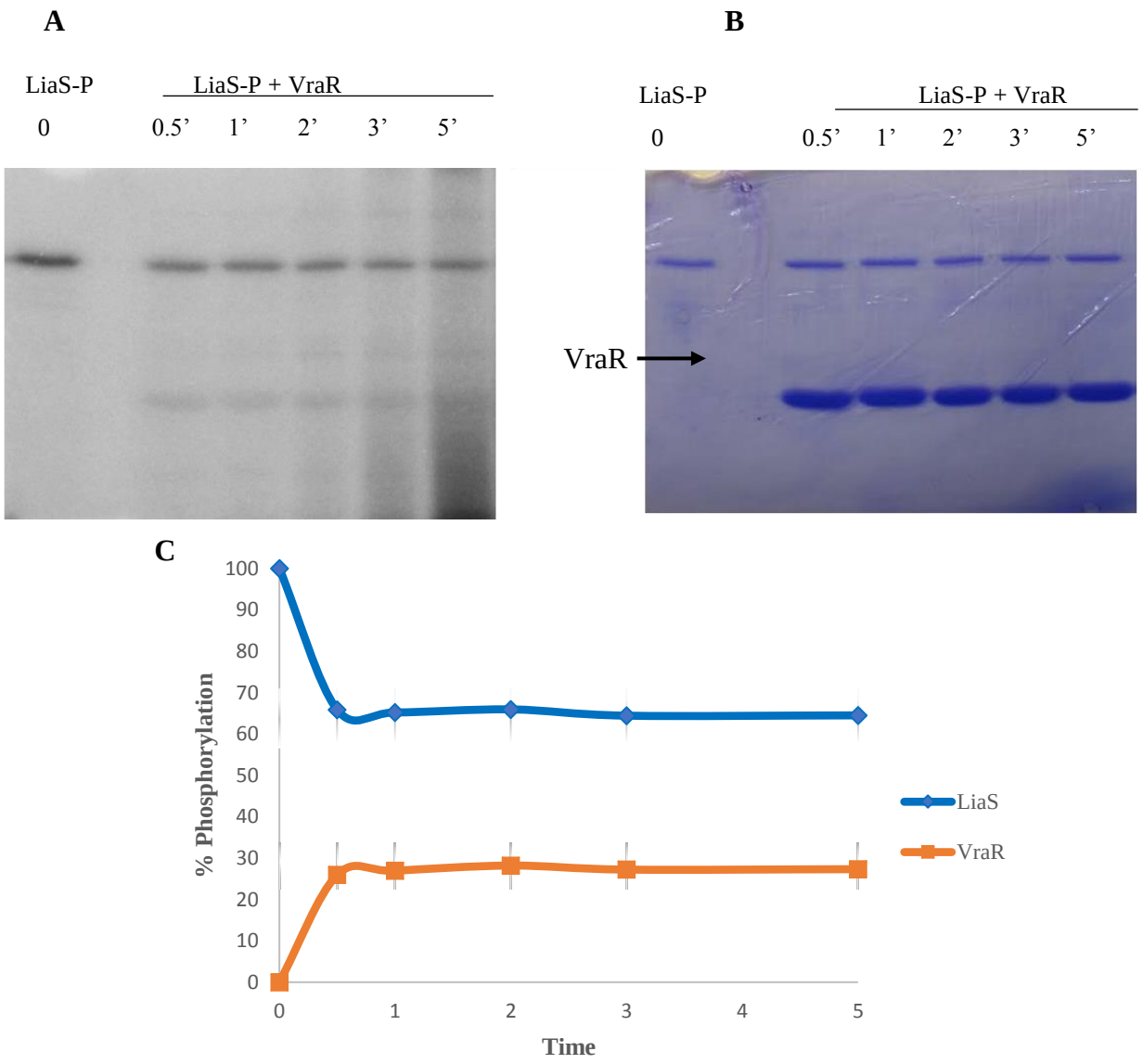

Figure 2.1.31 ***In vitro*** **Phosphotransfer between GST-LiaS and VraR using radioactive ATP at room temperature**

A: 5 µM of [γ - 32P]-ATP phosphorylated LiaS was used as the control. Phosphorylated GST-LiaS was added to VraR samples in a concentration ratio of 1:5. The samples were quenched with 5X SDS dye at time intervals ranging from 0.5 min to 5 min for the phosphotransfer to occur and was analysed using 15% SDS-PAGE. The gel was exposed to a phosphoscreen for 2 hr and scanned with a Typhoon scanner. **B**: Phosphorylated GST- LiaS mixed with VraR at room temperature. 15% SDS-PAGE gel stained with Coomassie Blue demonstrating loading concentrations **C**: Quantified data using the ImageJ software showing the rate of phosphotransfer.

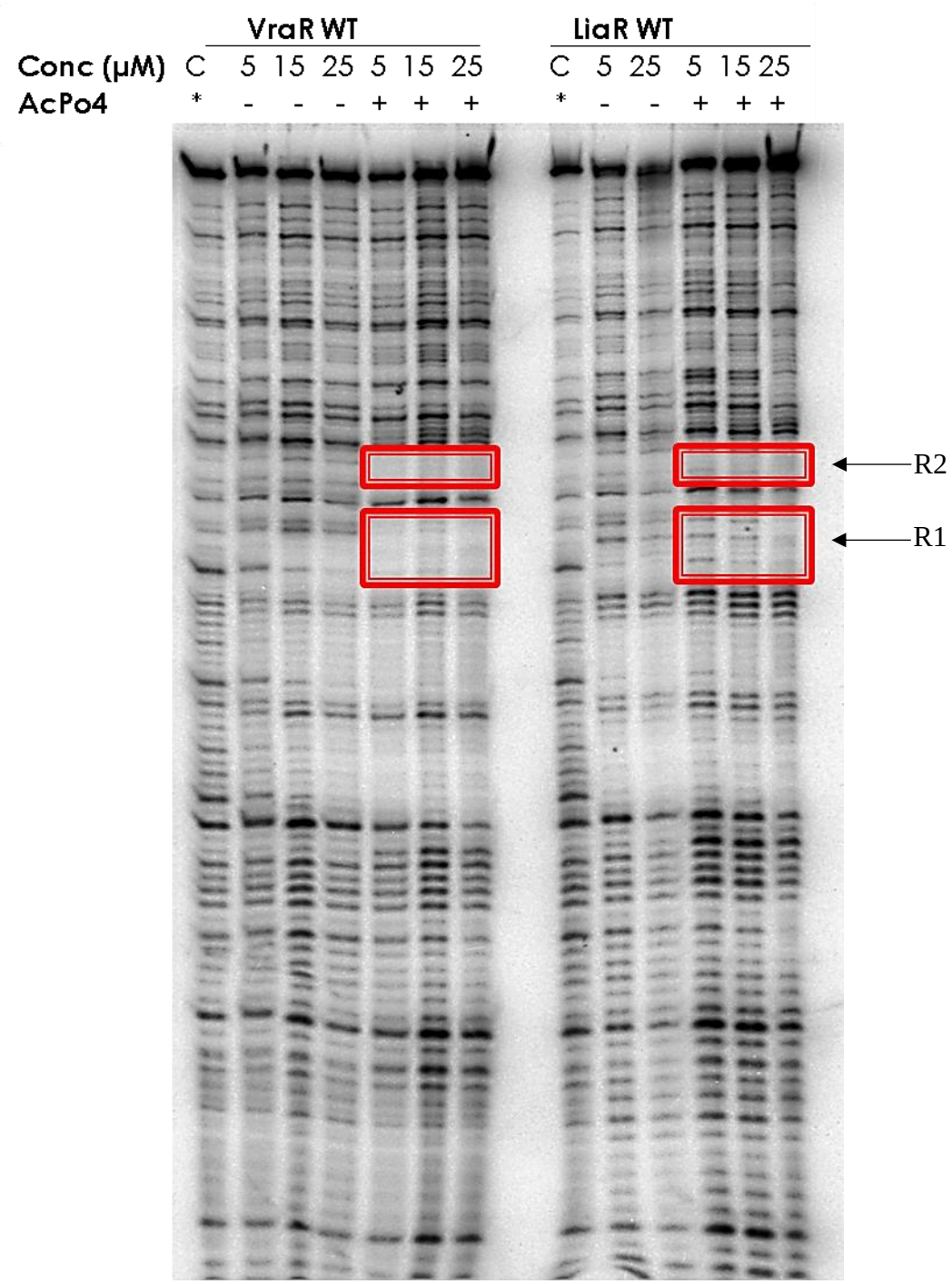

Figure 2.1.32 WT-LiaR and VraR WT terminal domain DNase-I footprinting on the labelled top strand of the *vraSR* promoter

Lanes 1 and 8 represent the controls having no protein. Lanes 2-7 represent different concentrations of unphosphorylated and phosphorylated VraR WT. Lanes 9-13 represent phosphorylated and unphosphorylated WT-LiaR

3.7.1 Investigation of protein-protein interactions by pull-down assays of GST-LiaS and LiaR, GST-LiaS and VraR, GST-VraS and LiaR and His-VraS and GST-LiaS

Analysis of heterodimer structures can provide insight into the principles of protein-protein complex formation and help develop models to predict interaction sites. In order to investigate the physical interaction between the HK and its cognate RR, resin-bound GST-LiaS was incubated with LiaR. LiaR displayed no physical interaction with LiaS despite the phosphor signal transfer between the two **(Figure 2.1.33 A)**. When GST-VraS was incubated with LiaR, no co-elution was observed **(Figure 2.1.33 B)** in antithesis to the results obtained from the phosphotransfer reactions.

Similarly, no protein-protein interaction was observed between GST-LiaS and VraR as seen in **Figure 2.1.33 C**.

Since the gene sequences of VraS and LiaS share a 53% sequence identity, we sought to investigate whether these two proteins interacted to form a heterodimer. His-VraS was immobilized on Ni-NTA resin and was co-incubated with its homolog GST-LiaS. As seen in **Figure 2.1.33 D**, the two proteins appear to co-elute together and thus interact. However, independent experiments using GST-tagged LiaS indicated that the GST tag can non-specifically bind to the Nickel column. Collectively these results demonstrate that a true interaction between the two proteins is unlikely. In conclusion, all the protein combinations did not demonstrate any binding with respect to heterodimer formation implying weak or no physical interactions.

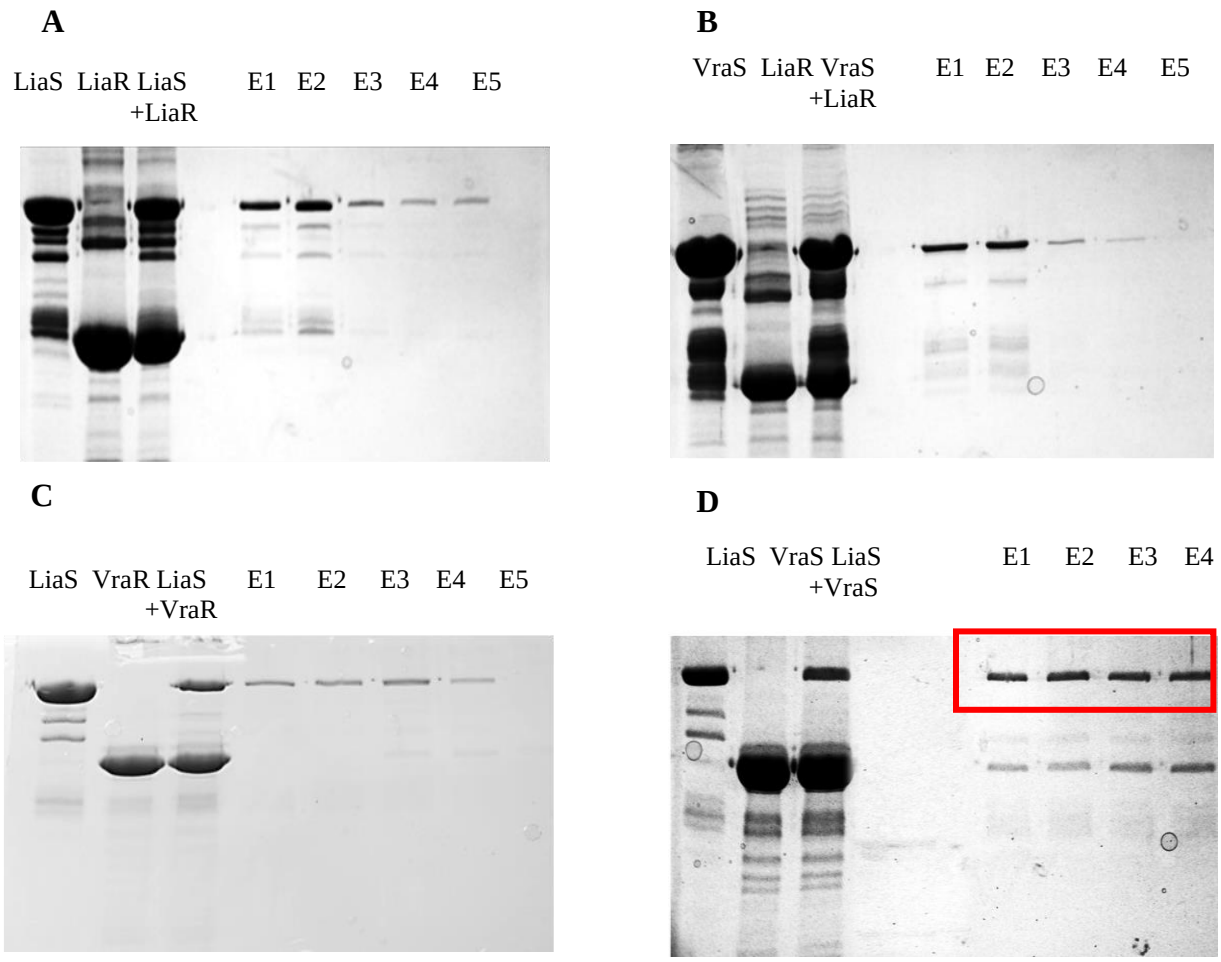

Figure 2.1.33 Pull down assays to study protein-protein interaction

A: GST-LiaS was immobilized onto glutathione resin and LiaR was co-incubated. Unbound proteins were washed and then eluted (E1-E5) with 10 mM reduced glutathione in 50 mM Tris (pH 8.0) buffer. **B:** GST-VraS was immobilized onto glutathione resin and LiaR was co-incubated. Unbound proteins were washed and then eluted (E1-E5) with 10 mM reduced glutathione in 50 mM Tris (pH 8.0) buffer. **C:** GST-LiaS was immobilized onto glutathione resin and VraR was co-incubated. Unbound proteins were washed and then eluted (E1-E5) with 10 mM reduced glutathione in 50 mM Tris (pH 8.0) buffer. **D:** His-VraS was immobilized onto Ni-NTA resin and was co-incubated with its homolog GST-LiaS. Unbound proteins were washed and then eluted (E1-E4) with 250 mM Sodium phosphate buffer (pH 8.0).

4 Discussion and Conclusions

The development of counter strategies to stress and resistance mechanisms, represent common survival strategies adopted by soil bacteria in an attempt to survive a hostile and unforgiving habitat (D'Costa et al., 2006). During infection, bacterial gene expression is modulated by multiple regulatory elements such as DNA-binding proteins, regulatory RNAs, sigma factors and TCSs (Kolar et al., 2011). The TCS is the primary modulator of gene expression in response to external stimuli. As the name suggests, TCSs are composed of two elements: a membrane-associated histidine kinase and a response regulator located within the cytoplasm. TCSs essentially counteract stress by detecting changes in the external environment and accordingly reprograming gene expression. *B. subtilis*, possesses four key TCSs involved in maintenance of cellular wall integrity (Jordan Sina, 2006). The LiaSR TCS responds to a relatively broad range of stimuli, in comparison to other TCSs which are very specific to drug sensing and detoxification only (Rietkötter et al., 2008).

Most of our current knowledge of the LiaSR TCS in *B. subtilis* (strain 168) is the product of research of homologs from other bacteria or the result of *in vivo* studies. My studies are unique because for the first time they attempt to investigate in detail the molecular mechanisms of signal transduction of the LiaSR TCS *in vitro* in *B. subtilis*.

LiaS' cytosolic portion (excluding the transmembrane domain) was successfully cloned, expressed and purified as previously described (Belcheva & Golemi-Kotra, 2008). The truncated version of LiaS (GST-LiaS), which only possessed the DHp and the CA domains was able to autophosphorylate in the presence of radiolabelled ATP. This finding is in accordance with previously published studies on IM-HK (Mascher, 2006). The affinity of LiaS towards ATP was very high as demonstrated by a Km value of ~ 3 µM, indicating that only a small concentration of

ATP is required for achieving 50% maximal phosphorylation. Because the intracellular levels of ATP are in the millimolar concentration, phosphorylation of LiaS in the cell is highly likely as a response to any stress related stimuli.

Depending on the nature of the environmental stimulus, HKs can either autophosphorylate and serve as phosphor-donors for the RR or promote their rapid dephosphorylation (Kenney, 2011). Similarly, *in vivo* studies have demonstrated that LiaS (a member of the HisKA_3 subfamily) is a bifunctional HK that also acts as a phosphatase on LiaR in the absence of a stress stimulus (Karen Schrecke, 2013). Like other known TCSs, LiaS can transfer its phosphate group to LiaR *in vitro* with 50% of the transfer occurring within the first 30 secs (rate constant = 0.0609 ± 0.0288 s^{-1}) **(Figure 2.1.12 & 2.1.13)**. This rapid phosphotransfer suggests that in the presence of cell wall stress this system is readily activated resulting in high levels of phosphorylated LiaR intracellularly. It was also demonstrated that phosphorylation levels of LiaR were tightly regulated by the phosphatase activity of LiaS as evident by phosphotransfer experiments and Phostag™ analysis **(Figure 2.1.19)**. The results obtained here, are particularly interesting in light of a recent *in vitro* study of the LiaSR TCS of *S. mutans* demonstrating that phosphorylated LiaR is relatively stable for up to 30 min as LiaS does not dephosphorylate LiaR (Manoharan Shankar, 2015).

In order to confirm the identity of the site of autophosphorylation on LiaS, mutation of histidine (residue 159) to alanine (LiaS H159A) was carried out based on available sequence information on Uniprot [(UniProtKB - O32198 (LIAS_BACSU)]. Mutation of the phosphohistidine severely curtailed autophosphorylation as demonstrated by the phosphor screen experiments. However, the phosphatase activity of LiaS H159A towards LiaR was unaltered as demonstrated by Native-PAGE and Phostag™ experiments. Phosphatase activity in the HisKA_3 subfamily of HKs is typically controlled by a conserved glutamine (residue 164 and a conserved DxxxQ motif recently

identified in DesK and NarX/Q (Albanesi et al., 2004; Schroder et al., 1994). Perhaps mutating glutamine 164 in the LiaS sequence would lead to an impairment in its phosphatase activity. The lack of phosphatase activity for LiaSH159A could also be attributed to the fact that in our *in vitro* model LiaF was absent. *In vivo*, LiaF acts as an inhibitor of the LiaSR signal transfer forming the stimulus perception complex (Karen Schrecke, 2013).

Phosphorylation of the aspartic acid residue on the RR is the hallmark of TCSs that orchestrates the adaptive responses of bacteria in response to their surroundings. The aspartylphosphate residue on the N-terminal of LiaR was mutated to alanine based on the Uniprot predicted site [(UniProtKB - O32197 (LIAR_BACSU)]. The mutation was tested to see if LiaR D54A could indeed accept phosphate groups from LiaS via phosphotransfer reactions at various time intervals. As demonstrated in **Figure 2.1.14**, while WT-LiaR readily accepted the phosphate transferred by LiaS, the D54A mutant, appeared largely unable to get phosphorylated. However, there appears to be a very faint band on the phosphotransfer gel portrayed in **Figure 2.1.14**. This very faint band could potentially be attributed to GST contamination, since LiaR and GST have almost identical molecular weights (23.125 KDa and 26 KDa respectively) and additionally GST protein gets phosphorylated. In addition, it is also possible that the signal diminishes after 5 min due to auto-dephosphorylation of LiaS when incubated with a |RR, not necessary that the RR picks up the signal. That is LiaS loses its signal but is not accepted by the response regulator, in this case because the mutant LiaR D54A lacks an aspartate group.

Acetyl phosphate is a small molecule phospho-donor capable of phosphorylating RRs *in vivo*, since it can reach intracellular concentrations comparable to those of ATP (McClearly et al., 1993). As can be demonstrated in **Figure 2.1.19**, WT-LiaR readily became phosphorylated as indicated by the retarded migration of phosphorylated LiaR during protein electrophoresis in the presence

of PhosTag^{TM}. Based on the aforementioned results, the rate of phosphorylation for LiaR was determined. It is worth mentioning that maximal phosphorylation occurs over a period of 1 hr where it tends to saturate. On the other hand, LiaRD54A remained unphosphorylated as revealed by the absence of a shift in electrophoretic mobility, indicating that phosphorylation by acetyl phosphate is unlikely.

The modular architecture of RRs comprises a conserved receiver domain and a variable effector domain which allow RRs to function as phosphorylation-regulated switches that manage a wide variety of cues (Barbieri et al., 2010). Studies on various RRs such as *S. aureus* VraR and the more widely characterized OmpR/PhoB winged-HTH transcription factor subfamilies have demonstrated a phosphorylation-dependent oligomerization assembly from monomers to dimers, responsible for the recognition of specific DNA target sites (Belcheva & Golemi-Kotra, 2008). The phosphorylation-dependent oligomerization and structure of LiaR from *E. faecium* has been studied using Beryllium Trifluoride ($BeF3^-$), a noncovalent mimic of a phosphoryl group aiding in the formation of a stable analog of the phosphorylated protein. In the same article the authors used analytical ultracentrifugation, and demonstrated that unphosphorylated *E. faecium* LiaR existed nearly exclusively as a monomer in solution with a dissociation constant of 1600 μM and that addition of BeF3 - promoted dimer formation (Kd = 15 μM) (Davlieva et al., 2016).

Upon phosphorylation with acetyl phosphate, *S. aureus* VraR displays a change in its oligomeric state as revealed by a shift in its spectrum using CD (Belcheva & Golemi-Kotra, 2008). Similarly, *B. subtilis* WT-LiaR also displayed a change in its spectrum prompting us, to further analyze its oligomeric state by using Native-PAGE. Surprisingly, these experiments indicated that LiaR existed as a mixture of monomers and dimers in its unphosphorylated state. Upon phosphorylation, a transition was observed between the monomeric and dimeric species present.

Because of this shift in equilibrium the apparent dissociation constant could not be calculated and thus no comparisons could be drawn regarding the rate of phosphorylation of LiaR by LiaS and acetyl phosphate.

Further we attempted to decipher the amino acids involved in maintaining the dimer interface of LiaR in *B. subtilis*. A recent study (Davlieva et al., 2015) on LiaR from *E. faecalis* (S613), showed a dimer-tetramer equilibrium model. Using Swiss PDB viewer we analysed the structure of the DNA-binding domain of LiaR from *E. faecalis* **(Figure 1.1.5)** to draw reference for our protein of interest. The C-terminus of LiaR from *B. subtilis* was subjected to sequence alignment with LiaR from *E. faecalis*. Three conserved amino acids at the dimerization interface, namely, threonine, isoleucine, and phenylalanine at positions 198, 202 and 205 respectively (refer to figure in the **APPENDIX D**) were identified. The relevant mutations on full-length LiaR and $LiaR^C$ were carried out with the presumption that loss of any one of the three residues would result in the loss of the ability of the protein to dimerize. However, mutants of $LiaR^C$ ($LiaR^C$ T198A, $LiaR^C$ V202A and $LiaR^C$ H205A) could not be efficiently purified and thereby characterized therefore the same mutations in the full-length LiaR protein. The resulting mutants (LiaR T198A, LiaR V202A and LiaR H205A) folded similarly to the WT protein as confirmed by their respective CD spectrums, as well as Native-PAGE and EMSA profiles. This in turn implies that perhaps the dimerization interface is rather located on the N-terminus of the protein.

LiaR from *B. subtilis* has been classified as a transcription factor, based on its ability to recognize and bind the promoter sequence (Mascher et al., 2004). My studies addressed the DNA binding ability of LiaR to the aforementioned *liaSR* promoter. Moreover, the transcriptional start site was mapped upstream of liaI using primer extension analysis. In the 60 nucleotides between the -35 region and the putative terminator of yvqJ, a 6-nucleotide direct repeat (TCCGGT) with a 12-

nucleotide spacing was identified as a candidate site for DNA binding by LiaR (Mascher, et al., 2004). In contrast to this study that demonstrated that phosphorylation was a prerequisite for DNA binding to the promoter, WT-LiaR in my experiments displayed a strong binding affinity towards the *liaSR* promoter pre and post-phosphorylation (Mascher et al., 2004). The K_D values obtained were lower than these described for homologous proteins like VraR (5 ± 2 μM) as well as LiaR (4.13 ± 0.48 μM), signifying a higher affinity for the promoter (Davlieva et al., 2015; Belcheva & Golemi-Kotra, 2008). Interestingly, the mutant LiaR D54A showed K_D values similar to that of the WT protein reiterating the fact that phosphorylation made little or no impact on the ability of LiaR to bind to the DNA. When the 192 bp *liaSR* promoter sequence was labeled and subjected to DNase I cleavage, a novel binding site was observed (designated as R1). In addition, upon phosphorylation of LiaR, a secondary binding site on the promoter is apparent (designated as R2) suggesting that LiaR either undergoes a conformational change (i.e. tetramer formation) or recruits more dimers to the vicinity of the promoter. Unfortunately, the exact base sequence of the protection area could not be determined as the sequencing standards were not working in the lab. However, the data supports previously published work with respect to LiaR binding site and sequence identity (Wolf et al., 2010). Furthermore, DNase I hypersensitive sites were observed above and below the R2 protected sequence where protection and reactivity increased. In turn, it is possible that WT-LiaR binding to the promoter induces structural alterations or changes in the curvature of the DNA thereby facilitating DNase I cleavage. Studies with other homologous response regulators (i.e. LiaR from *E. faecalis*) have also demonstrated similar findings with respect to hypersensitivity sites and thereby the probable bending of DNA (Davlieva et al., 2015). The DNA binding results on LiaR from *B. subtilis* obtained here are comparable to previously published data on LiaR from *E. faecium* and *E. faecalis* and its homolog VraR from *S. aureus*

(Belcheva & Golemi-Kotra, 2008; Davlieva et al., 2015; Davlieva et al., 2016). However, these findings with respect to the binding affinity and protection sites for LiaR from *B. subtilis* can be considered novel.

In order to gain insight into the structure and function of LiaR, its conserved receiver and effector domains were cloned independently. Site-directed mutagenesis to mutate Gly131 on the full-length gene was used to introduce a stop codon, creating $LiaR^N$. The purification was carried out by DEAE and size exclusion chromatography due to the absence of the DNA binding domain. $LiaR^N$ was subjected to phosphotransfer, to investigate whether the receiver domain was able to get phosphorylated to the same extent as full-length LiaR. The pseudo-first order rate constant for $LiaR^N$ was determined to be $0.0828 \pm 0.0325\ s^{-1}$, a value, significantly lower to that observed for the full-length protein. It is noteworthy that LiaS did not demonstrate phosphatase activity towards the receiver domain of LiaR, during the time intervals tested. This result was particularly intriguing because the HK and the RR often have a physical interaction aiding with the phosphotransfer and the subsequent phosphatase reaction. This interaction often occurs between the DHp domain of the HK and the α1 and α5 helices of the N-terminus of the RR (Leonard et al., 2013).

Phosphorylation induced by acetyl phosphate on $LiaR^N$ was estimated to be 4 times slower when compared to the rate of phosphorylation of the full-length protein. Analytical ultracentrifugation experiments also indicated that $LiaR^N$ was fit for a monomer-dimer model. In its native state, the N-terminal domain was shown to exist as a monomer/dimer mixture using Native-PAGE analysis, suggesting that the regulatory domain switches between an active and inactive state when there is interaction with the effector domain. Our findings help rule out the possibility that $LiaR^N$ function as a standalone module (Galperin M. , 2010).

The variable C-terminal effector domain is mostly involved in DNA-binding and its structural variability contributes to a wide range of functional diversity. LiaR is said to belong to the LuxR-type family of RRs, characterized by a conserved helix turn helix (HTH) motif. Structures of several LuxR-type (NarL family) have been resolved and shown that the DNA-binding domain is formed by a four-helix bundle (Barbieri et al., 2010). Surprisingly, $LiaR^{C}$ was unable to bind to the *liaSR* promoter as demonstrated by EMSA and DNase I footprinting assay. The inability of $LiaR^{C}$ to bind to the DNA emphasizes the importance of the N-terminus for the formation of a stable structure and a conformational change necessary for LiaR's binding to the gene promoter.

The inability of $LiaR^{C}$ to bind DNA is atypical of the NarL family of RRs. Recent crystal structures of RRs belonging to the NarL/LuxR family have demonstrated that a distinct surface (α1-α5 interface) is key in mediating phosphorylation-triggered dimerization. These α1-α5 helices are absent in $LiaR^{C}$ hence explaining the lack of dimerization and thereby DNA binding (Casino et al., 2010; Leonard et al., 2013). To my knowledge, only one study of DesR from *B. subtilis* (NarL family) has demonstrated similar results with respect to lack of binding to the DNA. Crystallography data on DesR indicates that phosphorylation of Asp54 induces significant rearrangements of residues Glu8, Asp9, Glu56, Thr80, and Thr81. This in turn, induces changes in protein folding, exposing the HTH motif that is responsible for DNA binding. Therefore, it is conceivable that the C-terminal domain of LiaR is unable to bind to DNA in the absence of phosphorylation on Asp54 (Trajtenberga et al., 2014). Although LiaR belongs to the NarL/LuxR family of RRs, it also shares a 28% sequence similarity to another distinct family of RRs (OmpR/PhoB family). In this family of proteins, the phosphorylation of the N-terminus is essential for C-terminal DNA binding (Martinez-Hackert & Stock, 1997). It is thus plausible that the absence of the N-terminus from LiaR affects its ability to bind to DNA.

Recent studies have also put forth the notion of the "mutual inhibition" model of function for RRs. According to this model, there is bidirectional communication between the receiver and output domains. In 2016, Correa & Gardner demonstrated that the C-terminus can affect the structure and dynamics of the receiver domain (active and inactive state). Likewise, the N-terminus can affect the ability of the C-terminus to bind to DNA (Correa & Gardner, 2016). Since $LiaR^{C}$ was unable to bind DNA in the absence of the N-terminal domain and $LiaR^{N}$ demonstrated lesser phosphorylation in the absence of the C-terminus, my findings are compatible with the aforementioned "mutual inhibition" concept.

My work also examined the interaction between the *B. subtilis* LiaSR and the well-characterized *S. aureus* VraSR TCSs. LiaS and VraS are bifunctional HKs, meaning they both possess kinase and phosphatase activities. Interestingly, LiaR and VraR responded differently in the absence of their cognate sensors. The signal transfer from GST-VraS to LiaR was significantly faster in comparison to the cognate TCS (LiaS to LiaR) with a pseudo first order rate of $3.2129 \pm 0.7339\ s^{-1}$. A sharp decline in phosphorylation of LiaR was also observed demonstrating, how VraS can serve as a more suitable phosphatase to LiaR than its cognate HK LiaS. These findings are contrary to the popular opinion that the domain alignment and physical bond formation between HKs and RRs are specific for cognate TCSs allowing for efficient signal transfer (Skerker et al., 2005; West & Stock, 2001). In contrast to the VraS and LiaR phosphotransfer reaction, VraR gets phosphorylated and maintains the phosphorylated state in the presence of LiaS as LiaS lacks phosphatase activity towards VraR. The structural similarities between LiaR and VraR were confirmed by DNase I footprinting showing LiaR binding to the *vraSR* gene promoter.

Physical interactions between the homologous TCSs were analysed using pull down assays. The pull-down assay is an *in vitro* technique used for determining the physical interaction between two

or more proteins (Uzma Muzamal, 2014). The potential interaction between GST-LiaS/LiaR was examined where GST-LiaS served as the bait and LiaR as the prey. The results obtained indicated no physical interactions between these two components. Next, we also determined if there a physical interaction between GST-VraS/LiaR and GST-LiaS/VraR since there was phosphotransfer observed in previous experiments. Similarly, no physical interactions were evident. Finally, physical interactions between the homologous proteins GST-LiaS and His-VraS was analyzed, but did not observe any co-elution. However, we need to consider that the protein preparation contains many impurities which may have impacted the analysis of these experiments.

In summary, my study provides novel insights into the molecular mechanisms of LiaSR-mediated signal transduction. Importantly, the truncated version of LiaS was shown to get phosphorylated in the presence of ATP *in vitro*. Furthermore, the bifunctional role of LiaS towards LiaR was addressed experimentally by determining the reaction rate constants. LiaR was shown to be phosphorylated by using acetyl phosphate, a small phospho-donor. WT-LiaR was shown to bind DNA strongly pre-and post phosphorylation as demonstrated by very small K_D values in comparison to other RRs. Footprinting analysis demonstrated the existence of an additional DNA binding site for phosphorylated WT-LiaR on the *liaSR* gene promoter. Mutants of the C-terminus of LiaR, demonstrated similar oligomeric state and DNA binding behaviour in comparison to the WT protein. The N and the C-terminal domains of LiaR showed novel structural dependency on each other. When LiaSR was compared to the VraSR TCS by various *in vitro* techniques/assays differences were observed in phosphorylation and dephosphorylation rates. Hopefully the research shown here would contribute towards the recent advancements in structural and functional characterization of other TCSs in order to develop new antibiotics.

5 Future Directions

My work provides important insights into the function and signaling mechanisms of the TCS in *B. subtilis*. However, there are a few interesting questions that require future investigation. For instance, it would be interesting to determine the exact binding location on the *liaSR* gene promoter where LiaR binds by using DNase I footprinting assay and the appropriate sequencing standards.

Additionally, the LiaSR TCS is often associated with a third protein (LiaF), forming a three-component system. *In vivo* studies have demonstrated that LiaF plays an inhibitory role in signal transduction between LiaS and LiaR. It would be interesting to study its involvement on signal transduction between LiaS and LiaR *in vitro* as well as its role in the ability of LiaR to bind to DNA. Studies have shown involvement of the *vraT* gene in the signal transduction from VraS to VraR. Similarly, the mechanisms by which VraT (homologous to LiaF) affects methicillin resistance are presently unclear (Boyle-Vavra et al., 2013). Studying the molecular characteristics of LiaF would contribute to understanding the signalling mechanisms operating in antibiotic resistant strains of *S. aureus*. A few studies have investigated the effect of ions (Mg^{+} and Ca^{2+}) on signal transfer in TCSs (Patel & Golemi-Kotra, 2015). It would thus be interesting to determine whether ion concentration can influence (i.e. induce or inhibit) kinase activity (LiaS) or even modify the rate of phosphorylation for LiaR.

The crystal structure of $LiaR^{C}$ from *E. faecalis* was used as a template for predicting the dimerization interface in its *B. subtilis* homolog. Unfortunately, the use of three full-length and C-terminus mutants, did not allow for the characterization of the identity of the dimerization interface. Thus, an interesting alternative approach would require mutating amino acid residues on the N-terminus of LiaR, that may potentially be involved in the dimerization interface. Because presently there is no crystal structure available for the N terminal domain of LiaR or its

homologues, it is hard to determine what exact amino acids are involved in dimer formation. Different crystallization conditions were tested by members of Dr. Vivian Saridakis lab in an attempt to crystallize the N-terminal domain of LiaR but with no success. Testing a variety of buffers and crystallization conditions and using $BeF3^-$ as a phosphate analog will help in solving the molecular architecture of phosphorylated and unphosphorylated LiaR.

Although a lot of *in vivo* studies have been conducted on the TCS, a few questions still need to be addressed. For example, there is very little information regarding alterations in gene expression following binding of LiaR to the *liaSR* promoter, or the overall phenotypic changes post signaling. Finally, investigation of the effect of LiaR deletion on the function and integrity of the cell wall by techniques such as NMR and electron microscopy can help address important questions relating to antimicrobial resistance.

References

Aguilar, P., Cronan, Jr., J., & Mendoza, D. (1998). A Bacillus subtilis gene induced by cold shock encodes a membrane phospholipid desaturase. *Journal of Bacteriology, 180(8)*, 2194-2000.

Aguilar, P., Hernandez-Arriaga, A., Cybulski, L., Erazo, A., & Mendoza, D. (2001). Molecular basis of thermosensing: a two-component signal transduction thermometer in Bacillus subtilis. *The EMBO Journal, 20(7)*, 1681-91.

Alanis, A. J. (2005). Resistance to Antibiotics: Are We in the Post-Antibiotic Era? *Archives of Medical Research, 36(6)*, 697–705.

Albanesi, D., Cecilia Mansilla, M., & de Mendoza, D. (2004). The Membrane Fluidity Sensor DesK of Bacillus subtilis Controls the Signal Decay of Its Cognate Response Regulator. *Journal of Bacteriology, 186(9)*, 2655–2663.

Ames, S., Frankema, N., & Kenney, L. (1999). C-terminal DNA binding stimulates N-terminal phosphorylation of the outer membrane protein regulator OmpR from Escherichia coli. *Proceedings of the National Academy of Sciences of the United States of America, 96(21)*, 11792–11797.

Bairoch, A. R. (2005). The Universal Protein Resource. *Nucleic Acids Research*, 154-159.

Bairoch, A., Apweiler, R., Wu, C., Barker, W., Boeckmann, B., Ferro, S., . . . Yeh, L.-S. (2005). The Universal Protein Resource . *33*.

Barbieri, C., Mack, T., Robinson, V., Miller, M., & Stock, A. (2010). Regulation of Response Regulator Autophosphorylation. *The Journal of Biological Chemistry, 285(42)*, 32325-35.

Barret, J., & Hoch, J. (1998). Two-Component Signal Transduction as a Target for Microbial Anti-Infective Therapy. *Antimicrobial Agents and Chemotherapy, 42(7)*, 1529-36.

Bassler, B. (1999). How bacteria talk to each other: regulation of gene expression by quorum sensing. *Currentopinion in Microbiology, 2*(6), 582-587.

Belcheva, A., & Golemi-Kotra, D. (2008). A Close-up View of the VraSR Two-component System. *The Journal of Biological Chemistry, 283(18)*, 12354-64.

Belcheva, A., & Golemi-Kotra, D. (2008). A Close-up View of the VraSR Two-component System A Mediator Of Staphylococcus Aureus Response To Cell Wall Damage. *Journal of Bacteriology, 283*, 2354-12364.

Bérdy, J. (2005). Bioactive Microbial Metabolites. *Journal of Antibiotics, 58(1)*, 1-26.

Bhate, M., Molnar, K., Goulian, M., & DeGrado, W. (2015). Signal Transduction in Histidine Kinases:Insights from New Structures. *Structure Review Cell Press, 23(6)*, 981-94.

Bisicchia, P., Noone, D., LioLiou, E., Howell, A., Quigley, S., Jensen, T., . . . Devine, K. (2007). The essential YycFG two-component system controls cell wall metabolism in Bacillus subtilis. *Molecular Microbiology, 65(1)*, 180-200.

Boyle-Vavra, S., Yin, S., Sun, D. J., Montgomery, C. P., & Dauma, R. S. (2013). VraT/YvqF Is Required for Methicillin Resistance and Activation of the VraSR Regulon in Staphylococcus aureus. *Antimicrob Agents Chemotherphy, 57(1)*, 83–95.

Burnside, K., & Rajagopal, L. (2012). Regulation of prokaryotic gene expression by eukaryotic-like enzymes. *Current opinion in Microbiology, 15(2)*, 125-31.

Bury-Moné, S., Nomane, Y., Reymon, N., Barbet, R., Jacquet, E., Imbeaud, S., . . . Bouloc, P. (2009). Global Analysis of Extracytoplasmic Stress Signaling in Escherichia coli. *PLOS Genetics*, e1000651.

Capra, E., & Laub, M. (2012). The Evolution of Two-Component Signal Transduction Systems. *Annual Review of Microbiology, 66*, 325-347.

Casino, P., Rubio, V., & Marina, A. (2010). The mechanism of signal transduction by two-component. *Current Opinion in Structural Biology, 20(6)*, 763-71.

Chen, G., Ramanathan, V., Law, D., Funchain, P., Chen, G., French, S., . . . Pham, B. (2010). Acute liver injury induced by weight-loss herbal supplements. *World Journal of Hepatology, 2(11)*, 410-415.

Cheung, J., & Hendrickson, W. (2010). Sensor domains of two-component regulatory systems. *Current Opinion in Microbiology, 13(2)*, 116-23.

Ciffo, F. (1984). Determination of the spectrum of antibiotic resistance of the "Bacillus subtilis" strains of Enterogermina. *Chemioterapia, 3(1)*, 45-52.

Correa, F., & Gardner, K. H. (2016). Basis of Mutual Domain Inhibition in a Bacterial Response Regulator. *Cell Press, 23(8)*, 945–954.

Davlieva, M., Shi, Y., Leonard, P., Johnson, T., Zianni, M., Arias, C., . . . Shamoo, Y. (2015). A variable DNA recognition site organization establishes the LiaR-mediated cell envelope stress response of enterococci to daptomycin. *Nucleic Acids Research, 43(9)*, 4758-73.

Davlieva, M., Tovar-Yanez, A., DeBruler, K., Leonard, P., Zianni, M., Arias, C., & Shamoo, Y. (2016, September). An Adaptive Mutation in Enterococcus faecium LiaR Associated with

Antimicrobial Peptide Resistance Mimics Phosphorylation and Stabilizes LiaR in an Activated State. *Journal of Molecular Biology, 428(22),* 4503-4519.

D'Costa, V., McGrann, K., Hughes, D., & Wright, G. (2006). Sampling the antibiotic resistome. *Science, 311(5759),* 374-7.

Dephoure, N., Gould, K., Gygi, S., & Kellogg, D. (2013). Mapping and analysis of phosphorylation sites: a quick guide for cell biologists. *Molecular Biology of the cell, 24(5),* 535-42.

Dintner, S., Heermann, R., Fang, C., Jung, K., & Gebhard, S. (2014). A sensory complex consisting of an ATP-binding cassette transporter and a two-component regulatory system controls bacitracin resistance in Bacillus subtilis. *Molecular Microbiology, 289(40),* 27899-910.

Dutta, R., Qin, L., & Inouye, M. (1999). Histidine kinases: diversity of domain organization. *34(4).*

Dworkin. (2015). Ser/Thr phosphorylation as a regulatory mechanism in bacteria. *Current opinion in Microbiology, 24,* 47-52.

Fabret, C., Feher, V., & Hoch, J. (1999). Two-component signal transduction in Bacillus subtilis: how one organism sees its world. *Journal of Bacteriology, 181(7),* 1975-1983.

Falord, M., Mäder, U., Hiron, A., Débarbouillé, M., & Msadek, T. (2011). Investigation of the Staphylococcus aureus GraSR regulon reveals novel links to virulence, stress response and cell wall signal transduction pathways. *PLoS One., 6(7),* e21323.

Frechette, R., Beach, M., Bernstein, J., Dow, T., Foleno, B., Johnson, C., . . . Barrett, J. (1997). Novel benzoxazine derivatives with inhibitory activity against bacteria. *ACS National Meeting, 2143*, 1529-1536.

Fredericks, C., Shibata, S., Shin-Ichi, A., Reimann, S., & Wolfe, A. (2006). Acetyl phosphate-sensitive regulation of flagellar biogenesis and capsular biosynthesis depends on the Rcs phosphorelay. *Molecular Microbiology, 61(3)*, 734-47.

Frederike, F., Mauder, N., Williams, T., Weiser, J., Oberle, M., & Beier, D. (2011). The cell envelope stress response mediated by the LiaFSRLm three-component system of Listeria monocytogenes is controlled via the phosphatase activity of the bifunctional histidine kinase LiaSLm. *Microbiology, 157*, 373-386.

Freiburg, B. (2016). *How To Bacillus subtilis.* Greifswald University (Germany): Munich iGEM 2012.

Fridman, M., Williams, D., Muzamal, U., Hunter, H., Siu, M., & Golemi-Kotra, D. (2013). Two unique phosphorylation-driven signaling pathways crosstalk in Staphylococcus aureus to modulate the cell-wall charge: Stk1/Stp1 meets GraSR. *Biochemistry, 52(45)*, 7975-86.

Galperin, M. (2010). Diversity of structure and function of response regulator output domains. *Current Opinion in Microbiology, 13(2)*, 150-9.

Galperin, M., & Gomelsky, M. (2005). Bacterial signal transduction modules: from genomics to biology. *ASM News, 7*, 326-333.

Galperin, M., Nikolskaya, A., & Koonin, E. (2001). Novel domains of the prokaryotic two-component signal transduction systems. *FEMS Microbiology Letters, 203(1)*, 11-21.

Gao, R., & Stock, A. (2009). Biological insights from structures of two-component proteins. *Annual Review of Microbiology, 63*, 133-154.

Gardete, S., Tomasz, A., Wu, S., & Gill, S. (2006). Role of VraSR in antibiotic resistance and antibiotic-induced stress response in Staphylococcus aureus. *Antimicrobial agents in Microbiology, 50(10)*, 3424–3434.

Gueriri, I., Bay, S., Dubrac, S., Cyncynatus, C., & Msadek, T. (2008). The Pta–AckA pathway controlling acetyl phosphate levels and the phosphorylation state of the DegU orphan response regulator both play a role in regulating Listeria monocytogenes motility and chemotaxis. *Molecular Microbiology, 70(6)*, 1342–1357.

Haijun Xu, M. J. (2010). Role of Acetyl-Phosphate in Activation of the Rrp2-RpoN-RpoS Pathway in Borrelia burgdorferi. *PLOS Pathogens*.

Hanks, S., Quinn, A., & Hunter, T. (1988). The protein kinase family: conserved features and deduced phylogeny of the catalytic domains. *Science, 241(4861)*, 42-55.

Heijenoort, J. v. (2007). Lipid Intermediates in the Biosynthesis of Bacterial Peptidoglycan. *Microbiology and Molecular Biology Reviews, 71(4)*, 620-635.

Howell, A., Dubrac, S., Noone, D., Varughese, K., & Devine, K. (2006). Interactions between the YycFG and PhoPR two-component systems in Bacillus subtilis: the PhoR kinase phosphorylates the non-cognate YycF response regulator upon phosphate limitation. *Molecular Microbiology, 59(4)*, 1199–1215.

Hsing, W., & Silhavy, T. (1997). Function of Conserved Histidine-243 in Phosphatase Activity of EnvZ, the Sensor for Porin Osmoregulation in Escherichia coli. *Journal of Bacteriology, 179(11)*, 3729–3735.

Hunter, T. (1991). Protein kinase classification. *Methods in Enzymology, 200*, 3-37.

Inouye, M. (2006). Signaling by Transmembrane Proteins Shifts Gears. *Cell, 126(5)*, 829–831.

Jordan Sina, J. A. (2006). Regulation of LiaRS-dependent gene expression in bacillus subtilis: identification of inhibitor proteins, regulator binding sites, and target genes of a conserved cell envelope stress-sensing two-component system. *J Bacteriology*.

Jordan, S., Hutchings, M., & Mascher, T. (2007). Cell envelope stress response in Gram-positive bacteria. *FEMS Microbiology Reviews, 32(1)*, 107-46.

Karen Schrecke, S. J. (2013). Stoichiometry and perturbation studies of the LiaFSR system of Bacillus subtilis. *Molecular Microbiology*.

Kenney, L. J. (2011). How Important Is the Phosphatase Activity of Sensor Kinases? *Current opinion in Microbiology*, 168–176.

Kinoshita, E., Kinoshita-Kikuta, E., Takiyama, K., & Koike, T. (2006). Phosphate-binding Tag, a New Tool to Visualize Phosphorylated Proteins. *Molecular and Cellular Proteomics, 5(4)*, 749-757.

Klinzing, D., Ishmael, N., Hotopp, J., Tettelin, H., Shields, K., Madoff, L., & Puopolo, K. (2013, July). The two-component response regulator LiaR regulates cell wall stress responses, pili expression and virulence in group B Streptococcus. *Microbiology, 159(7)*, 1521-34.

Kolar, S., Nagarajan, V., Oszmian, A., Rivera, F., Miller, H., Davenport, J., . . . Shaw, L. (2011). NsaRS is a cell-envelope-stress-sensing two component system of Staphylococcus aureus. *Microbiology, 157(8)*, 2206–2219.

Kristin Wuichet, B. J. (2012). Evolution and phyletic distribution of two-component signal transduction systems. *Current opinion in Microbiology*, 219–225.

Kuroda, M., Kuroda, H., Oshima, T., Takeuch, F., Mori, H., & Hiramatsu, K. (2003). Two-component system VraSR positively modulates the regulation of cell-wall biosynthesis pathway in Staphylococcus aureus. *Molecular Microbiology, 49(3)*, 807-21.

Kuroda, M., Kuwahara-Arai, K., & Hiramastu, K. (2000). Identification of the up- and down-regulated genes in vancomycin-resistant Staphylococcus aureus strains Mu3 and Mu50 by cDNA differential hybridization method. *Biochemical and Biophysical Research Communications, 269(2)*, 485-490.

Le Henry, Undergraduate Thesis, Alanine-scanning mutagenesis of residues involved in the dimerization interface of LiaR from *Bacillus subtilis,* York University (2017)

Lee, Y.-W., Jin, S., Sim, W.-S., & Nester, E. (1995). Genetic evidence for direct sensing of phenolic compounds by the VirA protein of Agrobacterium tumefaciens. *PNAS, 92*, 12245-12249.

Leonard, P. G., Golemi-Kotra, D., & Stock, A. M. (2013). Phosphorylation-dependent conformational changes and domain rearrangements in Staphylococcus aureus VraR activation. *National academy of Science*, 8525–8530.

Licata, L., Hilliard, J., Goldschmidt, R., Zaum, E., & Bush, K. (1998). In vitro characterization of a novel class of antibacterial agents that inhibit bacterial two-component systems. *American Society for Microbiology, 43,* 1693-1699.

Macielag, M., Bernstein, J., Demers, J., Dow, T., Foleno, B., Goldschmidt, R., . . . Barrett, J. (1997). Antibacterial salicylamides that inhibit bacterial two-component regulatory systems. *American society of Microbiology, Abstract F-228,* 87.

Madigan, M., Martinko, J., & Parker, J. (2003). *Brock Biology of Microorganisms.* Upper Saddle River NY: Pearson Education, Inc.

Manning, G., Whyte, D., Martinez, R., Hunter, T., & Sudarsanam, S. (2002). The protein kinase complement of the human genome. *Science, 298,* 1912-34.

Manoharan Shankar, S. S. (2015). Gene Regulation by the LiaSR Two-Component System in Streptococcus mutans. *PLOS one, e.0128083,* 1-10.

Martinez-Hackert, & Stock, A. (1997). Structural relationships in the OmpR family of winged-helix transcription factors. *Journal of Molecular Biology, 269(3),* 301-312.

Martinez-Hackert, E., & Stock, A. (1997). Structural relationships in the OmpR family of winged-helix transcription factors. *Journal of Molecular Biology, 269(3),* 301-312.

Martinez-Hackert, E., & Stock, A. (1997). The DNA-binding domain of OmpR: crystal structures of a winged helix transcription factor. *Cell Press, 5(1),* 109–124.

Mascher, T. (2006). Intramembrane-sensing histidine kinases: a new family of cell envelope stress sensors in Firmicutes bacteria. *FEMS Microbiology Letters, 264(2),* 133-144.

Mascher, T., Margulis, N., Wang, T., Ye, R., & Helmann, J. (2003). Cell wall stress responses in Bacillus subtilis: the regulatory network of the bacitracin stimulon. *Molecular Microbiology, 50(5)*, 1591-604.

Mascher, T., Zimmer, S., Smith, T.-A., & Helmann, J. (2004). Antibiotic-inducible promoter regulated by the cell envelope stress-sensing two-component system LiaRS of Bacillus subtilis. *Antimicrobial Agents and Chemotherapy, 48(8)*, 2888-96.

McClearly, W., Stock, J., & Ninfa, A. (1993). Is Acetyl Phosphate a Global Signal in Escherichia coli? *Journal of Bacteriology, 175(10)*, 2793-2798.

Meehl, M., Herbert, S., Götz, F., & Cheung, A. (2007). Interaction of the GraRS two-component system with the VraFG ABC transporter to support vancomycin-intermediate resistance in Staphylococcus aureus. *Antimicrobiaal Agents in Chemotherapy, 51(8)*, 2679-89.

Microbiology, D. o. (2017). *Bacterial Endospores*. Retrieved from Cornell University Department of Agriculture and Life Sciences: https://micro.cornell.edu/research/epulopiscium/bacterial-endospores

Möglich, A., Ayers, R., & Moffa, K. (2009). Design and signaling mechanism of light-regulated histidine kinases. *Journal of Molecular Biology, 385 (5)*, 1434-1444.

Munita, J., Mishra, N., Alvarez, D., Tran, T., Diaz, L., Panesso, D., . . . Arias, C. (2014). Failure of high-dose daptomycin for bacteremia caused by daptomycin-susceptible Enterococcus faecium harboring LiaSR substitutions. *Infectious Diseases Society of America, 59(9)*, 1277-80.

Nakano, M., & Zuber, P. (1998). Anaerobic growth of a "strict aerobe" (Bacillus subtilis). *Annual Review of Microbiology, 52*, 165-90.

Nathaniel, M., & Breukink, E. (2007). The expanding role of lipid II as a target for lantibiotics. *Future Microbiology, 2(5)*, 513-525.

Nicholson, W., Munakata, N., Horneck, G., Melosh, H., & Setlow, P. (2000). Resistance of Bacillus endospores to extreme terrestrial and extraterrestrial environments. *Microbial Molecular Biology Review, 64(3)*, 548-572.

Nohaile, M., Kern, D., Wemmer, D., Stedman, K., & Kustu, S. (1997). Structural and functional analyses of activating amino acid substitutions in the receiver domain of NtrC: evidence for an activating surface. *Journal of Molecular Biology, 273(1)*, 299-316.

Oggioni, M., Pozzi, G., & Valensin, P. (1998). Recurrent Septicemia in an Immunocompromised Patient Due to Probiotic Strains of Bacillus subtilis. *Journal of Clinincal Microbiology, 36(1)*, 325-348.

Pao, G., Tam, R., Lipschitz, L., & Saier, Jr., M. (1994). Response regulators: structure, function and evolution. *Research in Microbiology, 145(5)*, 356-62.

Patel, K., & Golemi-Kotra, D. (2015). Signaling mechanism by the Staphylococcus aureus two-component system LytSR: role of acetyl phosphate in bypassing the cell membrane electrical potential sensor LytS. *F1000 Research, 4(79)*, 49.

Pawelczyk, S., Scott, K., Hamer, R., Blades, G., Deane, C., & Wadha, G. (2012). Predicting Inter-Species Cross-Talk in Two-Component Signalling Systems. *PLOS One, 7(5)*, e37737.

Perego, M., & Hoch, J. (1996). Protein aspartate phosphatases control the output of two-component signal transduction systems. *Trends in Genetics, 12(3),* 97-101.

Petersohn, A., Brigulla, M., Haas, S., Hoheisel, J., Völker, U., & Hecker, M. (2001). Global analysis of the general stress response of Bacillus subtilis. *Journal of Bacteriology, 183(19),* 5617-31.

Pietiäinen, M., Gardemeister, M., Mecklin, M., Leskelä, S., Sarvas, M., & Kontinen, V. (2005). Cationic antimicrobial peptides elicit a complex stress response in Bacillus subtilis that involves ECF-type sigma factors and two-component signal transduction systems. *Microbiology, 151(5),* 1577-92.

Pirrung, M. (1999). Histidine kinases and two-component signal transduction systems. *Chemistry and Biology, 6(6),* 167-75.

Pöntinena, A., Lindströma, M., Skurnikb, M., & Korkeala, H. (2017). Screening of the two-component-system histidine kinases of Listeria monocytogenes EGD-e. LiaS is needed for growth under heat, acid, alkali, osmotic, ethanol and oxidative stresses. *Food Microbiology, 65,* 36-43.

Procaccini, A., Lunt, B., Szurmant , H., Hwa, T., & Marti. (2011). Dissecting the Specificity of Protein-Protein Interaction in Bacterial Two-Component Signaling: Orphans and Crosstalks. *PLOS one,* e19729.

Raivio, T., & Silhavy, T. (1997). Transduction of envelope stress in Escherichia coli by the Cpx two component. *Journal of Bacteriology, 179(24),* 7724-33.

Reyes, J., Panesso, D., Tran, T., Mishra, N., Cruz, M., Munita, J. M., . . . Arias, C. A. (2014). A liaR deletion restores susceptibility to Daptomycin and antimicrobial peptides in multidrug-resistant enterococcus faecalis. *Journal of Infectious Diseases*.

Rietkötter, E., Hoyer, D., & Mascher, T. (2008). Bacitracin sensing in Bacillus subtilis. *Molecular Microbiology, 68(3)*, 768–785.

Ryan, R., & Dow, M. (2008). Diffusible signals and interspecies communication in bacteria. *Microbiology, 154(7)*, 1845-1858.

Sara B. Estruch, 1. S. (2016). The language-related transcription factor FOXP2 is post-translationally modified with small ubiquitin-like modifiers. *Scientific Reports*.

Schroder, I., Wolin, C., Cavichioli, R., & Gunsalus, R. (1994). Phosphorylation and dephosphorylation of the NarQ, NarX, and NarL proteins of the nitrate-dependent two-component regulatory system of Escherichia coli. *Journal of Bacteriology, 176(16)*, 4985–4992.

Silhavy, T., Kahne, D., & Walke, S. (2010). The Bacterial Cell Envelope. *Cold Spring Harbor Perspectives in Biology, 2(5)*, a000414.

Skerker, J., Prasol, M., Perchuk, B., Biondi, E., & Laub, M. (2005). Two-component signal transduction pathways regulating growth and cell cycle progression in a bacterium: a system-level analysis. *PloS Biology, 3(10)*, e334.

Sonja, P., Scott, K., Hamer, R., Blades, G., Deane, C., & Wadhams, G. (2012). Predicting Inter-Species Cross-Talk in Two-Component Signalling Systems. *PLos One, 10.1371*, e.0037737.

Staroń, A., Sofia, H., Dietrich, S., Ulrich, L., Liesegang, H., & Mascher, T. (2009). The third pillar of bacterial signal transduction: classification of the extracytoplasmic function (ECF) sigma factor protein family. *Molecular Microbiology, 74(3),* 557-81.

Stein, T. (2005). Bacillus subtilis antibiotics: structures, syntheses and specific functions. *Molecular Microbiology, 56(4),* 845-57.

Stock, J., Park, P., Surette, M., & Levit, M. (1995). Two-component signal transduction:structure-function relationships and mechanisms of catalysis. *Annual Review of Biochemistry, Chp 3,* 183-215.

Storz, G., & Hengge-Aronis, R. (2000). *Bacterial Stress Responses* (Vol. 2). Washington: ASM Press.

Strauch, M., Mendoza, D., & Hoch, J. (1992). cis-unsaturated fatty acids specifically inhibit a signal-transducing protein kinase required for initiation of sporulation in Bacillus subtilis. *Mol Microbiology, 6(20),* 2909-17.

Strausa, S., & Hancockb, R. (2006). Mode of action of the new antibiotic for Gram-positive pathogens daptomycin: comparison with cationic antimicrobial peptides and lipopeptides. *Biochim Biophys Acta, 1758(9),* 1215-23.

Suntharalingam, P., Senadheera, M., Mair, R., Lévesque, C., & Cvitkovitch, D. (2009). The LiaFSR System Regulates the Cell Envelope Stress Response in Streptococcus mutans. *Journal of Bacteriology, 191(9),* 2973–2984.

Tam, L., Eymann, C., Albrecht, D., Sietmann, R., Schauer, F., Hecker, M., & Antelmann, H. (2006, August). Differential gene expression in response to phenol and catechol reveals different

metabolic activities for the degradation of aromatic compounds in Bacillus subtilis. *Environmental Microbiology, 8(8),* 1408-27.

Technology. (2009). *Missouri University of Science*. Retrieved from Ellen Kirk: http://web.mst.edu/~microbio/BIO221_2009/B_subtilis.html

Toymentseva, A. A., Schrecke, K., Sharipova, M., & Thorsten, M. (2012). The LIKE system, a novel protein expression toolbox for Bacillus subtilis based on the liaI promoter. *Microbial Cell Factories, 11 (143),* 1111-1143.

Trajtenberga, F., Albanesi, D., Ruétalo, N., Botti, H., Mechaly, A., Nieves, M., . . . Buschiazzo, A. (2014). Allosteric Activation of Bacterial Response Regulators: the Role of the Cognate Histidine Kinase Beyond Phosphorylation. *MbIo, 5(6),* e02105-14.

Ulrich, L. E., Koonin, E. V., & Zhulin, I. B. (2005). One-component systems dominate signal transduction in prokaryotes. *Trends in Microbiology, 13(2),* 52-6.

Uzma Muzamal, D. G.-K. (2014). Diversity of two-component systems: insights into the signal transduction mechanism by the Staphylococcus aureus two-component system GraSR. *F1000 Research, 2*, 352-359.

Volkman, B., Lipson, D., Wemmer, D., & Kern, D. (2001). Two-state allosteric behavior in a single-domain signaling protein. *Science, 5512,* 2429-33.

Wecke, T., & Mascher, T. (2011). Antibiotic research in the age of omics: from expression profiles to interspecies communication. *Journal of Antimicrobial Chemotherepy, 66(12),* 2689-704.

Wecke, T., Veith, B., Ehrenreich, A., & Mascher, T. (2006). Cell Envelope Stress Response in Bacillus licheniformis: Integrating Comparative Genomics, Transcriptional Profiling, and

Regulon Mining To Decipher a Complex Regulatory Network. *Journal of Bacteriology, 188(21)*, 7500-11.

Weidenmaier, C., Peschel, A., Kempf, V., Lucindo, N., Yeaman, M., & Bayer, A. (2005). DltABCD- and MprFmediated cell envelope modifications of Staphylococcus aureus confer resistance to platelet microbicidal proteins and contribute to virulence in a rabbit endocarditis model. *Infection and Immunology, 73(12)*, 8033-8.

West, A., & Stock, A. (2001). Histidine kinases and response regulator proteins in two-component signaling systems. *Trends in Biological sciences, 26(6)*, 369-76.

Wiegert, T., Homuth, G., Versteeg, S., & Schumann, W. (2001). Alkaline shock induces the Bacillus subtilis sigma(W) regulon. *Molecular Microbiology, 41(1)*, 59-71.

Wolf, D., Kalamorz, F., Wecke, T., Juszczak, A., Mäder, U., Homuth, G., … Mascher, T. (2010). In-Depth Profiling of the LiaR Response of *Bacillus subtilis* . *Journal of Bacteriology, 192*(18).

Wolfe, A. (2005). The Acetate Switch. *Microbiology and Molecular Reviews, 69(1)*, 12-50.

Wright, G., Holman, T., & Walsh, C. (1993). Purification and characterization of VanR and the cytosolic domain of VanS: a two-component regulatory system required for vancomycin resistance in Enterococcus faecium BM4147. *Biochemistry, 32(19)*, 5057-63.

Yassin, N. A., & Ahmad, A. M. (2012). Incidence and Resistotyping Profiles of Bacillus subtilis Isolated from Azadi Teaching Hospital in Duhok City, Iraq. *Materio Socio-Medica, 24(3)*, 194-197.

Yilmaz, M., Soran, H., & Beyatli, Y. (2006). Antimicrobial activities of some Bacillus spp. strains isolated from the soil. *Microbiological Research, 16(2),* 127-131.

Yin, S., Daum, R., & Boyle-Vavra, S. (2006). VraSR two-component regulatory system and its role in induction of pbp2 and vraSR expression by cell wall antimicrobials in Staphylococcus aureus. *Antimicrobial Agents Chemotherapy., 50(1),* 336-43.

Zhu, Y., Qin, L., Yoshida, T., & Inouye, M. (2000). Phosphatase activity of histidine kinase EnvZ without kinase catalytic domain. *PNAS, 97(14),* 7808-13.

APPENDICES

Appendix A: DNA sequencing results for GST-LiaS^{Ala126}, GST-LiaS^{Arg153}, GST-LiaSH159A, LiaRD54A, LiaR T198A, LiaR V202A, LiaR H205A, LiaR^{N}, LiaR^{C}, LiaR^{C} T198A, LiaR^{C} V202A and LiaR^{C} H205A

i) GST-LiaS ^{Ala126}

The sequence of GST-LiaS was amplified from the full-length gene from amino acids residues 126 to 360, shown by the bolded letters. With a total of 708 base pairs.

MRKKMLASLQWRAIRMTTGISLLLFVCLISFMMFYYRLDPLVLLSSSWFGIPFILILLLISV
TVGFASGYMYGNRLKTRIDTLIESILTFENGNFAYRIPPLGDDEIGLAADQLNEMAKRVE
LQV**ASLQKLSNERAEWQAQMKKSVISEERQRLARDLHDAVSQQLFAISMMTSAVL
EHVKDADDKTVKRIRMVEHMAGEAQNEMRALLLHLRPVTLEGKGLKEGLTELLD
EFRKKQPIDIEWDIQDTAISKGVEDHLFRIVQEALSNVFRHSKASKVTVILGIKNSQL
RLKVIDNGKGFKMDQVKASSYGLNSMKERASEIGGVAEVISVEGKGTQIEVKVPIF
PEEKGENERDSSIID**

Score	Expect	Identities	Gaps	Strand
1308 bits(708)	0.0	708/708(100%)	0/708(0%)	Plus/Plus

```
Query  1    GCATCCCTCCAGAAACTTTCCAATGAACGTGCGGAATGGCAGGCTCAAATGAAGAAGTCG  60
            ||||||||||||||||||||||||||||||||||||||||||||||||||||||||||||
Sbjct  1    GCATCCCTCCAGAAACTTTCCAATGAACGTGCGGAATGGCAGGCTCAAATGAAGAAGTCG  60

Query  61   GTTATCTCAGAAGAACGCCAGCGATTGGCCAGAGATCTTCATGATGCGGTCAGCCAGCAG  120
            ||||||||||||||||||||||||||||||||||||||||||||||||||||||||||||
Sbjct  61   GTTATCTCAGAAGAACGCCAGCGATTGGCCAGAGATCTTCATGATGCGGTCAGCCAGCAG  120

Query  121  CTCTTTGCCATATCGATGATGACATCAGCCGTGCTGGAACATGTCAAGGATGCTGATGAC  180
            ||||||||||||||||||||||||||||||||||||||||||||||||||||||||||||
Sbjct  121  CTCTTTGCCATATCGATGATGACATCAGCCGTGCTGGAACATGTCAAGGATGCTGATGAC  180

Query  181  AAAACAGTCAAGCGGATCAGGATGGTCGAGCATATGGCAGGCGAAGCCCAAAATGAGATG  240
            ||||||||||||||||||||||||||||||||||||||||||||||||||||||||||||
Sbjct  181  AAAACAGTCAAGCGGATCAGGATGGTCGAGCATATGGCAGGCGAAGCCCAAAATGAGATG  240

Query  241  AGGGCGCTGCTGCTCCATTTACGGCCTGTTACCCTTGAAGGAAAAGGGCTGAAGGAGGGC  300
            ||||||||||||||||||||||||||||||||||||||||||||||||||||||||||||
Sbjct  241  AGGGCGCTGCTGCTCCATTTACGGCCTGTTACCCTTGAAGGAAAAGGGCTGAAGGAGGGC  300

Query  301  CTTACGGAGCTTTTGGACGAGTTCCGAAAAAAGCAGCCGATTGATATTGAGTGGGATATA  360
            ||||||||||||||||||||||||||||||||||||||||||||||||||||||||||||
Sbjct  301  CTTACGGAGCTTTTGGACGAGTTCCGAAAAAAGCAGCCGATTGATATTGAGTGGGATATA  360

Query  361  CAGGACACAGCGATATCCAAGGGTGTTGAAGACCACTTGTTCAGAATCGTGCAGGAGGCC  420
            ||||||||||||||||||||||||||||||||||||||||||||||||||||||||||||
Sbjct  361  CAGGACACAGCGATATCCAAGGGTGTTGAAGACCACTTGTTCAGAATCGTGCAGGAGGCC  420

Query  421  CTTTCAAACGTATTTAGACATTCAAAAGCGTCAAAAGTAACCGTGATTCTGGGCATAAAG  480
            ||||||||||||||||||||||||||||||||||||||||||||||||||||||||||||
Sbjct  421  CTTTCAAACGTATTTAGACATTCAAAAGCGTCAAAAGTAACCGTGATTCTGGGCATAAAG  480

Query  481  AACAGCCAGCTCCGTCTGAAGGTGATTGATAATGGAAAAGGCTTTAAAATGGACCAGGTG  540
```

```
            ||||||||||||||||||||||||||||||||||||||||||||||||||||||||||||||||
Sbjct  481  AACAGCCAGCTCCGTCTGAAGGTGATTGATAATGGAAAAGGCTTTAAAATGGACCAGGTG  540

Query  541  AAAGCCTCCTCATACGGCTTGAATTCTATGAAAGAACGTGCAAGTGAAATCGGCGGTGTC  600
            ||||||||||||||||||||||||||||||||||||||||||||||||||||||||||||||||
Sbjct  541  AAAGCCTCCTCATACGGCTTGAATTCTATGAAAGAACGTGCAAGTGAAATCGGCGGTGTC  600

Query  601  GCCGAAGTGATTTCAGTAGAAGGAAAAGGCACTCAAATCGAAGTGAAGGTCCCGATTTTT  660
            ||||||||||||||||||||||||||||||||||||||||||||||||||||||||||||||||
Sbjct  601  GCCGAAGTGATTTCAGTAGAAGGAAAAGGCACTCAAATCGAAGTGAAGGTCCCGATTTTT  660

Query  661  CCGGAAGAAAAAGGAGAGAACGAACGTGATTCGAGTATTATTGATTGA  708
            ||||||||||||||||||||||||||||||||||||||||||||||||
Sbjct  661  CCGGAAGAAAAAGGAGAGAACGAACGTGATTCGAGTATTATTGATTGA  708
```

ii) GST-LiaS^{Arg153}

The sequence of GST-LiaS was amplified from the full-length gene from amino acids residues 153 to 360, shown by the bolded letters. With a total of 627 base pairs.

MRKKMLASLQWRAIRMTTGISLLLFVCLISFMMFYYRLDPLVLLSSSWFGIPFILILLLISV
TVGFASGYMYGNRLKTRIDTLIESILTFENGNFAYRIPPLGDDEIGLAADQLNEMAKRVE
LQVASLQKLSNERAEWQAQMKKSVISEERQ**RLARDLHDAVSQQLFAISMMTSAVLE**
HVKDADDKTVKRIRMVEHMAGEAQNEMRALLLHLRPVTLEGKGLKEGLTELLDE
FRKKQPIDIEWDIQDTAISKGVEDHLFRIVQEALSNVFRHSKASKVTVILGIKNSQLR
LKVIDNGKGFKMDQVKASSYGLNSMKERASEIGGVAEVISVEGKGTQIEVKVPIFP
EEKGENERDSSIID

Score	Expect	Identities	Gaps	Strand
1158 bits(627)	0.0	627/627(100%)	0/627(0%)	Plus/Plus

```
Query  1    CGATTGGCCAGAGATCTTCATGATGCGGTCAGCCAGCAGCTCTTTGCCATATCGATGATG  60
            ||||||||||||||||||||||||||||||||||||||||||||||||||||||||||||||||
Sbjct  1    CGATTGGCCAGAGATCTTCATGATGCGGTCAGCCAGCAGCTCTTTGCCATATCGATGATG  60

Query  61   ACATCAGCCGTGCTGGAACATGTCAAGGATGCTGATGACAAAACAGTCAAGCGGATCAGG  120
            ||||||||||||||||||||||||||||||||||||||||||||||||||||||||||||||||
Sbjct  61   ACATCAGCCGTGCTGGAACATGTCAAGGATGCTGATGACAAAACAGTCAAGCGGATCAGG  120

Query  121  ATGGTCGAGCATATGGCAGGCGAAGCCCAAAATGAGATGAGGGCGCTGCTGCTCCATTTA  180
            ||||||||||||||||||||||||||||||||||||||||||||||||||||||||||||||||
Sbjct  121  ATGGTCGAGCATATGGCAGGCGAAGCCCAAAATGAGATGAGGGCGCTGCTGCTCCATTTA  180

Query  181  CGGCCTGTTACCCTTGAAGGAAAAGGGCTGAAGGAGGGCCTTACGGAGCTTTTGGACGAG  240
            ||||||||||||||||||||||||||||||||||||||||||||||||||||||||||||||||
Sbjct  181  CGGCCTGTTACCCTTGAAGGAAAAGGGCTGAAGGAGGGCCTTACGGAGCTTTTGGACGAG  240

Query  241  TTCCGAAAAAAGCAGCCGATTGATATTGAGTGGGATATACAGGACACAGCGATATCCAAG  300
```

```
            ||||||||||||||||||||||||||||||||||||||||||||||||||||||||||||||||
Sbjct  241  TTCCGAAAAAAGCAGCCGATTGATATTGAGTGGGATATACAGGACACAGCGATATCCAAG  300

Query  301  GGTGTTGAAGACCACTTGTTCAGAATCGTGCAGGAGGCCCTTTCAAACGTATTTAGACAT  360
            ||||||||||||||||||||||||||||||||||||||||||||||||||||||||||||||||
Sbjct  301  GGTGTTGAAGACCACTTGTTCAGAATCGTGCAGGAGGCCCTTTCAAACGTATTTAGACAT  360

Query  361  TCAAAAGCGTCAAAAGTAACCGTGATTCTGGGCATAAAGAACAGCCAGCTCCGTCTGAAG  420
            ||||||||||||||||||||||||||||||||||||||||||||||||||||||||||||||||
Sbjct  361  TCAAAAGCGTCAAAAGTAACCGTGATTCTGGGCATAAAGAACAGCCAGCTCCGTCTGAAG  420

Query  421  GTGATTGATAATGGAAAAGGCTTTAAAATGGACCAGGTGAAAGCCTCCTCATACGGCTTG  480
            ||||||||||||||||||||||||||||||||||||||||||||||||||||||||||||||||
Sbjct  421  GTGATTGATAATGGAAAAGGCTTTAAAATGGACCAGGTGAAAGCCTCCTCATACGGCTTG  480

Query  481  AATTCTATGAAAGAACGTGCAAGTGAAATCGGCGGTGTCGCCGAAGTGATTTCAGTAGAA  540
            ||||||||||||||||||||||||||||||||||||||||||||||||||||||||||||||||
Sbjct  481  AATTCTATGAAAGAACGTGCAAGTGAAATCGGCGGTGTCGCCGAAGTGATTTCAGTAGAA  540

Query  541  GGAAAAGGCACTCAAATCGAAGTGAAGGTCCCGATTTTTCCGGAAGAAAAAGGAGAGAAC  600
            ||||||||||||||||||||||||||||||||||||||||||||||||||||||||||||||||
Sbjct  541  GGAAAAGGCACTCAAATCGAAGTGAAGGTCCCGATTTTTCCGGAAGAAAAAGGAGAGAAC  600

Query  601  GAACGTGATTCGAGTATTATTGATTGA  627
            |||||||||||||||||||||||||||
Sbjct  601  GAACGTGATTCGAGTATTATTGATTGA  627
```

iii) GST-LiaS H159A

GST LiaS^{Ala126} was used as template to mutate the histidine residue on position 159, shown in red.

ASLQKLSNERAEWQAQMKKSVISEERQRLARDLHDAVSQQLFAISMMTSAVLEHV KDADDKTVKRIRMVEHMAGEAQNEMRALLLHLRPVTLEGKGLKEGLTELLDEFR KKQPIDIEWDIQDTAISKGVEDHLFRIVQEALSNVFRHSKASKVTVILGIKNSQLRLK VIDNGKGFKMDQVKASSYGLNSMKERASEIGGVAEVISVEGKGTQIEVKVPIFPEE KGENERDSSIID

Histidine 159 was mutated to Alanine

Score	Expect	Identities	Gaps	Strand
1299 bits(703)	0.0	707/709(99%)	0/709(0%)	Plus/Plus

```
Query  1    CGCATCCCTCCAGAAACTTTCCAATGAACGTGCGGAATGGCAGGCTCAAATGAAGAAGTC  60
            ||||||||||||||||||||||||||||||||||||||||||||||||||||||||||||
```

```
Sbjct  1    CGCATCCCTCCAGAAACTTTCCAATGAACGTGCGGAATGGCAGGCTCAAATGAAGAAGTC  60

Query  61   GGTTATCTCAGAAGAACGCCAGCGATTGGCCAGAGATCTTGCTGATGCGGTCAGCCAGCA  120
            ||||||||||||||||||||||||||||||||||||||||  ||||||||||||||||||
Sbjct  61   GGTTATCTCAGAAGAACGCCAGCGATTGGCCAGAGATCTTCATGATGCGGTCAGCCAGCA  120

Query  121  GCTCTTTGCCATATCGATGATGACATCAGCCGTGCTGGAACATGTCAAGGATGCTGATGA  180
            ||||||||||||||||||||||||||||||||||||||||||||||||||||||||||||
Sbjct  121  GCTCTTTGCCATATCGATGATGACATCAGCCGTGCTGGAACATGTCAAGGATGCTGATGA  180

Query  181  CAAAACAGTCAAGCGGATCAGGATGGTCGAGCATATGGCAGGCGAAGCCCAAAATGAGAT  240
            ||||||||||||||||||||||||||||||||||||||||||||||||||||||||||||
Sbjct  181  CAAAACAGTCAAGCGGATCAGGATGGTCGAGCATATGGCAGGCGAAGCCCAAAATGAGAT  240

Query  241  GAGGGCGCTGCTGCTCCATTTACGGCCTGTTACCCTTGAAGGAAAAGGGCTGAAGGAGGG  300
            ||||||||||||||||||||||||||||||||||||||||||||||||||||||||||||
Sbjct  241  GAGGGCGCTGCTGCTCCATTTACGGCCTGTTACCCTTGAAGGAAAAGGGCTGAAGGAGGG  300

Query  301  CCTTACGGAGCTTTTGGACGAGTTCCGAAAAAAGCAGCCGATTGATATTGAGTGGGATAT  360
            ||||||||||||||||||||||||||||||||||||||||||||||||||||||||||||
Sbjct  301  CCTTACGGAGCTTTTGGACGAGTTCCGAAAAAAGCAGCCGATTGATATTGAGTGGGATAT  360

Query  361  ACAGGACACAGCGATATCCAAGGGTGTTGAAGACCACTTGTTCAGAATCGTGCAGGAGGC  420
            ||||||||||||||||||||||||||||||||||||||||||||||||||||||||||||
Sbjct  361  ACAGGACACAGCGATATCCAAGGGTGTTGAAGACCACTTGTTCAGAATCGTGCAGGAGGC  420

Query  421  CCTTTCAAACGTATTTAGACATTCAAAAGCGTCAAAAGTAACCGTGATTCTGGGCATAAA  480
            ||||||||||||||||||||||||||||||||||||||||||||||||||||||||||||
Sbjct  421  CCTTTCAAACGTATTTAGACATTCAAAAGCGTCAAAAGTAACCGTGATTCTGGGCATAAA  480

Query  481  GAACAGCCAGCTCCGTCTGAAGGTGATTGATAATGGAAAAGGCTTTAAAATGGACCAGGT  540
            ||||||||||||||||||||||||||||||||||||||||||||||||||||||||||||
Sbjct  481  GAACAGCCAGCTCCGTCTGAAGGTGATTGATAATGGAAAAGGCTTTAAAATGGACCAGGT  540

Query  541  GAAAGCCTCCTCATACGGCTTGAATTCTATGAAAGAACGTGCAAGTGAAATCGGCGGTGT  600
            ||||||||||||||||||||||||||||||||||||||||||||||||||||||||||||
Sbjct  541  GAAAGCCTCCTCATACGGCTTGAATTCTATGAAAGAACGTGCAAGTGAAATCGGCGGTGT  600

Query  601  CGCCGAAGTGATTTCAGTAGAAGGAAAAGGCACTCAAATCGAAGTGAAGGTCCCGATTTT  660
            ||||||||||||||||||||||||||||||||||||||||||||||||||||||||||||
Sbjct  601  CGCCGAAGTGATTTCAGTAGAAGGAAAAGGCACTCAAATCGAAGTGAAGGTCCCGATTTT  660

Query  661  TCCGGAAGAAAAAGGAGAGAACGAACGTGATTCGAGTATTATTGATTGA  709
            ||||||||||||||||||||||||||||||||||||||||||||||||
Sbjct  661  TCCGGAAGAAAAAGGAGAGAACGAACGTGATTCGAGTATTATTGATTGA  709
```

iv) LiaR D54A

WT-LiaR was used as the template for mutating the aspartate residue at position 54, to alanine.

MIRVLLIDDHEMVRMGLAAFLEAQPDIEVIGEASDGSEGVRLAVELSPDVILM**D**LVMEG

MDGIEATKQICRELSDPKIIVLTSFIDDDKVYPVIEAGALSYLLKTSKAAEIADAIRAASK

GEPKLESKVAGKVLSRLRHSGENALPHESLTKRELEILCLIAEGKTNKEIGEELFITIKTVK

THITNILSKLDVSDRTQAAVYAHRNHLVN

Aspartate 54 was mutated to Alanine

Score	Expect	Identities	Gaps	Strand
1168 bits(632)	0.0	634/635(99%)	0/635(0%)	Plus/Plus

```
Query  2    TGATTCGAGTATTATTGATTGATGATCATGAAATGGTCAGAATGGGGCTCGCGGCTTTTT  61
            ||||||||||||||||||||||||||||||||||||||||||||||||||||||||||||
Sbjct  2    TGATTCGAGTATTATTGATTGATGATCATGAAATGGTCAGAATGGGGCTCGCGGCTTTTT  61

Query  62   TGGAGGCGCAGCCCGATATTGAAGTCATCGGCGAAGCATCGGACGGCAGCGAAGGTGTTC  121
            ||||||||||||||||||||||||||||||||||||||||||||||||||||||||||||
Sbjct  62   TGGAGGCGCAGCCCGATATTGAAGTCATCGGCGAAGCATCGGACGGCAGCGAAGGTGTTC  121

Query  122  GGCTTGCTGTGGAACTGTCGCCTGATGTCATTTTAATGGACCTTGTCATGGAGGGCATGG  181
            |||||||||||||||||||||||||||||||||||| ||||||||||||||||||||||
Sbjct  122  GGCTTGCTGTGGAACTGTCGCCTGATGTCATTTTAATGGCCCTTGTCATGGAGGGCATGG  181

Query  182  ATGGCATTGAAGCTACAAAGCAAATTTGCCGGGAGCTTTCCGACCCGAAAATTATTGTGC  241
            ||||||||||||||||||||||||||||||||||||||||||||||||||||||||||||
Sbjct  182  ATGGCATTGAAGCTACAAAGCAAATTTGCCGGGAGCTTTCCGACCCGAAAATTATTGTGC  241

Query  242  TCACTAGCTTCATTGATGATGACAAAGTGTACCCGGTTATTGAAGCTGGCGCGCTCAGCT  301
            ||||||||||||||||||||||||||||||||||||||||||||||||||||||||||||
Sbjct  242  TCACTAGCTTCATTGATGATGACAAAGTGTACCCGGTTATTGAAGCTGGCGCGCTCAGCT  301

Query  302  ATCTGTTGAAAACCTCAAAAGCGGCAGAAATCGCCGATGCCATCCGCGCCGCAAGCAAGG  361
            ||||||||||||||||||||||||||||||||||||||||||||||||||||||||||||
Sbjct  302  ATCTGTTGAAAACCTCAAAAGCGGCAGAAATCGCCGATGCCATCCGCGCCGCAAGCAAGG  361

Query  362  GAGAGCCGAAGCTGGAGTCAAAAGTGGCGGGAAAAGTATTATCCAGGCTGCGCCACTCAG  421
            ||||||||||||||||||||||||||||||||||||||||||||||||||||||||||||
Sbjct  362  GAGAGCCGAAGCTGGAGTCAAAAGTGGCGGGAAAAGTATTATCCAGGCTGCGCCACTCAG  421

Query  422  GTGAAAACGCGCTCCCGCATGAATCGCTTACAAAACGGGAGCTCGAAATACTCTGCCTGA  481
            ||||||||||||||||||||||||||||||||||||||||||||||||||||||||||||
Sbjct  422  GTGAAAACGCGCTCCCGCATGAATCGCTTACAAAACGGGAGCTCGAAATACTCTGCCTGA  481

Query  482  TCGCAGAAGGAAAGACAAACAAAGAAATAGGCGAGGAACTGTTTATTACGATTAAAACAG  541
            ||||||||||||||||||||||||||||||||||||||||||||||||||||||||||||
Sbjct  482  TCGCAGAAGGAAAGACAAACAAAGAAATAGGCGAGGAACTGTTTATTACGATTAAAACAG  541

Query  542  TCAAAACACATATTACGAATATTTTATCAAAGCTGGATGTCAGTGACCGGACGCAGGCGG  601
            ||||||||||||||||||||||||||||||||||||||||||||||||||||||||||||
Sbjct  542  TCAAAACACATATTACGAATATTTTATCAAAGCTGGATGTCAGTGACCGGACGCAGGCGG  601

Query  602  CGGTGTACGCACACCGAAATCATCTCGTGAATTAG  636
            ||||||||||||||||||||||||||||||||||
Sbjct  602  CGGTGTACGCACACCGAAATCATCTCGTGAATTAG  636
```

v) LiaR T198A

WT-LiaR was used as the template for mutating the threonine residue at position 198, to alanine.

MIRVLLIDDHEMVRMGLAAFLEAQPDIEVIGEASDGSEGVRLAVELSPDVILMDLVMEG

MDGIEATKQICRELSDPKIIVLTSFIDDDKVYPVIEAGALSYLLKTSKAAEIADAIRAASK

GEPKLESKVAGKVLSRLRHSGENALPHESLTKRELEILCLIAEGKTNKEIGEELFITIKTVK

THITNILSKLDVSDR**T**QAAVYAHRNHLVN

Threonine was mutated to Alanine

Score	Expect	Identities	Gaps	Strand
1170 bits(633)	0.0	635/636(99%)	0/636(0%)	Plus/Plus

```
Query  1    ATGATTCGAGTATTATTGATTGATGATCATGAAATGGTCAGAATGGGGCTCGCGGCTTTT  60
            ||||||||||||||||||||||||||||||||||||||||||||||||||||||||||||
Sbjct  1    ATGATTCGAGTATTATTGATTGATGATCATGAAATGGTCAGAATGGGGCTCGCGGCTTTT  60

Query  61   TTGGAGGCGCAGCCCGATATTGAAGTCATCGGCGAAGCATCGGACGGCAGCGAAGGTGTT  120
            ||||||||||||||||||||||||||||||||||||||||||||||||||||||||||||
Sbjct  61   TTGGAGGCGCAGCCCGATATTGAAGTCATCGGCGAAGCATCGGACGGCAGCGAAGGTGTT  120

Query  121  CGGCTTGCTGTGGAACTGTCGCCTGATGTCATTTTAATGGACCTTGTCATGGAGGGCATG  180
            ||||||||||||||||||||||||||||||||||||||||||||||||||||||||||||
Sbjct  121  CGGCTTGCTGTGGAACTGTCGCCTGATGTCATTTTAATGGACCTTGTCATGGAGGGCATG  180

Query  181  GATGGCATTGAAGCTACAAAGCAAATTTGCCGGGAGCTTTCCGACCCGAAAATTATTGTG  240
            ||||||||||||||||||||||||||||||||||||||||||||||||||||||||||||
Sbjct  181  GATGGCATTGAAGCTACAAAGCAAATTTGCCGGGAGCTTTCCGACCCGAAAATTATTGTG  240

Query  241  CTCACTAGCTTCATTGATGATGACAAAGTGTACCCGGTTATTGAAGCTGGCGCGCTCAGC  300
            ||||||||||||||||||||||||||||||||||||||||||||||||||||||||||||
Sbjct  241  CTCACTAGCTTCATTGATGATGACAAAGTGTACCCGGTTATTGAAGCTGGCGCGCTCAGC  300

Query  301  TATCTGTTGAAAACCTCAAAAGCGGCAGAAATCGCCGATGCCATCCGCGCCGCAAGCAAG  360
            ||||||||||||||||||||||||||||||||||||||||||||||||||||||||||||
Sbjct  301  TATCTGTTGAAAACCTCAAAAGCGGCAGAAATCGCCGATGCCATCCGCGCCGCAAGCAAG  360

Query  361  GGAGAGCCGAAGCTGGAGTCAAAAGTGGCGGGAAAAGTATTATCCAGGCTGCGCCACTCA  420
            ||||||||||||||||||||||||||||||||||||||||||||||||||||||||||||
Sbjct  361  GGAGAGCCGAAGCTGGAGTCAAAAGTGGCGGGAAAAGTATTATCCAGGCTGCGCCACTCA  420

Query  421  GGTGAAAACGCGCTCCCGCATGAATCGCTTACAAAACGGGAGCTCGAAATACTCTGCCTG  480
            ||||||||||||||||||||||||||||||||||||||||||||||||||||||||||||
Sbjct  421  GGTGAAAACGCGCTCCCGCATGAATCGCTTACAAAACGGGAGCTCGAAATACTCTGCCTG  480

Query  481  ATCGCAGAAGGAAAGACAAACAAAGAAATAGGCGAGGAACTGTTTATTACGATTAAAACA  540
            ||||||||||||||||||||||||||||||||||||||||||||||||||||||||||||
Sbjct  481  ATCGCAGAAGGAAAGACAAACAAAGAAATAGGCGAGGAACTGTTTATTACGATTAAAACA  540
```

```
Query  541  GTCAAAACACATATTACGAATATTTTATCAAAGCTGGATGTCAGTGACCGGACGCAGGCG  600
            ||||||||||||||||||||||||||||||||||||||||||||||||||| ||||||||
Sbjct  541  GTCAAAACACATATTACGAATATTTTATCAAAGCTGGATGTCAGTGACCGGGCGCAGGCG  600

Query  601  GCGGTGTACGCACACCGAAATCATCTCGTGAATTAG  636
            ||||||||||||||||||||||||||||||||||
Sbjct  601  GCGGTGTACGCACACCGAAATCATCTCGTGAATTAG  636
```

vi) LiaR V202A

WT-LiaR was used as the template for mutating the valine residue at position 202, to alanine.

MIRVLLIDDHEMVRMGLAAFLEAQPDIEVIGEASDGSEGVRLAVELSPDVILMDLVMEG

MDGIEATKQICRELSDPKIIVLTSFIDDDKVYPVIEAGALSYLLKTSKAAEIADAIRAASK

GEPKLESKVAGKVLSRLRHSGENALPHESLTKRELEILCLIAEGKTNKEIGEELFITIKTVK

THITNILSKLDVSDRTQAA**V**YAHRNHLVN

Valine was mutated to Alanine

Score	Expect	Identities	Gaps	Strand
1170 bits(633)	0.0	635/636(99%)	0/636(0%)	Plus/Plus

```
Query  1    ATGATTCGAGTATTATTGATTGATGATCATGAAATGGTCAGAATGGGGCTCGCGGCTTTT  60
            ||||||||||||||||||||||||||||||||||||||||||||||||||||||||||||
Sbjct  1    ATGATTCGAGTATTATTGATTGATGATCATGAAATGGTCAGAATGGGGCTCGCGGCTTTT  60

Query  61   TTGGAGGCGCAGCCCGATATTGAAGTCATCGGCGAAGCATCGGACGGCAGCGAAGGTGTT  120
            ||||||||||||||||||||||||||||||||||||||||||||||||||||||||||||
Sbjct  61   TTGGAGGCGCAGCCCGATATTGAAGTCATCGGCGAAGCATCGGACGGCAGCGAAGGTGTT  120

Query  121  CGGCTTGCTGTGGAACTGTCGCCTGATGTCATTTTAATGGACCTTGTCATGGAGGGCATG  180
            ||||||||||||||||||||||||||||||||||||||||||||||||||||||||||||
Sbjct  121  CGGCTTGCTGTGGAACTGTCGCCTGATGTCATTTTAATGGACCTTGTCATGGAGGGCATG  180

Query  181  GATGGCATTGAAGCTACAAAGCAAATTTGCCGGGAGCTTTCCGACCCGAAAATTATTGTG  240
            ||||||||||||||||||||||||||||||||||||||||||||||||||||||||||||
Sbjct  181  GATGGCATTGAAGCTACAAAGCAAATTTGCCGGGAGCTTTCCGACCCGAAAATTATTGTG  240

Query  241  CTCACTAGCTTCATTGATGATGACAAAGTGTACCCGGTTATTGAAGCTGGCGCGCTCAGC  300
            ||||||||||||||||||||||||||||||||||||||||||||||||||||||||||||
Sbjct  241  CTCACTAGCTTCATTGATGATGACAAAGTGTACCCGGTTATTGAAGCTGGCGCGCTCAGC  300

Query  301  TATCTGTTGAAAACCTCAAAAGCGGCAGAAATCGCCGATGCCATCCGCGCCGCAAGCAAG  360
            ||||||||||||||||||||||||||||||||||||||||||||||||||||||||||||
Sbjct  301  TATCTGTTGAAAACCTCAAAAGCGGCAGAAATCGCCGATGCCATCCGCGCCGCAAGCAAG  360
```

```
Query  361  GGAGAGCCGAAGCTGGAGTCAAAAGTGGCGGGAAAAGTATTATCCAGGCTGCGCCACTCA  420
            ||||||||||||||||||||||||||||||||||||||||||||||||||||||||||||
Sbjct  361  GGAGAGCCGAAGCTGGAGTCAAAAGTGGCGGGAAAAGTATTATCCAGGCTGCGCCACTCA  420

Query  421  GGTGAAAACGCGCTCCCGCATGAATCGCTTACAAAACGGGAGCTCGAAATACTCTGCCTG  480
            ||||||||||||||||||||||||||||||||||||||||||||||||||||||||||||
Sbjct  421  GGTGAAAACGCGCTCCCGCATGAATCGCTTACAAAACGGGAGCTCGAAATACTCTGCCTG  480

Query  481  ATCGCAGAAGGAAAGACAAACAAAGAAATAGGCGAGGAACTGTTTATTACGATTAAAACA  540
            ||||||||||||||||||||||||||||||||||||||||||||||||||||||||||||
Sbjct  481  ATCGCAGAAGGAAAGACAAACAAAGAAATAGGCGAGGAACTGTTTATTACGATTAAAACA  540

Query  541  GTCAAAACACATATTACGAATATTTTATCAAAGCTGGATGTCAGTGACCGGACGCAGGCG  600
            ||||||||||||||||||||||||||||||||||||||||||||||||||||||||||||
Sbjct  541  GTCAAAACACATATTACGAATATTTTATCAAAGCTGGATGTCAGTGACCGGACGCAGGCG  600

Query  601  GCGGTGTACGCACACCGAAATCATCTCGTGAATTAG  636
            |||| ||||||||||||||||||||||||||||||
Sbjct  601  GCGGCGTACGCACACCGAAATCATCTCGTGAATTAG  636
```

vii) LiaR H205A

WT-LiaR was used as the template for mutating the histidine residue at position 205, to alanine.

MIRVLLIDDHEMVRMGLAAFLEAQPDIEVIGEASDGSEGVRLAVELSPDVILMDLVMEG

MDGIEATKQICRELSDPKIIVLTSFIDDDKVYPVIEAGALSYLLKTSKAAEIADAIRAASK

GEPKLESKVAGKVLSRLRHSGENALPHESLTKRELEILCLIAEGKTNKEIGEELFITIKTVK

THITNILSKLDVSDRTQAAVYA**H**RNHLVN

Histidine was mutated to Alanine

Score	Expect	Identities	Gaps	Strand
1164 bits(630)	0.0	634/636(99%)	0/636(0%)	Plus/Plus

```
Query  1    ATGATTCGAGTATTATTGATTGATGATCATGAAATGGTCAGAATGGGGCTCGCGGCTTTT  60
            ||||||||||||||||||||||||||||||||||||||||||||||||||||||||||||
Sbjct  1    ATGATTCGAGTATTATTGATTGATGATCATGAAATGGTCAGAATGGGGCTCGCGGCTTTT  60

Query  61   TTGGAGGCGCAGCCCGATATTGAAGTCATCGGCGAAGCATCGGACGGCAGCGAAGGTGTT  120
            ||||||||||||||||||||||||||||||||||||||||||||||||||||||||||||
Sbjct  61   TTGGAGGCGCAGCCCGATATTGAAGTCATCGGCGAAGCATCGGACGGCAGCGAAGGTGTT  120

Query  121  CGGCTTGCTGTGGAACTGTCGCCTGATGTCATTTTAATGGACCTTGTCATGGAGGGCATG  180
            ||||||||||||||||||||||||||||||||||||||||||||||||||||||||||||
Sbjct  121  CGGCTTGCTGTGGAACTGTCGCCTGATGTCATTTTAATGGACCTTGTCATGGAGGGCATG  180

Query  181  GATGGCATTGAAGCTACAAAGCAAATTTGCCGGGAGCTTTCCGACCCGAAAATTATTGTG  240
```

```
            ||||||||||||||||||||||||||||||||||||||||||||||||||||||||||||||||
Sbjct  181  GATGGCATTGAAGCTACAAAGCAAATTTGCCGGGAGCTTTCCGACCCGAAAATTATTGTG  240

Query  241  CTCACTAGCTTCATTGATGATGACAAAGTGTACCCGGTTATTGAAGCTGGCGCGCTCAGC  300
            ||||||||||||||||||||||||||||||||||||||||||||||||||||||||||||||||
Sbjct  241  CTCACTAGCTTCATTGATGATGACAAAGTGTACCCGGTTATTGAAGCTGGCGCGCTCAGC  300

Query  301  TATCTGTTGAAAACCTCAAAAGCGGCAGAAATCGCCGATGCCATCCGCGCCGCAAGCAAG  360
            ||||||||||||||||||||||||||||||||||||||||||||||||||||||||||||||||
Sbjct  301  TATCTGTTGAAAACCTCAAAAGCGGCAGAAATCGCCGATGCCATCCGCGCCGCAAGCAAG  360

Query  361  GGAGAGCCGAAGCTGGAGTCAAAAGTGGCGGGAAAAGTATTATCCAGGCTGCGCCACTCA  420
            ||||||||||||||||||||||||||||||||||||||||||||||||||||||||||||||||
Sbjct  361  GGAGAGCCGAAGCTGGAGTCAAAAGTGGCGGGAAAAGTATTATCCAGGCTGCGCCACTCA  420

Query  421  GGTGAAAACGCGCTCCCGCATGAATCGCTTACAAAACGGGAGCTCGAAATACTCTGCCTG  480
            ||||||||||||||||||||||||||||||||||||||||||||||||||||||||||||||||
Sbjct  421  GGTGAAAACGCGCTCCCGCATGAATCGCTTACAAAACGGGAGCTCGAAATACTCTGCCTG  480

Query  481  ATCGCAGAAGGAAAGACAAACAAAGAAATAGGCGAGGAACTGTTTATTACGATTAAAACA  540
            ||||||||||||||||||||||||||||||||||||||||||||||||||||||||||||||||
Sbjct  481  ATCGCAGAAGGAAAGACAAACAAAGAAATAGGCGAGGAACTGTTTATTACGATTAAAACA  540

Query  541  GTCAAAACACATATTACGAATATTTTATCAAAGCTGGATGTCAGTGACCGGACGCAGGCG  600
            ||||||||||||||||||||||||||||||||||||||||||||||||||||||||||||||||
Sbjct  541  GTCAAAACACATATTACGAATATTTTATCAAAGCTGGATGTCAGTGACCGGACGCAGGCG  600

Query  601  GCGGTGTACGCACACCGAAATCATCTCGTGAATTAG  636
            ||||||||||||  ||||||||||||||||||||||
Sbjct  601  GCGGTGTACGCAGCCCGAAATCATCTCGTGAATTAG  636
```

viii) LiaR^{N}

WT-LiaR was used as the template for mutating the glycine residue at position 131, to stop codon.

The bolded sequence shows the N-terminal LiaR sequence 1-131.

MIRVLLIDDHEMVRMGLAAFLEAQPDIEVIGEASDGSEGVRLAVELSPDVILMDLV

MEGMDGIEATKQICRELSDPKIIVLTSFIDDDKVYPVIEAGALSYLLKTSKAAEIADA

IRAASKGEPKLESKVA*G*KVLSRLRHSGENALPHESLTKRELEILCLIAEGKTNKEIGEE

LFITIKTVKTHITNILSKLDVSDRTQAAVYAHRNHLVN

Glycine was mutated to stop codon

Score	Expect	Identities	Gaps	Strand

726 bits(393) 0.0 395/393(99%) 0/396(0%) Plus/Plus

```
Query  1    ATGATTCGAGTATTATTGATTGATGATCATGAAATGGTCAGAATGGGGCTCGCGGCTTTT  60
            ||||||||||||||||||||||||||||||||||||||||||||||||||||||||||||
Sbjct  1    ATGATTCGAGTATTATTGATTGATGATCATGAAATGGTCAGAATGGGGCTCGCGGCTTTT  60

Query  61   TTGGAGGCGCAGCCCGATATTGAAGTCATCGGCGAAGCATCGGACGGCAGCGAAGGTGTT  120
            ||||||||||||||||||||||||||||||||||||||||||||||||||||||||||||
Sbjct  61   TTGGAGGCGCAGCCCGATATTGAAGTCATCGGCGAAGCATCGGACGGCAGCGAAGGTGTT  120

Query  121  CGGCTTGCTGTGGAACTGTCGCCTGATGTCATTTTAATGGACCTTGTCATGGAGGGCATG  180
            ||||||||||||||||||||||||||||||||||||||||||||||||||||||||||||
Sbjct  121  CGGCTTGCTGTGGAACTGTCGCCTGATGTCATTTTAATGGACCTTGTCATGGAGGGCATG  180

Query  181  GATGGCATTGAAGCTACAAAGCAAATTTGCCGGGAGCTTTCCGACCCGAAAATTATTGTG  240
            ||||||||||||||||||||||||||||||||||||||||||||||||||||||||||||
Sbjct  181  GATGGCATTGAAGCTACAAAGCAAATTTGCCGGGAGCTTTCCGACCCGAAAATTATTGTG  240

Query  241  CTCACTAGCTTCATTGATGATGACAAAGTGTACCCGGTTATTGAAGCTGGCGCGCTCAGC  300
            ||||||||||||||||||||||||||||||||||||||||||||||||||||||||||||
Sbjct  241  CTCACTAGCTTCATTGATGATGACAAAGTGTACCCGGTTATTGAAGCTGGCGCGCTCAGC  300

Query  301  TATCTGTTGAAAACCTCAAAAGCGGCAGAAATCGCCGATGCCATCCGCGCCGCAAGCAAG  360
            ||||||||||||||||||||||||||||||||||||||||||||||||||||||||||||
Sbjct  301  TATCTGTTGAAAACCTCAAAAGCGGCAGAAATCGCCGATGCCATCCGCGCCGCAAGCAAG  360

Query  361  GGAGAGCCGAAGCTGGAGTCAAAAGTGGCGGGA  393
            |||||||||||||||||||||||||||| ||
Sbjct  361  GGAGAGCCGAAGCTGGAGTCAAAAGTGGCGTGA  393
```

ix) LiaR^{C}

WT-LiaR was used as the template for amplifying the C-terminal. The LiaR^{C} sequence is bolded with just 73 amino acids.

MIRVLLIDDHEMVRMGLAAFLEAQPDIEVIGEASDGSEGVRLAVELSPDVILMDLVMEG

MDGIEATKQICRELSDPKIIVLTSFIDDDKVYPVIEAGALSYLLKTSKAAEIADAIRAASK

GEPKLESKVAGKVLSRLRH**SGENALPHESLTKRELEILCLIAEGKTNKEIGEELFITIK**

TVKTHITNILSKLDVSDRTQAAVYAHRNHLVN

Score	Expect	Identities	Gaps	Strand
405 bits(219)	5e-118	219/219(100%)	0/219(0%)	Plus/Plus

```
Query  1    TCAGGTGAAAACGCGCTCCCGCATGAATCGCTTACAAAACGGGAGCTCGAAATACTCTGC  60
            ||||||||||||||||||||||||||||||||||||||||||||||||||||||||||||
Sbjct  1    TCAGGTGAAAACGCGCTCCCGCATGAATCGCTTACAAAACGGGAGCTCGAAATACTCTGC  60

Query  61   CTGATCGCAGAAGGAAAGACAAACAAAGAAATAGGCGAGGAACTGTTTATTACGATTAAA  120
            ||||||||||||||||||||||||||||||||||||||||||||||||||||||||||||
Sbjct  61   CTGATCGCAGAAGGAAAGACAAACAAAGAAATAGGCGAGGAACTGTTTATTACGATTAAA  120

Query  121  ACAGTCAAAACACATATTACGAATATTTTATCAAAGCTGGATGTCAGTGACCGGACGCAG  180
            ||||||||||||||||||||||||||||||||||||||||||||||||||||||||||||
Sbjct  121  ACAGTCAAAACACATATTACGAATATTTTATCAAAGCTGGATGTCAGTGACCGGACGCAG  180

Query  181  GCGGCGGTGTACGCACACCGAAATCATCTCGTGAATTAG  219
            |||||||||||||||||||||||||||||||||||||||
Sbjct  181  GCGGCGGTGTACGCACACCGAAATCATCTCGTGAATTAG  219
```

x) LiaR^{C} T198A

WT-LiaR^{C} was used as the template for mutating the threonine residue at position 198, to alanine.

SGENALPHESLTKRELEILCLIAEGKTNKEIGEELFITIKTVKTHITNILSKLDVSDRT

QAAVYAHRNHLVN

Threonine mutated to Alanine

-Score	Expect	Identities	Gaps	Strand
399 bits(216)	2e-116	218/219(99%)	0/219(0%)	Plus/Plus

```
Query  1    TCAGGTGAAAACGCGCTCCCGCATGAATCGCTTACAAAACGGGAGCTCGAAATACTCTGC  60
            ||||||||||||||||||||||||||||||||||||||||||||||||||||||||||||
Sbjct  1    TCAGGTGAAAACGCGCTCCCGCATGAATCGCTTACAAAACGGGAGCTCGAAATACTCTGC  60

Query  61   CTGATCGCAGAAGGAAAGACAAACAAAGAAATAGGCGAGGAACTGTTTATTACGATTAAA  120
            ||||||||||||||||||||||||||||||||||||||||||||||||||||||||||||
Sbjct  61   CTGATCGCAGAAGGAAAGACAAACAAAGAAATAGGCGAGGAACTGTTTATTACGATTAAA  120

Query  121  ACAGTCAAAACACATATTACGAATATTTTATCAAAGCTGGATGTCAGTGACCGGACGCAG  180
            |||||||||||||||||||||||||||||||||||||||||||||||||||||| |||||
```

```
Sbjct  121  ACAGTCAAAACACATATTACGAATATTTTATCAAAGCTGGATGTCAGTGACCGGGCGCAG  180

Query  181  GCGGCGGTGTACGCACACCGAAATCATCTCGTGAATTAG  219
            ||||||||||||||||||||||||||||||||||||||
Sbjct  181  GCGGCGGTGTACGCACACCGAAATCATCTCGTGAATTAG  219
```

xi) LiaR^{C} V202A

WT-LiaR^{C} was used as the template for mutating the valine residue at position 202, to alanine.

SGENALPHESLTKRELEILCLIAEGKTNKEIGEELFITIKTVKTHITNILSKLDVSDRT

QAAVYAHRNHLVN

Valine mutated to Alanine

Score	Expect	Identities	Gaps	Strand
399 bits(216)	2e-116	218/219(99%)	0/219(0%)	Plus/Plus

```
Query  1    TCAGGTGAAAACGCGCTCCCGCATGAATCGCTTACAAAACGGGAGCTCGAAATACTCTGC  60
            ||||||||||||||||||||||||||||||||||||||||||||||||||||||||||||
Sbjct  1    TCAGGTGAAAACGCGCTCCCGCATGAATCGCTTACAAAACGGGAGCTCGAAATACTCTGC  60

Query  61   CTGATCGCAGAAGGAAAGACAAACAAAGAAATAGGCGAGGAACTGTTTATTACGATTAAA  120
            ||||||||||||||||||||||||||||||||||||||||||||||||||||||||||||
Sbjct  61   CTGATCGCAGAAGGAAAGACAAACAAAGAAATAGGCGAGGAACTGTTTATTACGATTAAA  120

Query  121  ACAGTCAAAACACATATTACGAATATTTTATCAAAGCTGGATGTCAGTGACCGGACGCAG  180
            ||||||||||||||||||||||||||||||||||||||||||||||||||||||||||||
Sbjct  121  ACAGTCAAAACACATATTACGAATATTTTATCAAAGCTGGATGTCAGTGACCGGACGCAG  180

Query  181  GCGGCGGTGTACGCACACCGAAATCATCTCGTGAATTAG  219
            ||||||| |||||||||||||||||||||||||||||||
Sbjct  181  GCGGCGGCGTACGCACACCGAAATCATCTCGTGAATTAG  219
```

xii) LiaR^{C} H205A

WT-LiaR^{C} was used as the template for mutating the histidine residue at position 205, to alanine.

SGENALPHESLTKRELEILCLIAEGKTNKEIGEELFITIKTVKTHITNILSKLDVSDRT

QAAVYAHRNHLVN

Histidine mutated to Alanine

Score	Expect	Identities	Gaps	Strand
394 bits(213)	8e-115	217/219(99%)	0/219(0%)	Plus/Plus

```
Query  1    TCAGGTGAAAACGCGCTCCCGCATGAATCGCTTACAAAACGGGAGCTCGAAATACTCTGC  60
            ||||||||||||||||||||||||||||||||||||||||||||||||||||||||||||
Sbjct  1    TCAGGTGAAAACGCGCTCCCGCATGAATCGCTTACAAAACGGGAGCTCGAAATACTCTGC  60

Query  61   CTGATCGCAGAAGGAAAGACAAACAAAGAAATAGGCGAGGAACTGTTTATTACGATTAAA  120
            ||||||||||||||||||||||||||||||||||||||||||||||||||||||||||||
Sbjct  61   CTGATCGCAGAAGGAAAGACAAACAAAGAAATAGGCGAGGAACTGTTTATTACGATTAAA  120

Query  121  ACAGTCAAAACACATATTACGAATATTTTATCAAAGCTGGATGTCAGTGACCGGACGCAG  180
            ||||||||||||||||||||||||||||||||||||||||||||||||||||||||||||
Sbjct  121  ACAGTCAAAACACATATTACGAATATTTTATCAAAGCTGGATGTCAGTGACCGGACGCAG  180

Query  181  GCGGCGGTGTACGCACACCGAAATCATCTCGTGAATTAG  219
            ||||||||||||||  ||||||||||||||||||||||
Sbjct  181  GCGGCGGTGTACGCAGCCCGAAATCATCTCGTGAATTAG  219
```

Appendix B: Band intensity of phosphorylated response regulators, via phosphotransfer reactions, were quantified using ImageJ and plotted against time. The data were fitted using GraFit software to pseudo first order equation to calculate rate constant.

i) Phosphotransfer reaction between GST-VraS to LiaR

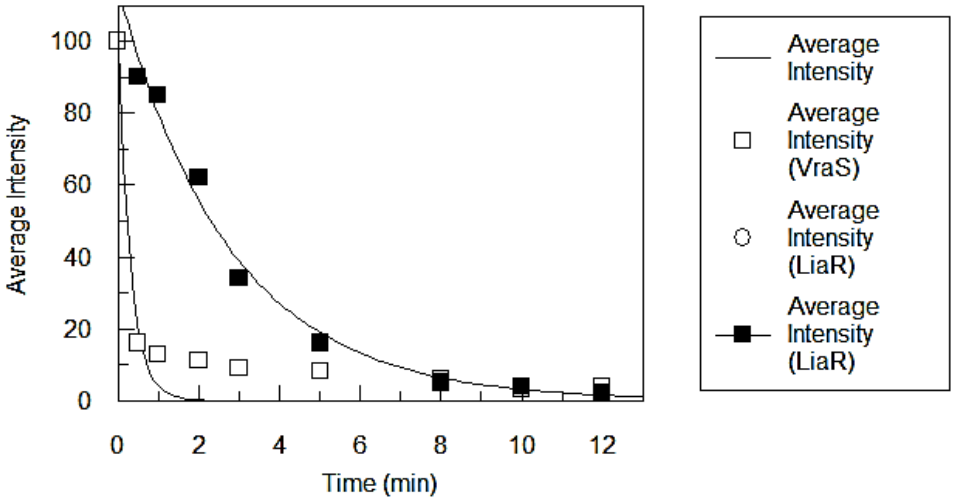

Parameter	Value	Std. Error
rate constant	3.2129	0.7339
proportionality constant	99.5824	7.7424

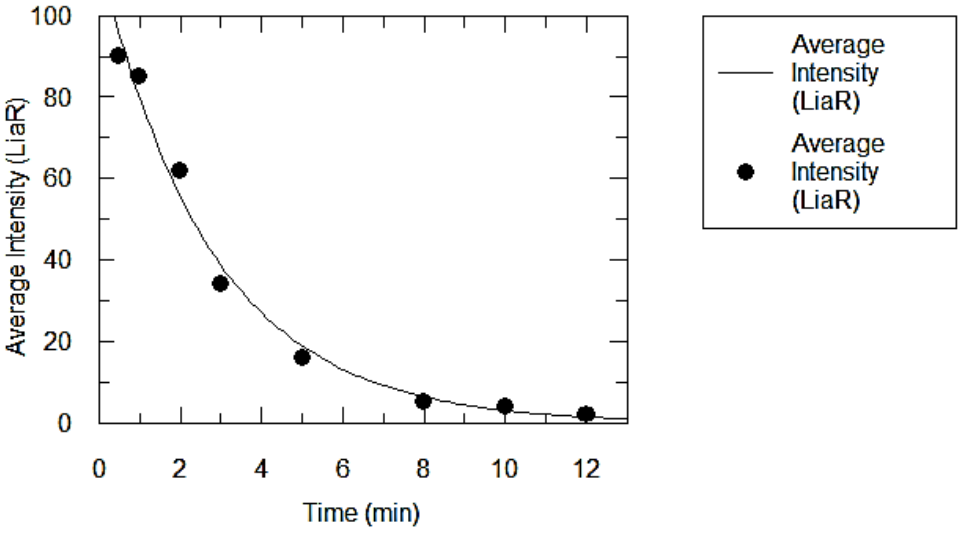

Parameter	Value	Std. Error
rate constant for dephosphorylation	0.3604	0.0336
proportionality parameter	114.3756	5.8396

ii) Phosphotransfer reaction between GST-LiaS to VraR

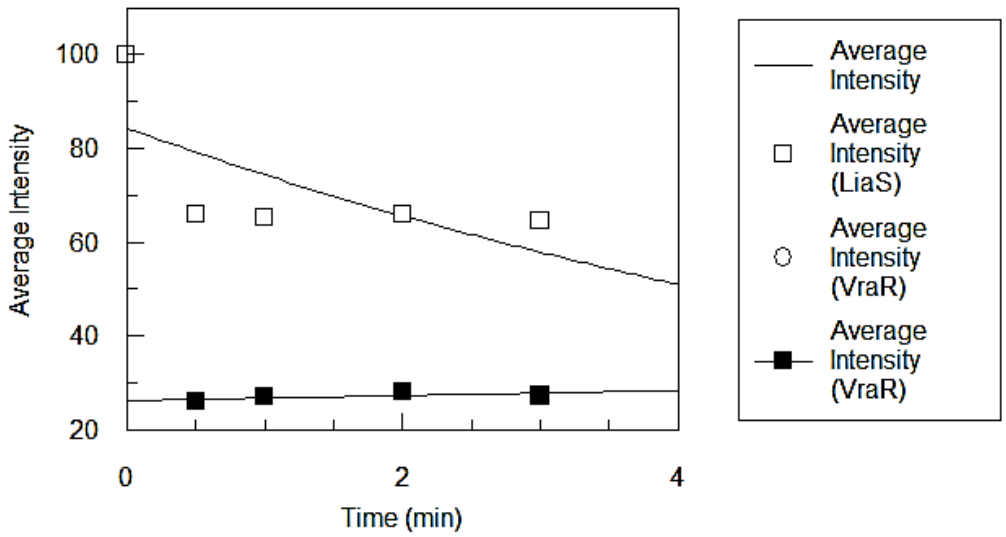

Parameter	Value	Std. Error
rate constant	0.1257	0.0828
proportionality constant	84.2888	10.0619

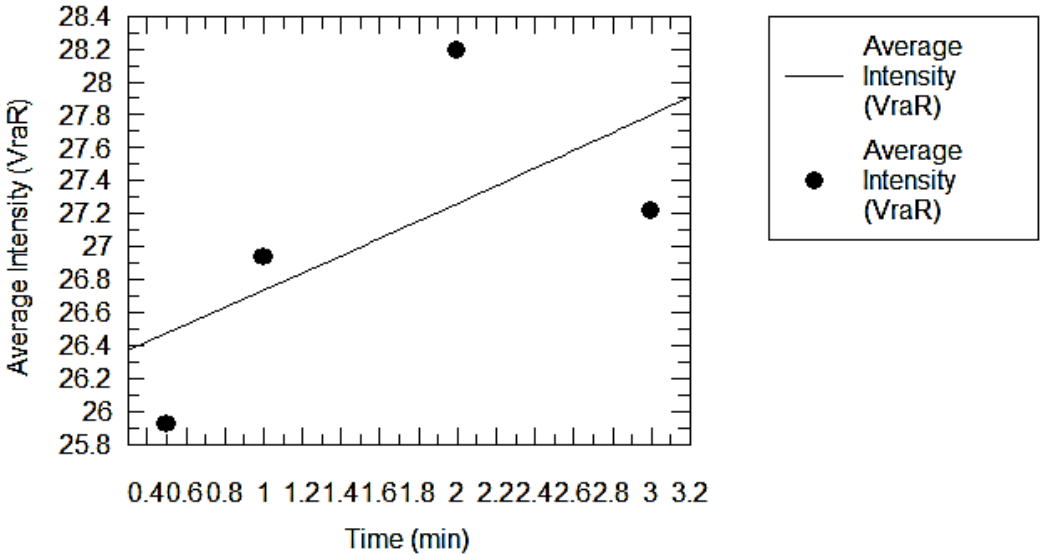

Parameter	Value	Std. Error
rate constant for dephosphorylation	-0.0195	0.0168
proportionality parameter	26.2178	0.8480

Appendix C: Quantification of DNase I footprinting data for WT-LiaR and D54A

Percentage of protected DNA is plotted against protein concentration. The intensity of three to four most prominent bands in the protected regions were measured by ImageJ software and averaged them out to calculate the protected DNA percentage.

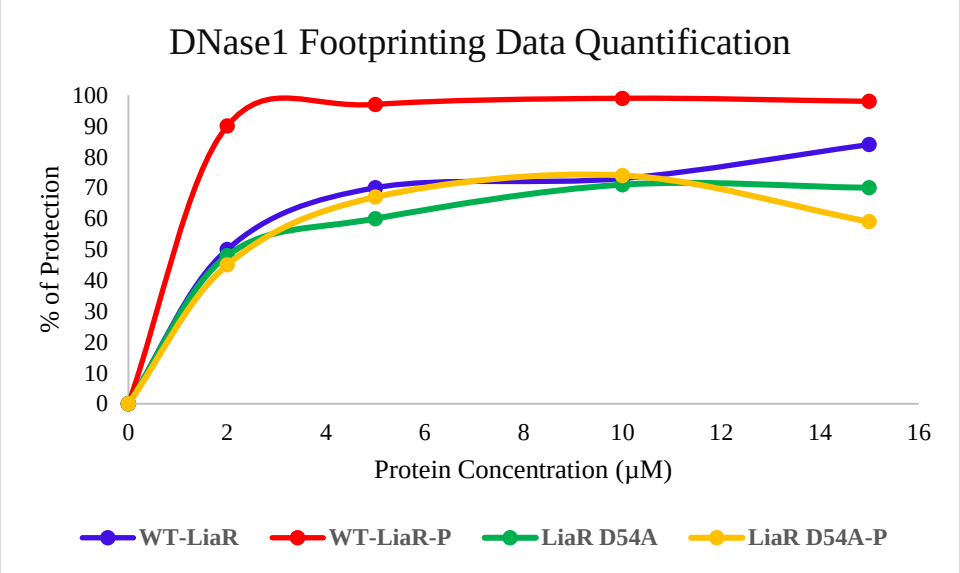

Appendix D: Crystal structure of LiaR C-Terminus from E. faecalis, modified through PyMOL software to show residues interacting amino acids

Conserved sites of LiaR *E. faecalis* that were used to create mutants in *B. subtilis* LiaR T198A, LiaR V202A and LiaR H205A

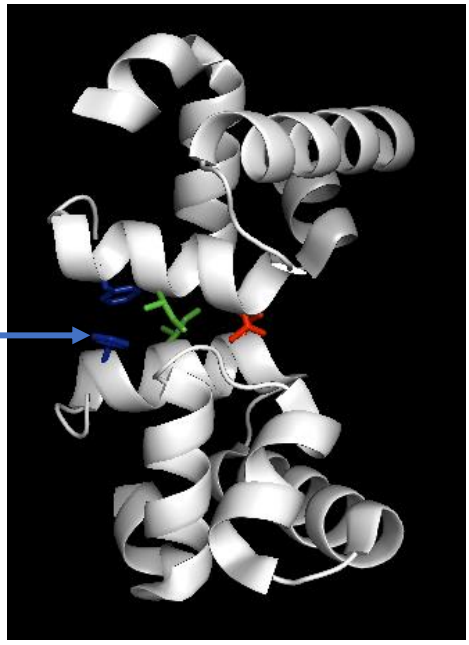

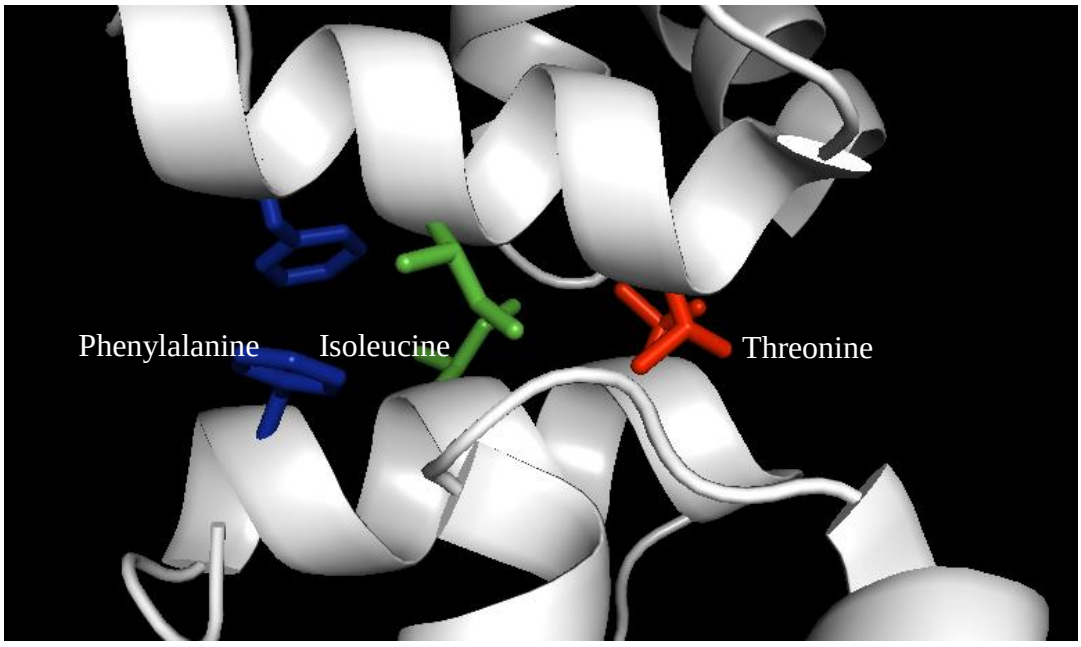

Appendix E: Sequence alignment of LiaR from *Enterococcus faecalis* and *Bacillus subtilis* to identify the conserved sites on the C-terminal, bolded and colored here.

```
E.faecalis    1   MLVDDHEMVRLGVSSYLSIQEDIEVVGEAENGKIGYEKALELRPDVILMDLVMEEMDGID  60
                      +L+DDHEMVR+G++++L  Q DIEV+GEA +G  G   A+EL PDVILMDLVME MDGI+
B.subtilis    5   LLIDDHEMVRMGLAAFLEAQPDIEVIGEASDGSEGVRLAVELSPDVILMDLVMEGMDGIE  64

E.faecalis   61   STKAILKDWPEAKIIIVTSFIDDEKVYPAIEAGAAGYLLKTSTAHEIADAIRATYRGERV 120
                   +TK I ++  + KII++TSFIDD+KVYP IEAGA  YLLKTS A EIADAIRA  +GE
B.subtilis   65   ATKQICRELSDPKIIVLTSFIDDDKVYPVIEAGALSYLLKTSKAAEIADAIRAASKGEPK 124

E.faecalis  121  LEPEVTHKMMERLTKKQEPVL-HEDLTNREHEILMLIAQGKSNQEIADELFITLKTVKTH  179
                      LE +V  K++ RL    E  L HE LT RE EIL LIA+GK+N+EI+ELFIT+KTVKTH
B.subtilis  125  LESKVAGKVLSRLRHSGENALPHESLTKRELEILCLIAEGKTNKEIGEELFITIKTVKTH  184

E.faecalis  180  VSNILAKLDVDDRTQAAIYAFQHGL  204
                 ++NIL+KLDV DRTQAA+YA++ L
B.subtilis  185  ITNILSKLDVSDRTQAAVYAHRNHL  209
```

Appendix F: List of Primers

Underlined bases represent the restriction sites and the italicized and bolded sequences represent the mutated amino acids

Vector name	Forward Primer (5′- 3′)	Reverse Primer (5′- 3′)
pGEX-4T-1:: *liaS*^{Ala126}	CATGGATCCCGATTGGCCAGAGATCTTC	ACGCCCGGGTTATCAATCAATAATACTCGAATC
pGEX-4T-1:: *liaS*^{Arg153}	CATGGATCCGCATCCCTCCAGAAACTTTC	ACGCCCGGGTTATCAATCAATAATACTCGAATC
pGEX-4T-1:: *liaS H159A*	CCAGAGATCTT***GCT***GATGCGGTCAG	CTGACCGCATCAGCAAGATCTCTGG
pET26b::*liaR*	ACGCATATGATGATTCGAGTATTATTGAT	ACGAAGCTTCTAATTCACGAGATGATTT
pET26b::*liaR D54A*	GATGTCATTTTAATG***GCC***CTTGTCATGG	CCATGACAAGG*GCC*ATTAAAATGACATC
pET26b::*liaR*^{N}	AAAGTGGCG***TGA***AAAGTATTATCCAGGCT	AGCCTGGATAATACTTTTCACGCCACTTT
pET26b::*liaR*^{C}	ACGCATATGTCAGGTGAAAACGC	ACGAAGCTTCTAATTCACGAGATGATTT
pET26b::*liaR*^{C}*T198A*	TCAGTGACCGG***GCG***CAGGCGGCG	CGCCGCCTGCGCCCGGTCACTGA
pET26b::*liaR*^{C}*V202A*	CGCAGGCGGCG***GCG***TACGCACACC	GGTGTGCGTACGCCGCCGCCTGCG
pET26b::*liaR*^{C}*H205A*	CGGTGTACGCA***GCC***CGAAATCATCTC	GAGATGATTTCG*GGC*TGCGTACACCG
pET26b::*liaRT198A*	TCAGTGACCGG***GCG***CAGGCGGCG	CGCCGCCTGCGCCCGGTCACTGA
pET26b::*liaRV202A*	CGCAGGCGGCG***GCG***TACGCACACC	GGTGTGCGTACGCCGCCGCCTGCG
pET26b::*liaRH205A*	CGGTGTACGCA***GCC***CGAAATCATCTC	GAGATGATTTCGGGCTGCGTACACCG
pT7Blue-3::*liaSR*	GAAAGGGAAGCAAGTGTTCATCTGTAAAG	TTCATGCAGATCCTCCTTTCGTTTT
vraSR promoter	GAAAGGGAAGCAAGTGTTCATCTGTAAAG	TTCATGCAGATCCTCCTTTCGTTTT